جمهورية العراق
وزارة التعليم العالي والبحث العلمي
جامعة بابل
كلية الهندسة
قسم الهندسة الميكانيكية

تحري نظري للاهتزاز الحر المتناظر محورياً للقشريات النحيفة المتماثلة الكروية المفلطحة

رسالة

قدمت إلى كلية الهندسة في جامعة بابل كجزءً من متطلبات نيل شهادة
ماجستير علوم في الهندسة الميكانيكية
(ميكانيك تطبيقي)

تقدمت بها

نوا ل حسين عبد الأمير الرهيمي

بكالوريوس هندسة ميكانيك
(1993)

تموز 2005

The Republic of Iraq
Ministry of Higher Education and Scientific Research
Babylon University
College of Engineering
Department of Mechanical Engineering

THEORETICAL INVESTIGATION OF THE AXISYMMETRIC FREE VIBRATION OF AN ISOTROPIC THIN OBLATE SPHEROID SHELLS

A Thesis
Submitted to the College of Engineering
of the University of Babylon in Partial
Fulfillment of the Requirements
for the Degree of Master of
Science in Mechanical
Engineering
(Applied Mechanics **)**

By

Nawal Hussein A. Al – Reheimy
B.S.C.
(1993)

July 2005

بسم الله الرَحمن الرَحيم

((وقل رَبِ زِدني علماً))

صدَقَ اللهُ ألعليُ العظيم
سورة طه (114)

الخلاصة

تتناول هذه الرسالة دراسة نظرية للاهتزازات الحرة للقشريات نحيفة الجدران شبه البيضوية الشكل المتناضرة المحور والمتشابهة الخواص في جميع الاتجاهات. التحليل النظري يعتمد على طريقتين هما طريقة (Rayliegh – Ritz) وطريقة (Boundary Matching) وقد تم استخدام كلاً من النظريتين (نظرية القشريات القليلة العمق) و (نظرية القشريات العميقة) في التحليل.

تعد نموذجاً تقريبياً في (Rayliegh – Ritz) وبالرغم من إنّ طريقة محاولة تخمين الترددات الطبيعية للقشريات، تكون هذه ألتقنيه مبنية على أساس القشرية الشبه بيظويه كمنظومة مستمرة مركبه من قشرتين نصف كرويتين متناظرتين على طول حدودها المستمرة.

بعض الاختبارات العملية والتي كانت مأخوذة من احد المراجع استعملت لدعم الجانب النظري، حيث إن الشكل الذي تم اعتماده بالاختبار يحقق نفس متطلبات و شروط هذه الرسالة.

من خلال النتائج, تبين بأنه عندما تصل اللامركزية إلى الصفر يكون ظاهر للعيان بالضبط حل لقشرية نحيفة كروية الشكل وعندما تكون اللامركزية تقريباً مساوية إلى الواحد يكون ظاهر للعيان بالضبط حل لصحيفة نحيفة دائرية الشكل, وبناءً عليه فان اللامركزية للشكل شبه البيضوي يقع عند قيمة متوسطة ما بين تلك القيمتين.

تكون ملائمة لقيم من اللامركزية (Rayliegh) تبين النتائج إنّ طريقة (Rayliegh – Ritz)و Boundary اقل من (0,6) بينما تكون طريقتي matching ملائمتين لكل قيم اللامركزية.

إن تأثير الشروط ألحديه المختلفة (مثل: مثبّت – مثبّت , مثبّت –حر , مفصل - مفصل) للقشرية الشبه بيضوية على خواص الاهتزاز الحر تم بحثها.

CHAPTER ONE

INTRODUCTION

1 . 1 General

Shells like other structures are familiar enough in the nature but the use of such structures as containers, aircraft fuselages, submarine hulls and roofing structures is only of recent origin. That the inherent strength of shells for structures has not been utilized much in the past is probably due to the difficulty in obtaining suitable material with which they are constructed. Such difficulties no longer exist and shell structures in general are constructed of such varied materials as steel, light alloys, plastics, wood, and reinforced concrete.

In general, a shell structure may be defined as the solid material enclosed between two closely spaced doubly curved surfaces. The distances between these two surfaces are the thickness of the shell. If the thickness is small compared with the overall dimensions of the bounding surfaces then the shell is defined as a "thin" shell ; if not, it is termed "thick" [29].

Problems concerning the vibration of shells are considerably more complicated than their counterparts for beams or plates. Primarily this is caused by the effects of the curvature on the dynamic behavior. For beams and plates it is possible to consider separately the flexural and extensional vibrations and only necessary to combine these effects for complex problems; for shells membrane and flexural deformations are coupled, and any theory must consider these effects simultaneously. For

flexural vibrations of beams and plates there are well established theories, which lead to equations (1 . 1 . 1) and (1 . 1 . 2), respectively, in terms of displacement;

$$\rho A \frac{\partial^2 v}{\partial t^2} + \frac{\partial^2}{\partial x^2}\left[E I \frac{\partial^2 v}{\partial x^2} \right] = p(x)\ f(t) \qquad \ldots (1 . 1 . 1)$$

$$D_b \left[\frac{\partial^4 w}{\partial x^4} + 2 \frac{\partial^4 w}{\partial x^2 \partial y^2} + \frac{\partial^4 w}{\partial y^4} \right] + \rho h \frac{\partial^2 w}{\partial t^2} = p(x,y)\ f(t) \qquad \ldots (1 . 1 . 2)$$

where,

$p(x)\ f(t)$ an applied force per unit length, which is a function of time $f(t)$ and act in the Y – direction, is distributed along the length of the beam.

$p(x,y)\ f(t)$ an applied force per unit area, which is a function of time $f(t)$.

For shells, because of the coupling, mutually perpendicular components of displacement must be considered and thus three equilibrium equations in terms of these displacement components should be derived. However, there is no universally accepted set of equations; in fact, many sets of slightly different equations exist. The differences depend upon the assumptions made in the derivation [27].

The model vibration characteristics of thin elastic shells of revolution have been of interest to engineers and scientists for over a century. General understanding of the fundamentals of the behavior of shells is essential in all branches of engineering including aeronautical, civil and mechanical engineering as well as industrial applications of shell structures. In connection to the latter, the natural frequencies of shell structures must be known in order to avoid destructive effects of resonance which might be caused by nearby rotating or oscillating equipment such as jet and reciprocating – aircraft engines, electrical

machinery, marine turbines and screws and exhaust flames from the rocket motors. Furthermore, the pre – knowledge of the free vibration characteristics of any structure is essential in determining its acoustical response, estimating its forced vibration behavior and obtaining its stiffened dynamical characteristics.

One of the commonly used types of elastic thin shells which has a particular interest in this thesis is the spheroid shells. Based on geometry, these shells may be classified as prolate and oblate shells. A prolate spheroid shell is a shell of revolution with elliptical intersection curves with respect to two perpendicular axes. It is the locus surface resulting from rotating an ellipse around the major axis. On the other hand, an oblate spheroid shell is defined as the locus surface resulting from rotating an ellipse around its minor axis, Fig. (1 – 1).

The latter type of shells has many practical applications. To cite a few, the liquid oxygen tanks used in several upper stages of space vehicles have essentially the shape of an oblate spheroid shell. These tanks represent sloshing problems difficult to analyze. These tanks when become only partially full, coupled oscillations of the liquid and the wall of the tank may be indices by various dynamic effects, such as sudden changes in the direction or magnitude of the thrust applied to the vehicle. An introductory approach to the problem involves consideration of the free vibration characteristics of an elastic thin oblate spheroid shell.

Another interesting application of oblate spheroid shells includes the protective shell used as the housing of the early – warning scanner of the Airborne Warning And Control System Aircraft (AWACS).

It is essential to study the free vibration of such shells in order to exclude the chances of resonance with the diffused and reflected electromagnetic waves along with other sources of vibrations. Any resonance may cause a catastrophic accident [33].

1 . 2 Theories in Shells

The most common shell theories are based on linear elasticity concepts. Linear shell theories adequately predict stresses and deformation for shells exhibiting small elastic deformations, that is deformations for which it is assumed that the equilibrium – equation conditions for deformed elements are the same as if they were not deformed and Hook's law applies.

The nonlinear theory of elasticity forms the basis for the finite – deflection and stability theories of shells. Large – deflection theories are often required when dealing with shallow shells, highly elastic membranes' and buckling problems. The nonlinear shell equations are considerably more difficult to solve and for this reason are more limited in use.

Practical difficulties in both theory and experiment have to the development and application of applied engineering method for the analysis of shells. While these methods are approximate and are valid only under specific conditions, they generally are very useful and give good accuracy for the analysis of practical engineering shell structures. Linear theory of shells can be classified into :-

1 – Bending shell theory.

2 – Membrane shell theory.

1 . 2 . 1 Bending shell theory :

The bending theory is more general than the membrane theory because it permits the use of all possible boundary conditions. This theory includes the bending résistance of shell and predict accurate stresses whenever bending is involved. The bending modes vary with thickness, therefore when the bending theory is employed, then the frequency interval of modes extends to infinity for every value of thickness that is greater than zero.

1 . 2 . 2 Membrane shell theory :

This theory studies the equilibrium of a shell, all moments expressions are neglected, the shell is incapable of withstanding any bending moments. The membrane modes are practically independent of thickness. It is apparent that two types of shells comply with this definition of a membrane : (1) shells with bending stiffness sufficiently small so that they are physically incapable of resisting bending and (2) shells that are flexurally stiff but loaded and supported in a manner that avoids the introduction of bending strain.

1 . 3 Geometry of Shells

The geometry of a shell is entirely defined by specifying the form of the middle surface and the thickness of thin shell at each point. To describe the form of the middle surface, it is necessary to present some of the important geometrical properties of the surface.

In the engineering applications of thin shells, a shell whose reference surface is in the form of a surface of revolution has extensive usage. A surface of revolution is obtained by rotation of a plane curve

about an axis lying in the plane of the curve. This curve is called the meridian, and its plane is the meridian plane. The intersection of the surface with planes perpendicular to the axis of rotation are parallel circles. For such a shell the lines of principal curvature are its meridians and parallels. The following nomenclature is given in Fig. (1 – 2)

Φ : angle between the axis of shell and the shell normal at the point under consideration on the middle surface of the shell.

R_Φ : radius of curvature of meridian

R_θ : length of the normal between any point on the middle surface and the axis of rotation

r : radius of curvature of parallel circle

The following geometrical relation is of fundamental importance:

$r = R_\theta \sin \Phi$ [25].

1 . 4 Applications of Shells

Shells have application in different fields such as buildings, chemical application, industrial, etc. The following are the main applications of shells.

1 . 4 . 1 Architecture and building :

The development of masonry domes and vaults in the middle ages made possible the construction of more spacious buildings. In more recent times the availability of reinforced concrete has stimulated interest in the use of shells for roofing purposes.

1 . 4 . 2 Power and chemical engineering :

The development of steam power during the industrial revolution depended to some extent on the construction of suitable boilers. These

boilers are thin shells which were constructed from plates suitable formed and joined by riveting. More recently the used of welding in pressure vessel construction has led to more efficient designs. Pressure vessels and associated pipe work are key components in thermal and nuclear power plants, and in all branches of the chemical and petroleum industries.

1 . 4 . 3 Structural engineering :

An important problem in the early development of steel for structural purposes was to design compression members against buckling. A striking advance was the use of tubular members in the construction of the Fourth Railway Bridge in 1889: steel plates were riveted together to form reinforced tubes as large as 12 feet in diameter, and having a radius/thickness ratio of between 60 and 180.

1 . 4 . 4 Vehicle body structures :

The construction of vehicle bodies in the early days of road transport involved a system of structural ribs and non-structural paneling or sheeting. The modern form of vehicle construction, in which the skin plays an important structural role, followed the introduction of sheet-metal components, preformed into thin doubly curved shells by large power presses, and firmly connected to each other by welds along the boundaries. The use of the curved skin of vehicles as a load bearing member has similarly revolutionized the construction of railway carriages and aircraft. In the construction of all kinds of spacecraft the idea of a thin but strong skin has been used from the beginning.

1 . 4 . 5 Composite construction :

The introduction of fiberglass and similar lightweight composite materials has impacted the construction of vehicles ranging from boats,

racing cars, fighter and stealth aircraft, and so on. The exterior skin can be used as a strong structural shell.

1 . 4 . 6 Miscellaneous Examples :

Other examples of the impact of shell structures include water cooling towers for power stations, grain silos, armour, arch dams, tunnels, submarines, and so forth [32].

1 . 5 Work Objectives

The main objectives of this work may be summarized as follows :

1. An exact formulation of the problem of the free vibrations of an oblate spheroidal shell will be attempted. However, since an exact closed form solution is not possible, an energy approach using Rayleigh – Ritz's Method will be used to investigate the free vibration characteristics of this type of shells.
2. Using the method of matching the boundary conditions and Rayliegh – Ritz's Method to obtain the vibration characteristics of shallow and non – shallow spheroidal shell for various eccentricity ratios.
3. Using two methods (matching the boundary conditions and Rayliegh – Ritz's) to obtain the effect of thickness ratio on natural frequency.
4. Using the matching of boundary method to obtain the effect of various boundary conditions on natural frequency of oblate spheroidal shell such as: (Clamped – free, Clamped – clamped and Pined – pined).

1 . 6 Layout of the Thesis

The thesis falls into five chapter. Chapter one is an introduction. Chapter two is concerned with a brief literature review. Chapter three is divided into five sections; section one presents the introduction for modeling and mathematical analysis used in this work, section two presents the first method (Rayleigh – Ritz's energy method), section three presents the engineering model by non – shallow shell theory, section four presents engineering model by shallow shell theory, and section five presents the computational procedure. Chapter four presents the results and their discussion and chapter five presents the conclusions drawn from this work with some suggestions for further work.

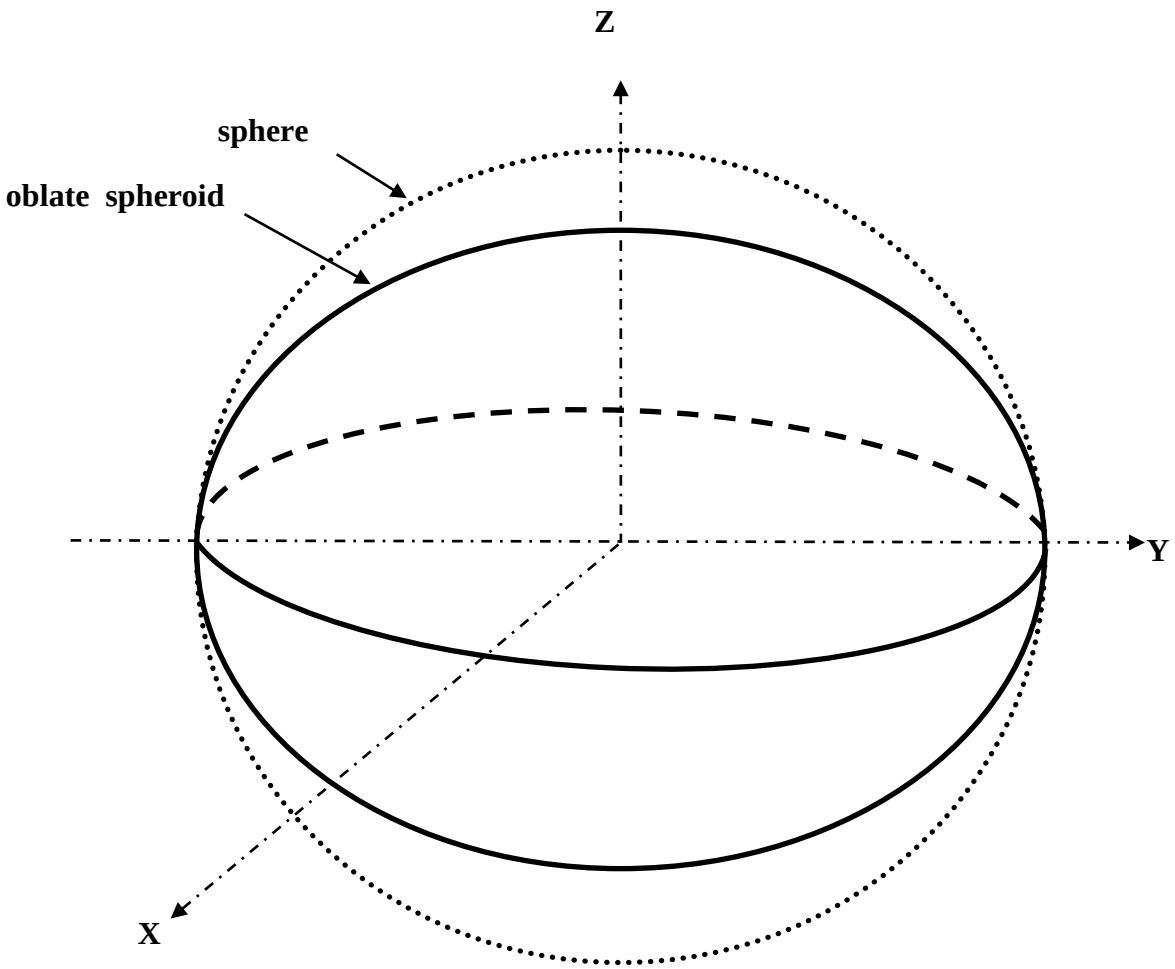

Fig. (1 – 1): An Oblate Spheroidal Shell

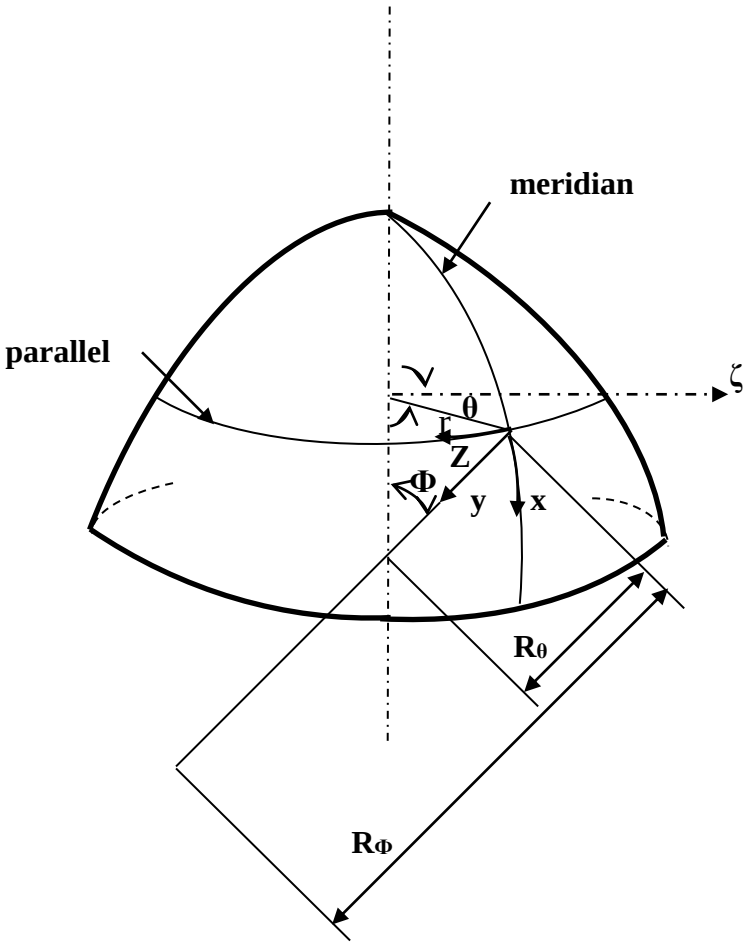

Fig. (1 – 2): Shell of Revolution

CHAPTER FOUR

RESULTS and DISCUSSIONS

4 .1 Introduction:

In this thesis a study of the axisymmetric vibrational characteristics of an oblate spheroidal shell has been performed.

Two basic theoretical techniques were employed; the first was based on the energy method using Rayliegh – Ritz's approach; the second was based on approximating the oblate spheroid as a structure composed of two open thin spherical shell elements joined rigidly at their circumferential. Using this approximation, the non – shallow and the shallow spherical shell theories were applied to investigate the free vibration characteristics of the oblate spheroid.

Finally some experiments which taken from [33] to justify the theoretical results as well as to observe the free axisymmetric vibration problem at hand.

In this chapter, the results of the theoretical work of chapter three and the available experiments are compared and thoroughly discussed. Also some conclusions drawn from the present work will be given at the end of the chapter.

4.2 Validity of the Employed Methods :

The lack of numerical results in the literature and the complexity of obtaining a closed form solution for the free vibrational characteristics of an oblate spheroid oblige us to seek alternative approaches for justifying the feasibility of the theoretical methods used in this thesis.

Eventually, these methods are general and may be used for any physical and geometrical parameters of the oblate spheroid. Therefore, the natural frequency for a thin sphere which is considered as an ultimate shape of the oblate spheroid may be determined by using these methods and the results are compared with the literature.

Table (4–1) shows the natural frequency of the three first axisymmetric modes of a full thin sphere of (0.1143) m radius and (5.7) mm thickness with material properties of E = 207GPa, ρ = 7800 kg / m^3 and υ = 0.3. These frequencies were obtained from applying the direct analytical solution (DAS), the state space method (SSM), the finite element method (FEM) where a forty elements of axisymmetrical model was used [31], Rayliegh Method (RM) [33], and the two methods derived in this thesis, namely the Rayleigh – Ritz Method (RRM) and the Boundary Matching Method (BMM). The results of the latter methods were obtained by setting the eccentricity ratio to zero in equation (3.2.7) and the boundary condition matching was applied to two hemispherical shell elements.

From this table it can be concluded that the (RRM) and (BMM) give the natural frequencies within computational error of the used computers.

Also it can be seen that the Rayleigh–Ritz's Method predicts frequencies higher than the other methods given in the table. This fact is inherited to this method for its higher bounds prediction. However, it may

be stated from this table that the two methods of solution presented in this work are dependable and may be used for other shell geometrical and physical parameters.

4.3 Comparison between RRM and BMM Methods :

Figure (4–1) shows the non–dimensional natural frequencies $\left(\lambda = \sqrt{\rho / E}\ \omega . a\right)$ of the first three modes of vibration as functions of the eccentricity ratio obtained by the Rayleigh Ritz's Method and the Matching Boundary Condition Method using the non – shallow shell theory. This figure shows clearly the tendency of the natural frequencies towards lower values as the eccentricity increases. Also it is indicated that the curve obtained by the Rayleigh – Ritz's Method, adjoin to that obtained by the Boundary Matching Method, although with slightly higher value for all values of eccentricity ratio.

This behavior could be explained by the fact that the mode shapes of a closed spherical shell would resemble those of an oblate spheroid up to certain eccentricity ratio. As the eccentricity ratio increases, the oblate spheroid tends to flatten up. Such "flattening" causes the uncoupling of the radial (or transverse motion) and the tangential motion where the latter is minimized and the radial or transverse motion mode shape approaches that of a circular plate (a plate is an oblate spheroid with approach unity eccentricity ratio). Another reason is that the spherical shape is stiffer than the oblate spheroid due to the flattening in the geometry.

4 . 4 Comparison between the Non – Shallow and Shallow Shell Theories Using BMM and RRM

Figures (4 – 2) and (4 – 3) represent a comparison of the lowest natural frequency predicted by the non – shallow as well as the shallow spherical shell theories using the (BMM) and (RRM) respectively, to approximate oblate spheroidal shells with (0.9 to 0.98) range of eccentricity ratios. The full line curve represents the non – shallow shell theory while the dashed line represents the shallow shell theory. The difference between the two curves diminishes as the eccentricity ratio increases.

Recalling that an oblate spheroid of (0.93) and larger eccentricities might be modeled as a structure composed of two spherical shells joined together at their edges with an opening angle (25°)and less as shown in Fig. (3 – 7). Evidently, for such a shape, both the shallow and the non – shallow spherical shell theories are applicable and the results predicted by both of them show acceptable convergence in that region. However, as the eccentricity ratio becomes less than (0.93), the opening angle of the approximate spherical shell model exceeds twenty five degrees, thus for such oblate spheroidal shells the assumptions used to derive equations (3 . 4) will not hold due to the fact that the ratio of the radial (transverse) motion to the tangential (longitudinal) motion will be maximized. However, this ratio tends to decrease by increasing the opening angle.

4 . 5 Effect of Thickness Ratio on Natural Frequency :

In oblate spheroidal shells the thickness ratio is defined as the shell thickness (h) to the major semi axis length (a). Figures (4 – 4) and (4 – 5) give the first few natural frequencies as function of the thickness ratio for an oblate spheroid with (e = 0) obtained by BMM and RRM respectively. However, Fig. (4 – 6) shows the same results as given by Kraus [17], for complete sphere. The three figures are in good agreement and justify very well the validity of the method used in this thesis.

Further, Figs. (4 – 7) and (4 – 8) show the first few frequencies as functions of thickness ratio with (e = 0.6). All these figures are for ($\upsilon = 0.3$) and they show the bending as well as the membrane modes using the non – shallow shell theory. It can be noted that the variation of the natural frequency of the bending modes increases with thickness and with the mode number. This phenomena can be elaborated due to the fact that the strain energy increased with increasing the thickness ratio. Also, for larger eccentricity ratio, the variations are more pronounced than for smaller eccentricity ratio.

Since the membrane modes occur at relatively high values of the non – dimensional frequency parameter value of λ in comparison to the first bending modes, the variation of only few of the membrane modes with the thickness ratio are investigated. A conclusion is reached that the membrane modes have very small variation – if no variation at all – with thickness ratio. This can be further explained by considering the strain energy expression of the two spherical shell elements.

If the strain energy due to the stretching of the middle surface of the shell is represented by U_m and due to the bending of the shell by U_b where,[11]

$$U_m = \frac{E\,h\,\pi\,R_r^{\,2}}{1-\upsilon^{\,2}} \int_0^{\Phi_0} \left(\varepsilon_\Phi^{\,2} + 2\upsilon\,\varepsilon_\Phi\,\varepsilon_\theta + \varepsilon_\theta^{\,2}\right) \sin\Phi\; d\Phi$$

$$U_b = \frac{E\,h^{\,3}\,\pi\,R_r^{\,2}}{1-\upsilon^{\,2}} \int_0^{\Phi_0} \left(k_\Phi^{\,2} + 2\upsilon\,k_\Phi\,k_\theta + k_\theta^{\,2}\right) \sin\Phi\; d\Phi$$

The middle surface strains may be expressed as,[11] :

$$\varepsilon_\Phi = \frac{1}{R_r}\left(U_\Phi' + W\right)$$

$$\varepsilon_\theta = \frac{1}{R_r}\left(\cot\Phi\; U_\Phi \; + W\right)$$

and the bending strains as :

$$k_\Phi = \frac{1}{R_r^{\,2}}\left(U_\Phi' - W''\right)$$

$$k_\theta = \frac{1}{R_r^{\,2}}\left(U_\Phi - W'\right)\cot\Phi$$

For membrane modes, the stretching effect strain energy is dominant as given by equation (3 . 2 . 7) while for bending modes, the bending effect on strain energy is dominant.

To have some quantitative feeling of this fact consider a complete sphere (an oblate spheroid with zero eccentricity ratio) with thickness ratio of (0.05).

Let ($\eta = U_b/ (U_b + U_m)$ which represent the ratio of the bending strain energy to the total strain energy, the numerical values of η for the first and second bending modes and for the first membrane mode are :

First bending mode = 0.015

Second bending mode = 0.283

First membrane mode = 0.000

Eventually, these values elaborate the preceding explanation. For further illustration of the effect of thickness on the bending modes, Figures (4 – 9) and (4 – 10) show the first two bending modes of an

oblate spheroid with an eccentricity ratio of (0.3 and 0.8) respectively for several thickness ratios, obtained by applying the BMM and RRM. However, Figures (4 – 11) and (4 – 12) show the first four bending modes of an oblate spheroid with (0.95) eccentricity ratio for several thickness ratios obtained by applying the shallow and the non – shallow spherical shell theories. Also for Figures (4 – 13) and (4 – 14) show the first four bending modes of an oblate spheroid with (0.95) eccentricity ratio for several thickness ratios obtained by the BMM and RRM by applying the non – shallow and shallow spherical shell theories respectively. It is well indicated that the figures obey the previous observation of the effect of thickness on bending modes. However, it is further observed that (RRM) in Figures (4 – 9 , 4 – 10 , 4 – 13 and 4 – 14) still predict higher values than the (BMM).

Figures (4 – 11) and (4 – 12) show similar features as those of the previous though, the shallow shell theory is more sensitive to the increasing thickness. On the other hand, it is shown that the shallow shell generally predicts higher values than those of the non – shallow theory.

4 . 6 The Effect of Eccentricity Ratio on Natural Frequencies :

To study the effect of the eccentricity ratio on natural frequencies, the two classified modes, namely the bending mode (in which the bending strain energy is dominant) and the membrane modes (in which the stretching strain energy is dominant), will be referred to.

Taking this into consideration, Figures (4 – 15, 16 and 17) illustrate the boundaries of the first three bending modes and the first membrane mode respectively with increasing the eccentricity ratio (e). It may be observed from Figures (4 – 15) and (4 – 16) that as the eccentricity ratio increased, the natural frequency slowly decrease until reaching close

to (0.5) where steeper variation occurs and the three curves converge to very close values. On the other hand, Fig. (4 – 17) shows other features concerning the behavior of the first membrane mode with increasing eccentricity ratios.

It is clearly seen that the first membrane natural frequency obtained by the BMM represented by the full line increases with increasing eccentricity ratios. Such trend is also related to the same argument stated before concerning the geometrical structure of the shell. However, in this case as the geometrical structure reaches a circular plate, membrane frequencies in which the stretching strain energy is dominant, becomes naturally higher in value. The dashed line curve obtained by applying the (RRM) emphasizes this conclusion.

4 . 7 The Effect of Boundary Conditions on Natural Frequencies

Fugures (4 – 18) , (4 – 19) and (4 – 20) show the non – dimensional natural frequencies $\left(\lambda = \sqrt{\rho / E}\ \omega . a\right)$ of the first three modes of vibration obtained by using the matching of boundary condition method for variouse boundary conditions as a function of eccentricity ratio.

It is well indicated that the three figures obey the previous obsarvation of the effect of eccentricity ratio on bending modes. However, it is further observed that the curve of clamped – clamped boundary conditions in three figures predict higher values than the other two curves for other boundary conditions. This is attributed to the fact that the structure for clamped – clamped boundary conditions are in general stiffer than the structure for other two boundary conditions.

4 . 8 Comparison between Theoretical and Experimental Results:

In order to verify the theoretical results, some experiments, which are related to the present work, were taken from [33].

The experimental and the theoretical frequencies for shell models 1 and 2 with the specifications given in Table (4 – 2) are presented in Tables (4 – 3 and 4 – 4) respectively. The theoretical values are obtained by using the Rayliegh, Rayleigh – Ritz Method and the Boundary Matching Method with non – shallow shell theory.

Table (4 – 3) indicates that the theoretical results predicted by the (BBM) are higher than the experimental values. This is attributed to the fact that the theoretical spherical caps are in general stiffer than the corresponding experimental oblate spheroidal shell. Also, it is indicated that the Rayliegh and Rayleigh – Ritz's Method predicts frequencies higher than both of the experimental and the (BMM). This is inherited to this particular method.

Table (4 – 4), however, indicates that the (BMM) predicts frequencies lower than the experimental values for the second and third modes. This may be explained by considering that the theoretical model with (e = 0.921) approaches a plate which in general has less stiffness.

However it may be noticed that the value predicted by the Rayleigh – Ritz Method (RRM) is higher than that by the Boundary Matching Method (BMM) for the first three modes and lower than the experimental values for the second and third modes. Also, it may be noticed that the value predicted by the (RM) is very high. Its results are undependable due to the fact that this method cannot be used as stated earlier for this range of eccentricities ratio.

Figures from (4 – 21 through 4 – 32), showed that the main features of the modes shapes associated with the first three natural frequencies rest in the number of the nodal lines in the upper and the lower shell parts. The number of these nodal lines is related to the order of the associated natural frequency.

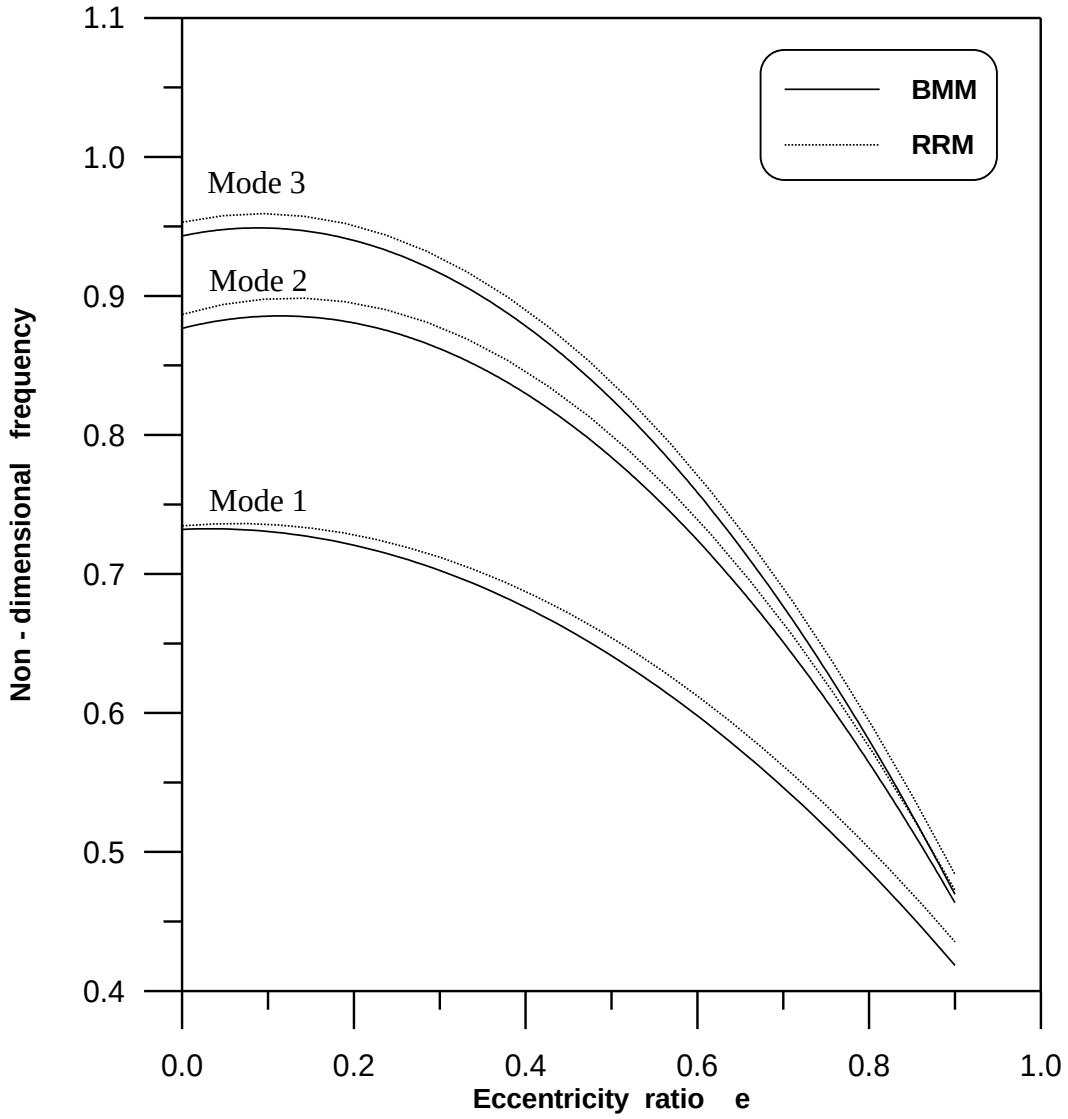

Fig. (4 – 1) Effect of eccentricity ratio on the first three bending modes of vibration.

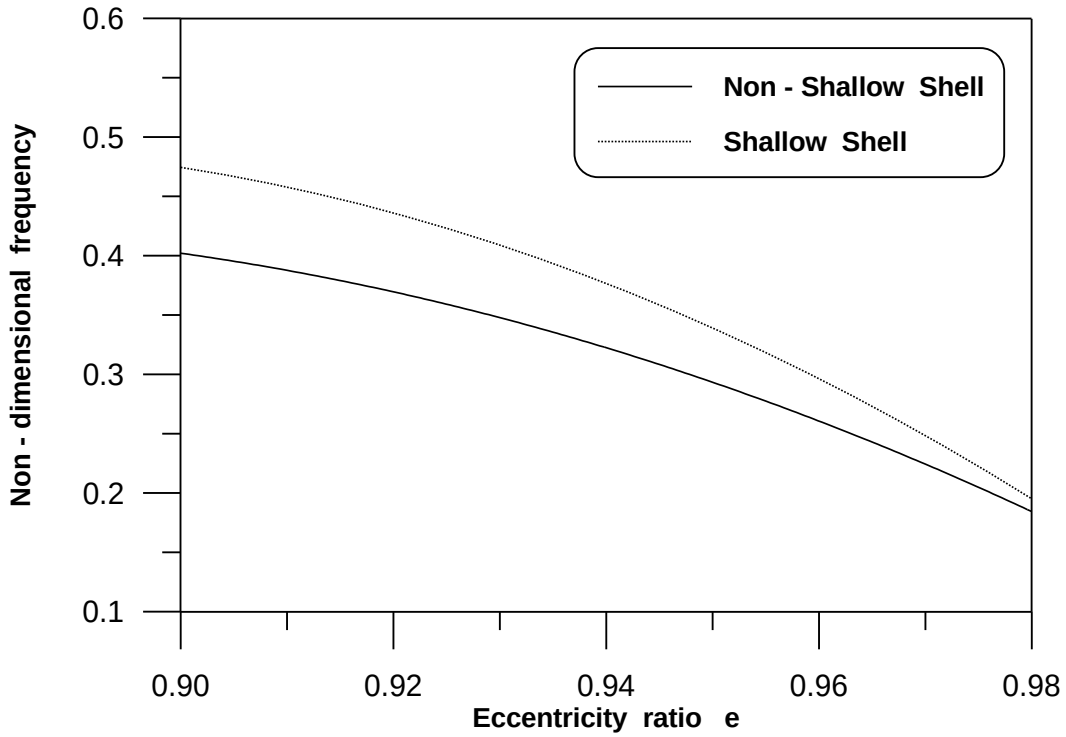

Fig. (4 – 2) A comparison between the shallow and the non – shallow shell theories prediction of the first bending mode vs. eccentricity obtained by BMM

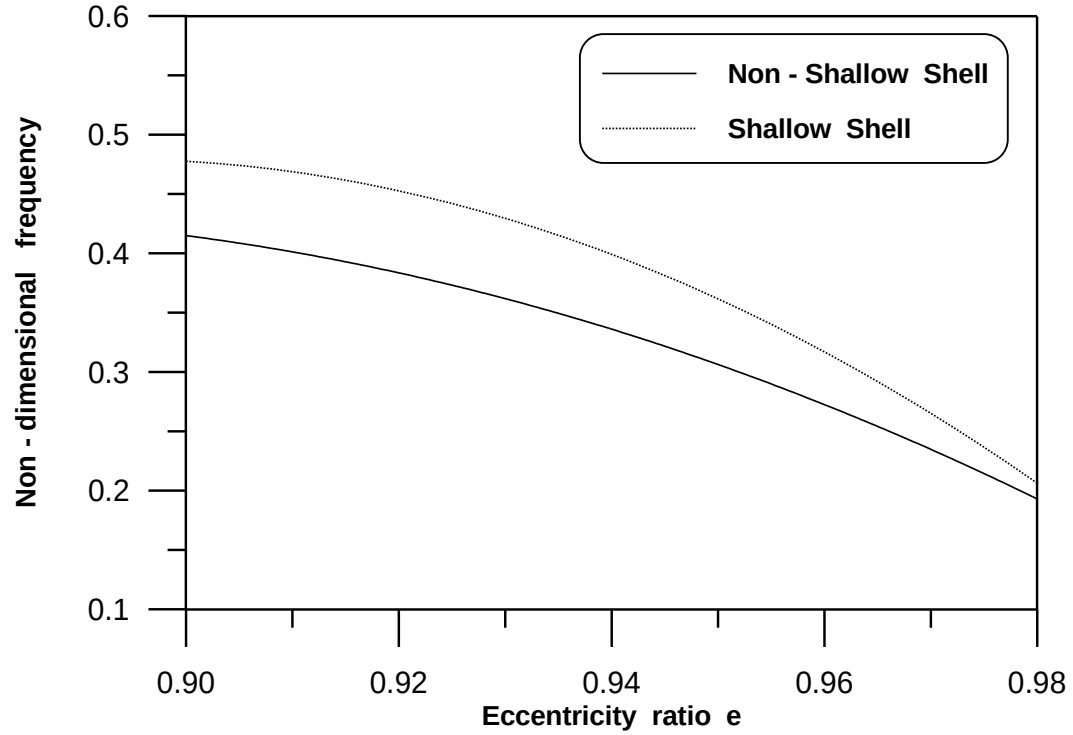

Fig. (4 – 3) A comparison between the shallow and the non – shallow shell theories prediction of the first bending mode vs. eccentricity obtained by RRM

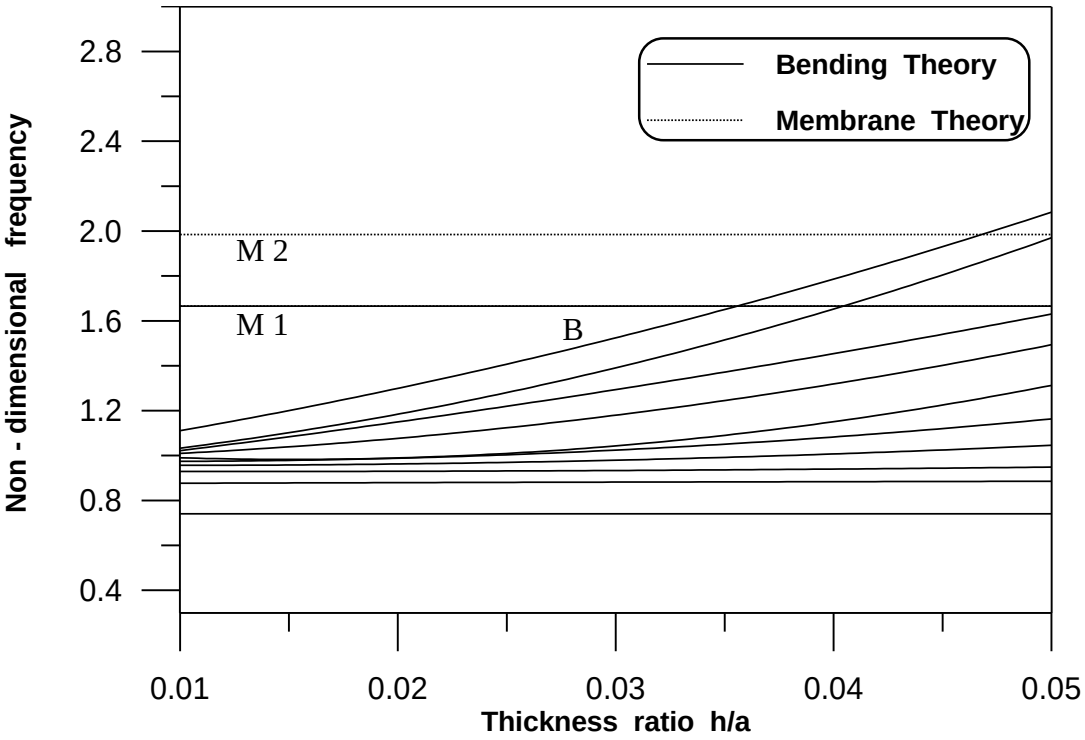

Fig. (4 – 4) Effect of the thickness ratio on the natural frequencies of a full sphere or an oblate spheroidal shell (e = 0) obtained by BMM

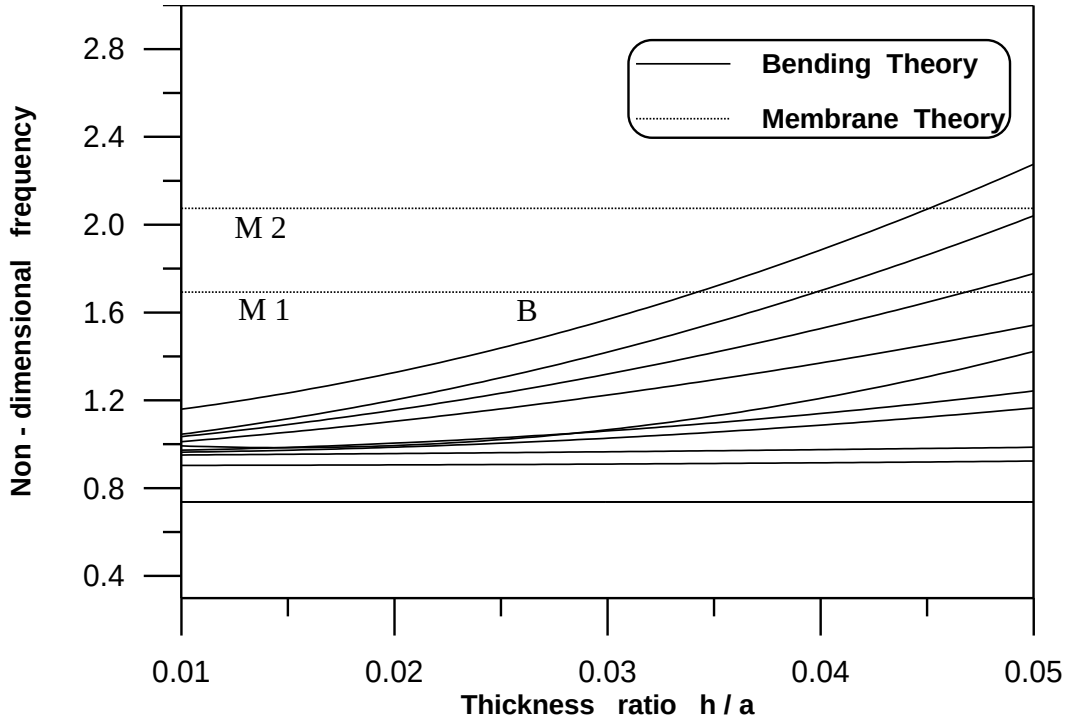

Fig. (4 – 5) Effect of the thickness ratio on the natural frequencies of a full sphere or an oblate spheroidal shell (e = 0) obtained by RRM

Fig. (4 – 7) Effect of the thickness ratio on the natural frequencies of a full sphere extracted from [17]

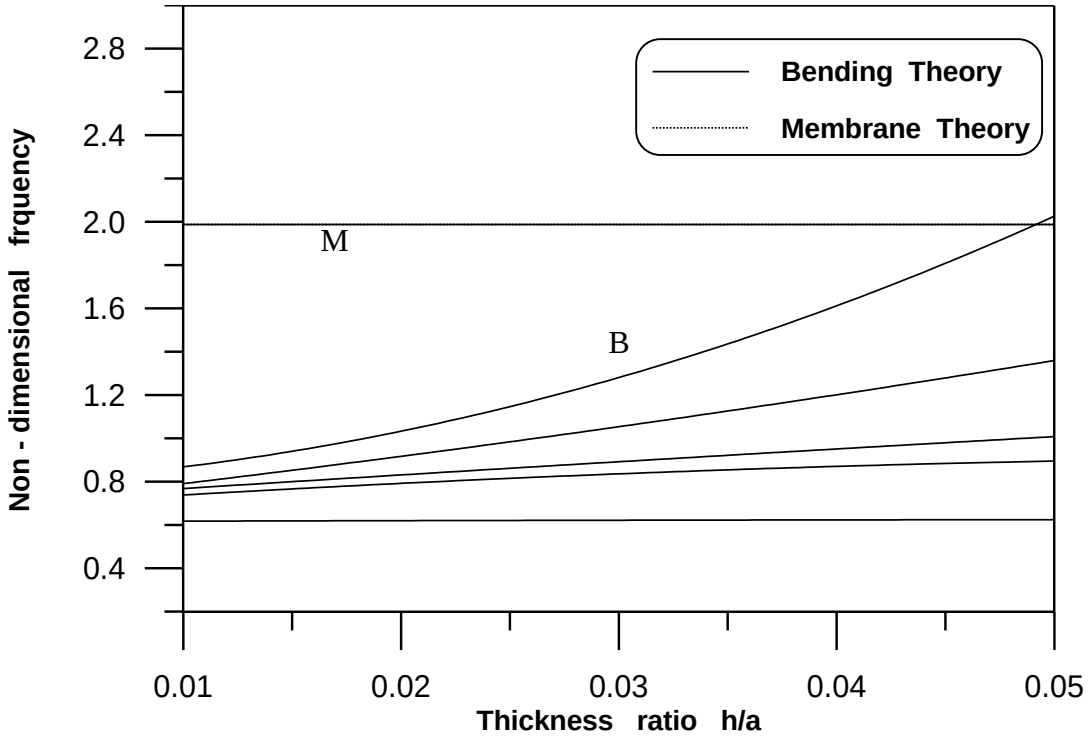

Fig. (4 – 7) Effect of the thickness ratio on the natural frequencies of an oblate spheroidal shell (e = 0.6) obtained by BMM

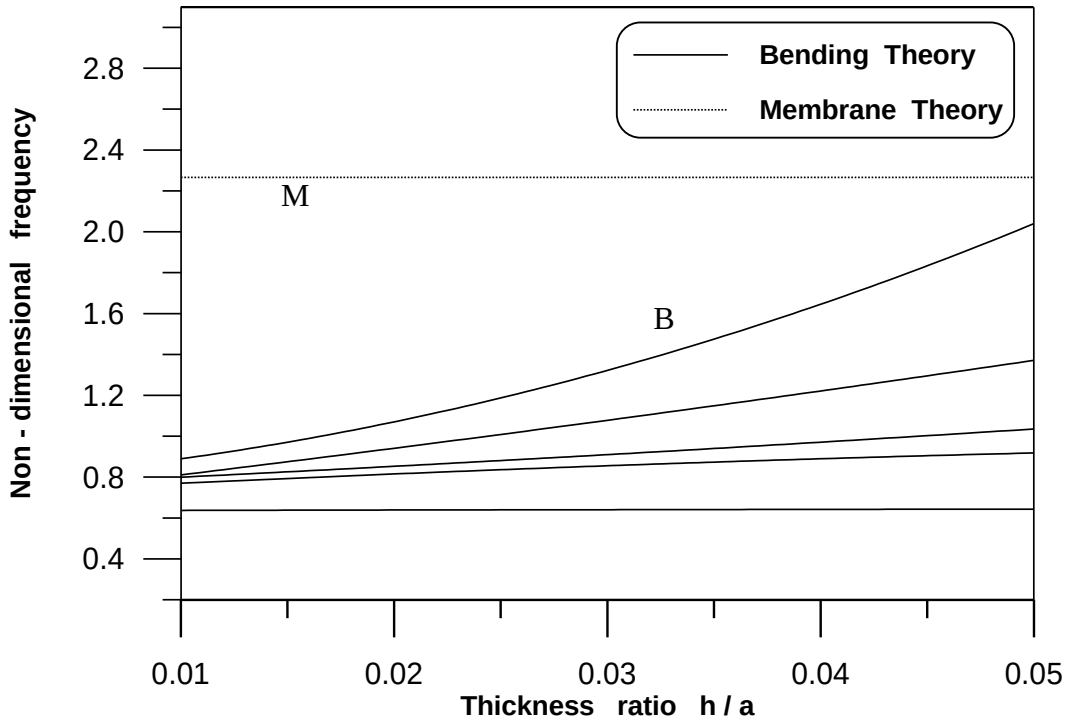

Fig. (4 – 8) Effect of the thickness ratio on the natural frequencies of an oblate spheroidal shell (e = 0.6) obtained by RRM

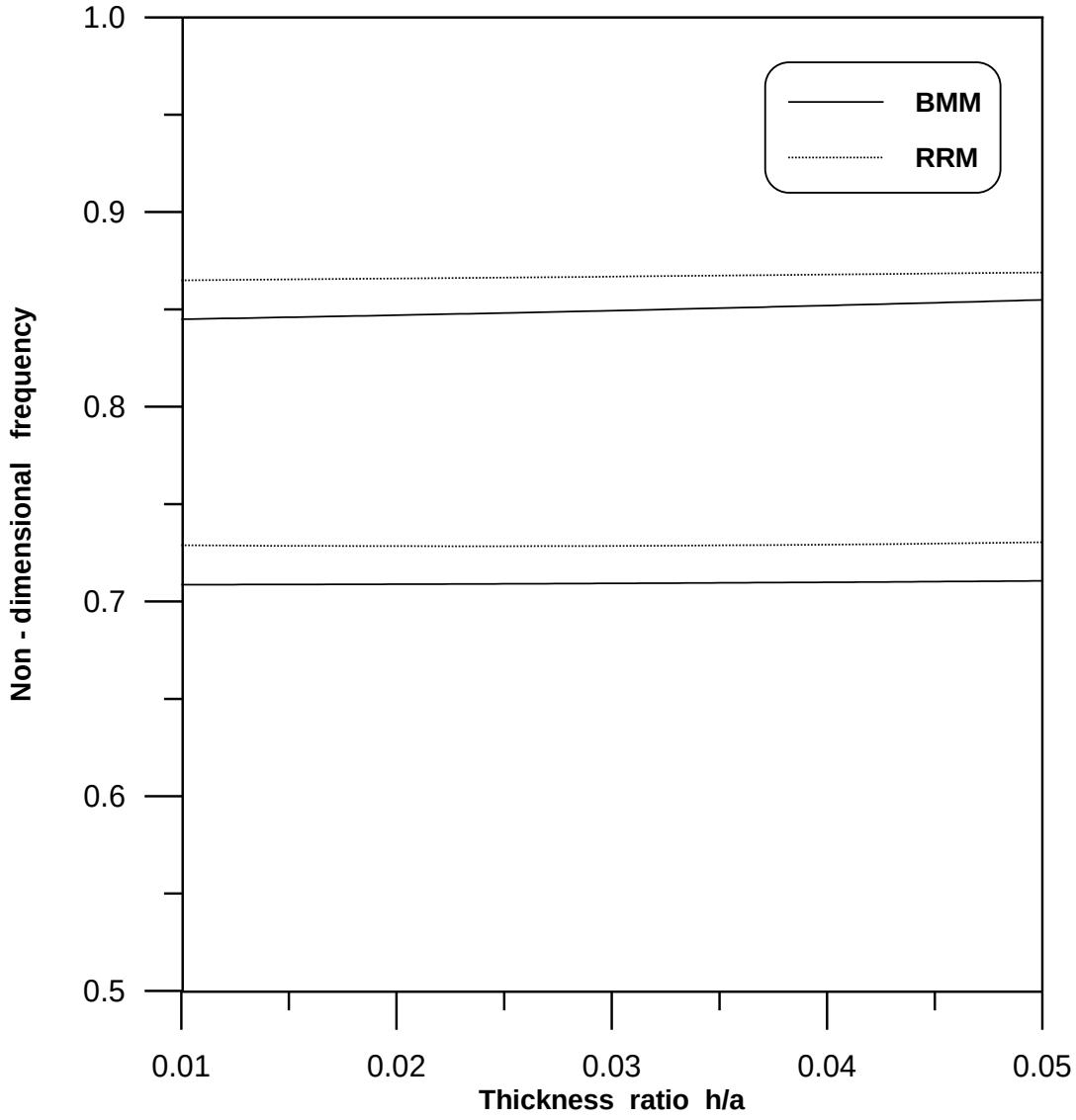

Fig. (4 – 9) Effect of thickness ratio on the first and second bending modes of an oblate spheroidal shell (e = 0.3)

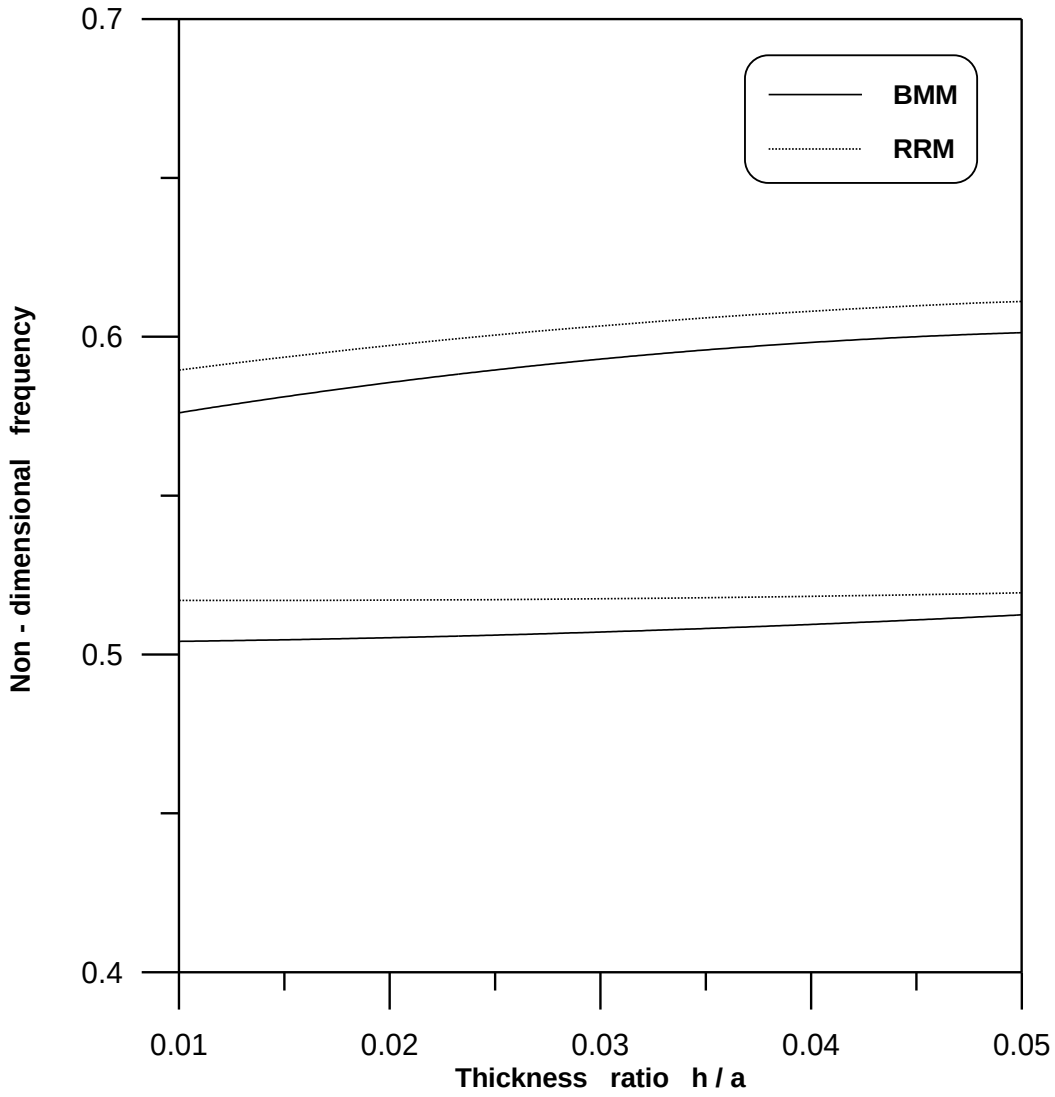

Fig. (4 – 10) Effect of thickness ratio on the first and second bending modes of an oblate spheroidal shell (e = 0.8)

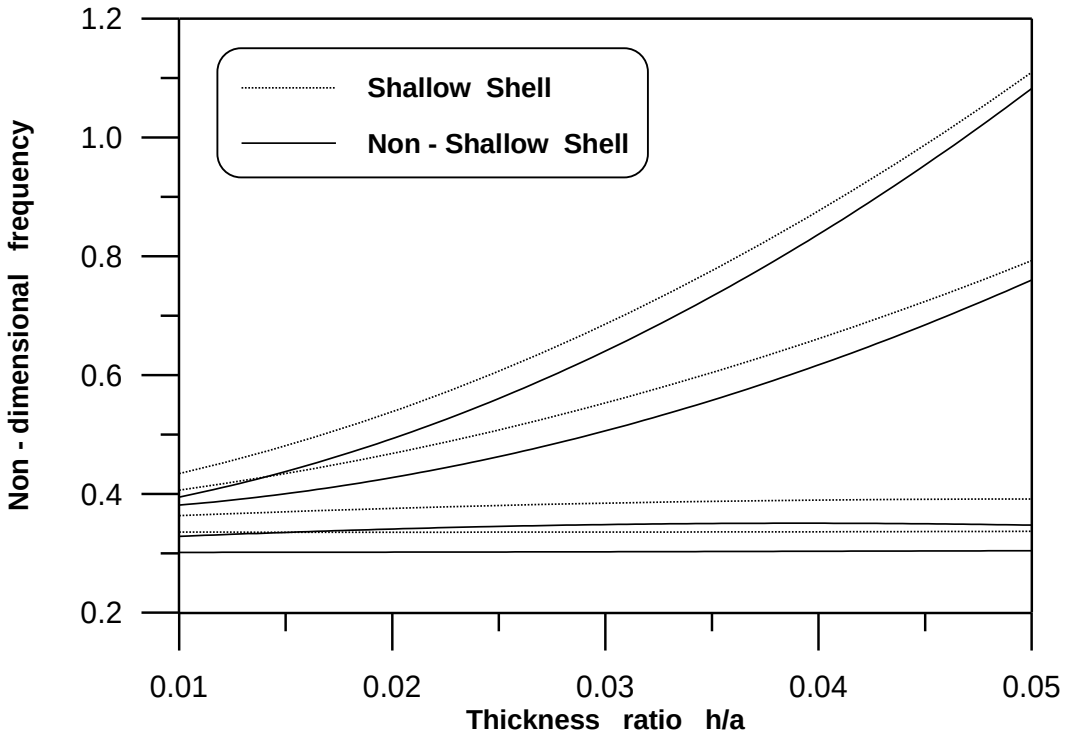

Fig. (4 – 11) A comparison between the shallow and non – shallow shell theories prediction of the first four bending modes of an oblate spheroidal shell (e = 0.95) showing the effect of thickness ratio obtained by BMM

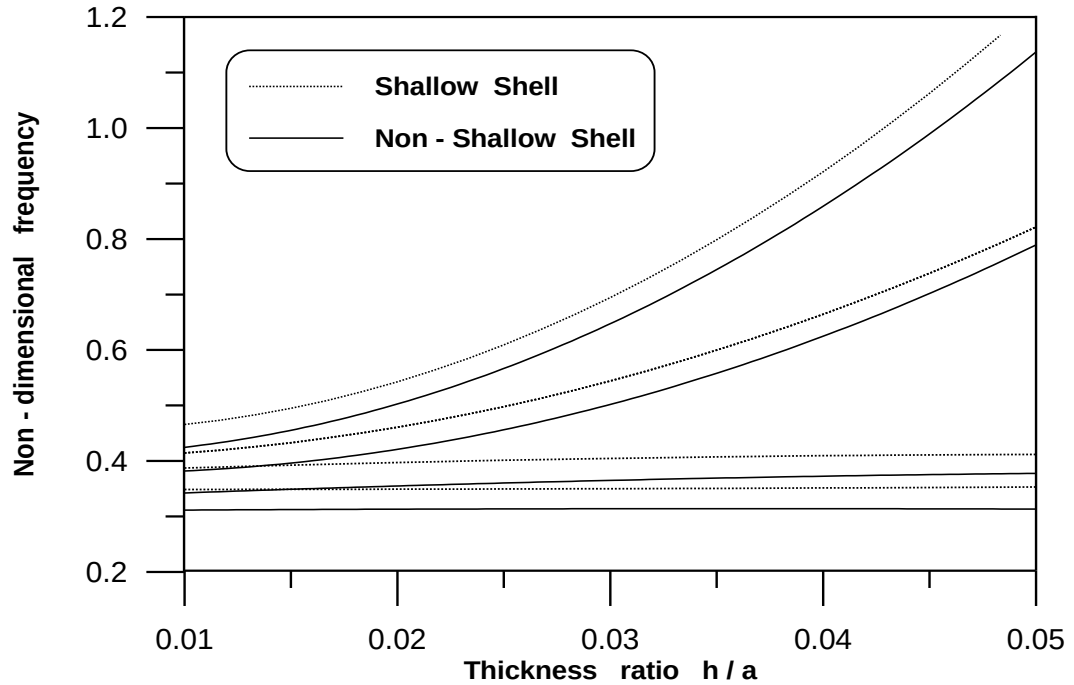

Fig. (4 – 12) A comparison between the shallow and non – shallow shell theories prediction of the first four bending modes of an oblate spheroidal shell (e = 0.95) showing the effect of thickness ratio obtained by RRM

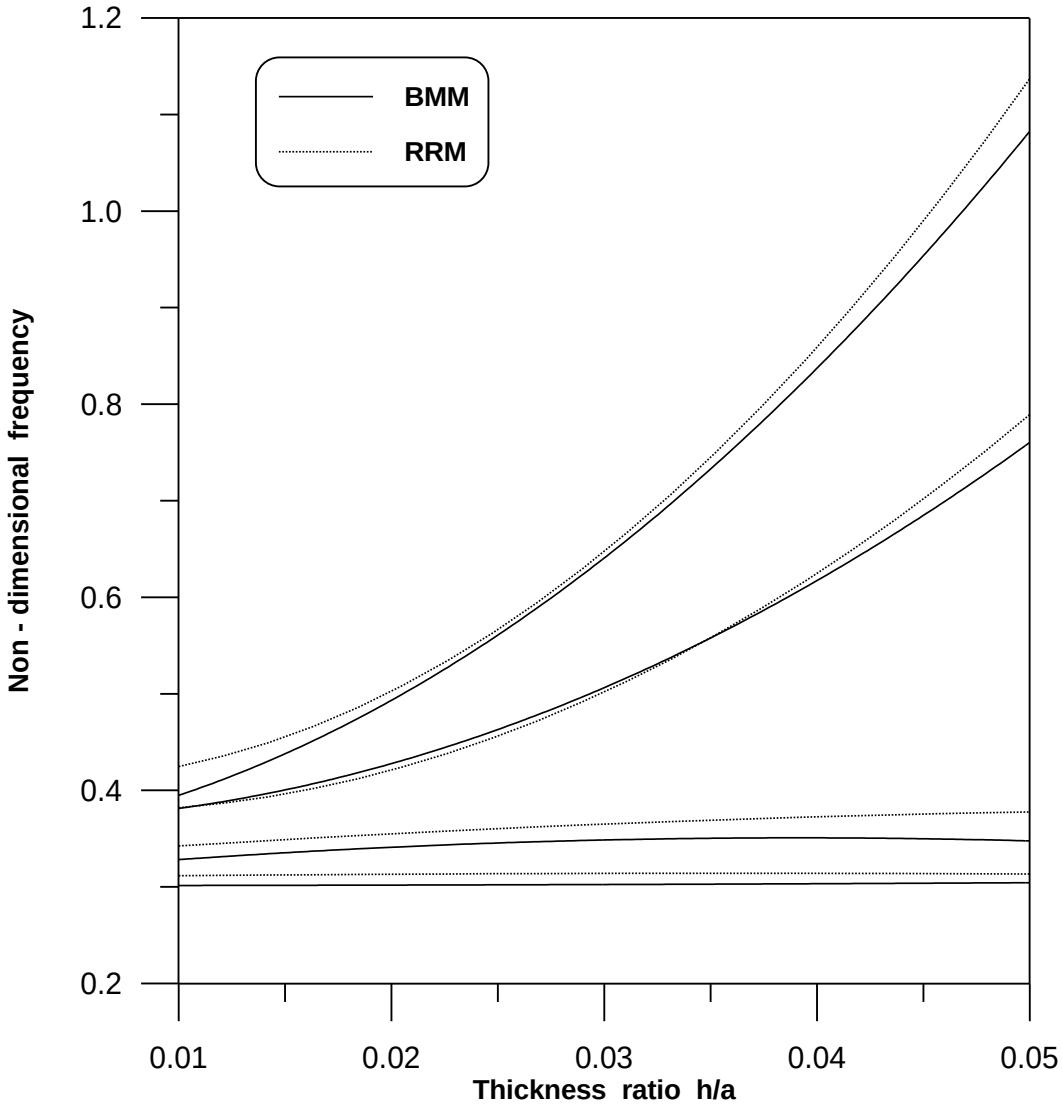

Fig. (4 – 13) Effect of thickness ratio on the first four bending modes of an oblate spheroidal shell (e = 0.95) by using the non – shallow shell theory

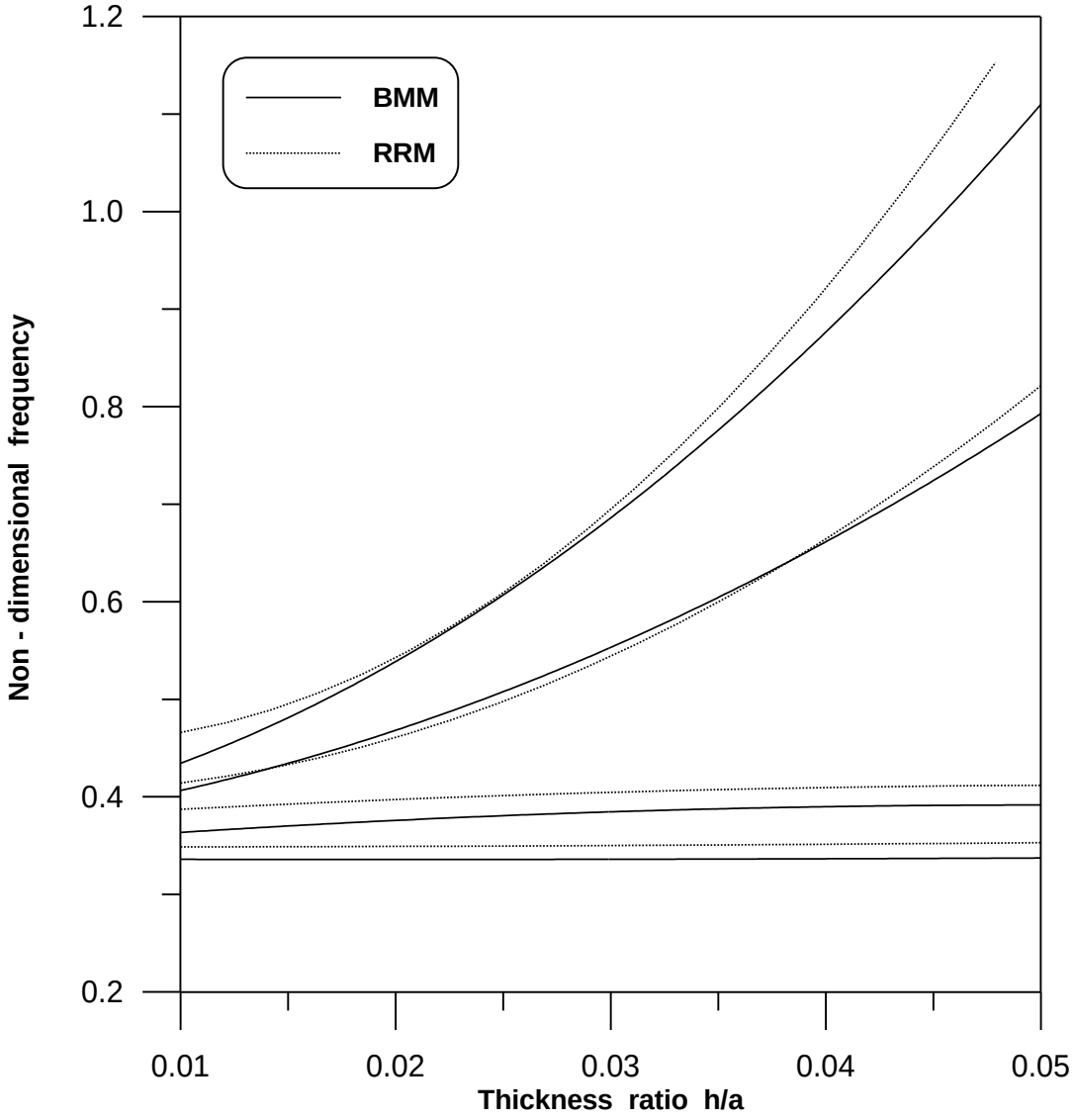

Fig. (4 – 14) Effect of thickness ratio on the first four bending modes of an oblate spheroidal shell (e = 0.95) by using the shallow shell theory

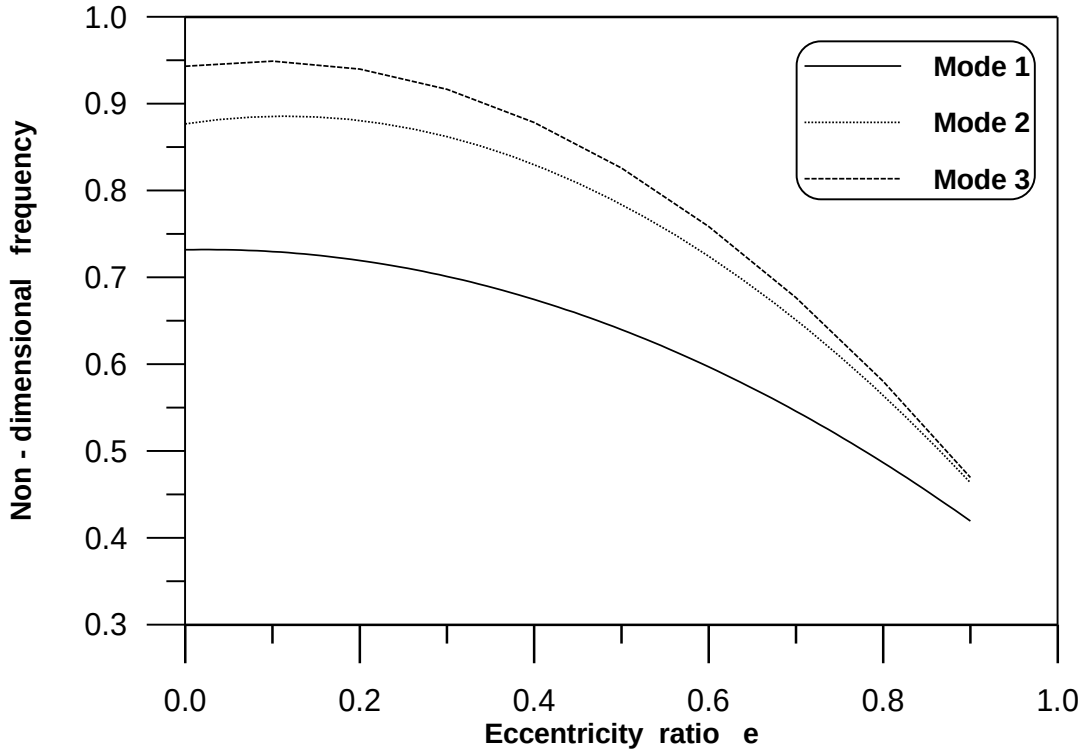

Fig. (4 – 15) Effect of eccentricity on the three first bending modes obtained by BMM

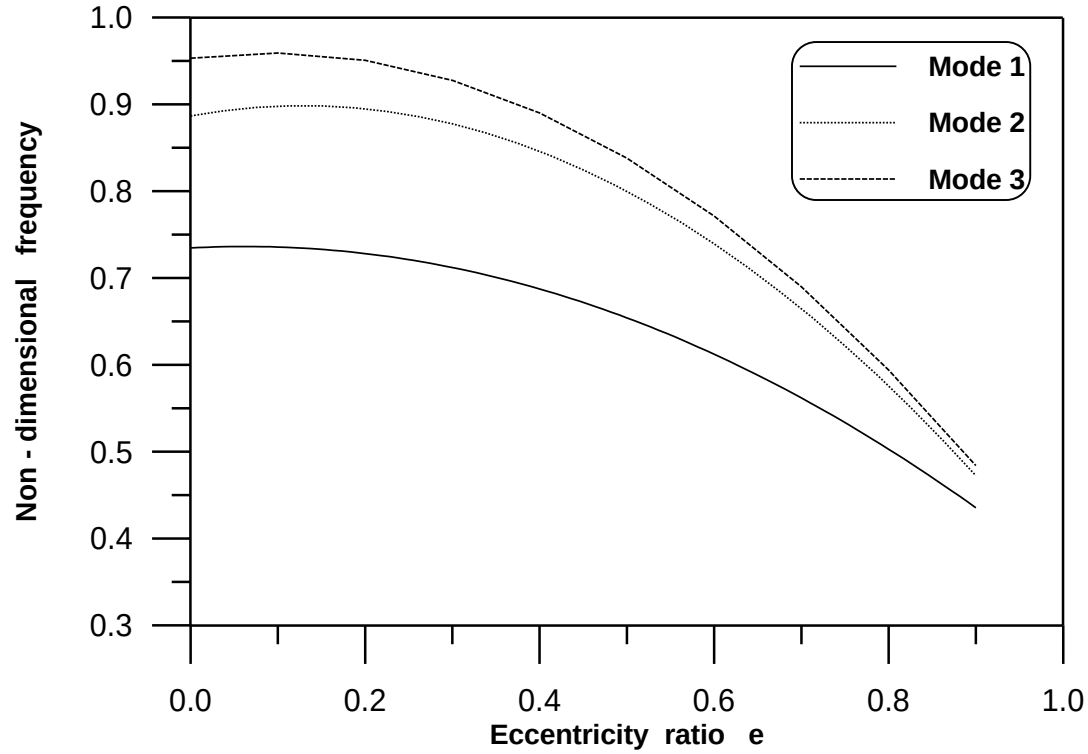

Fig. (4 – 16) Effect of eccentricity on the three first bending modes obtained by RRM

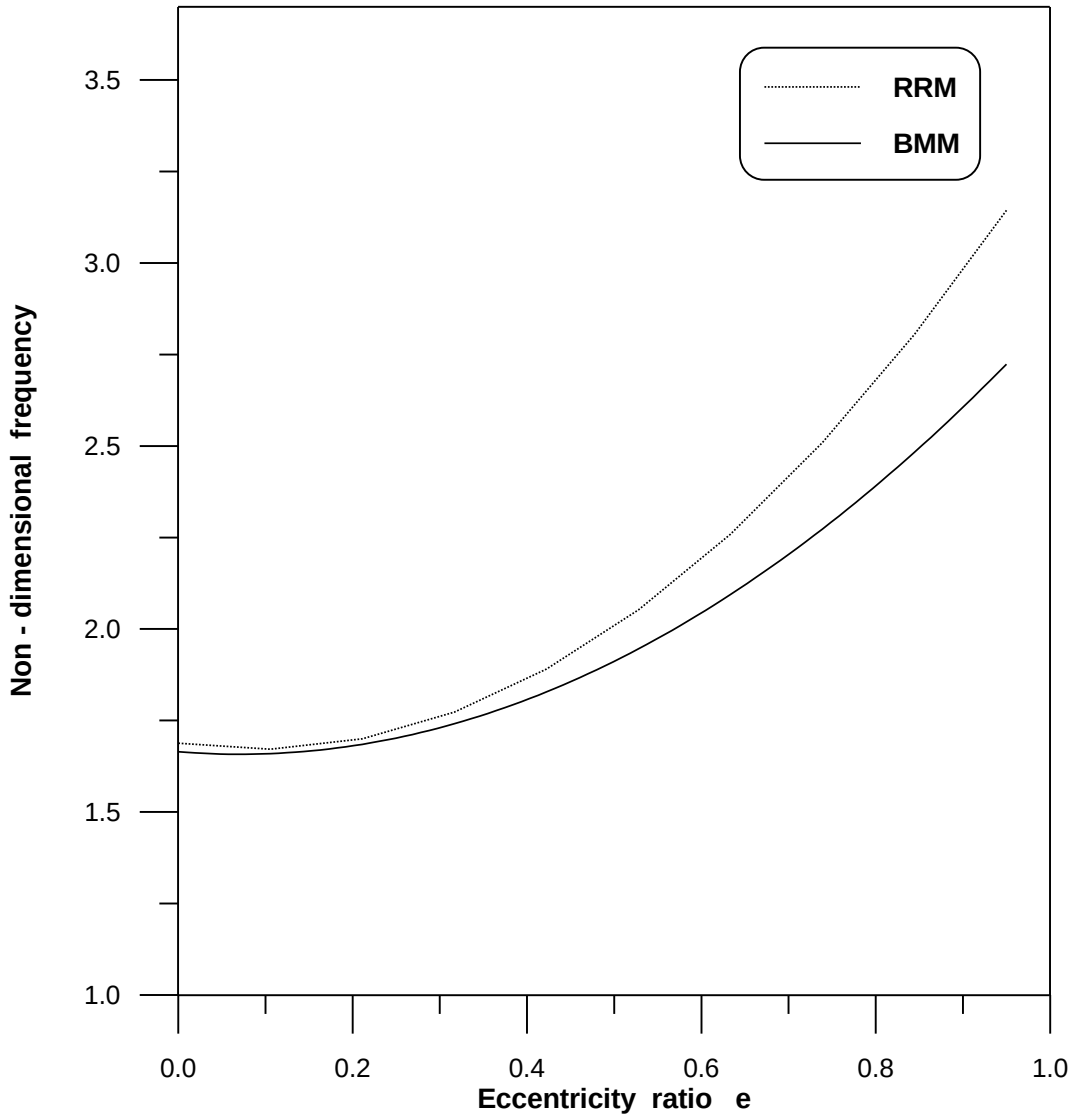

Fig. (4 – 17) Effect of eccentricity on the first membrane modes

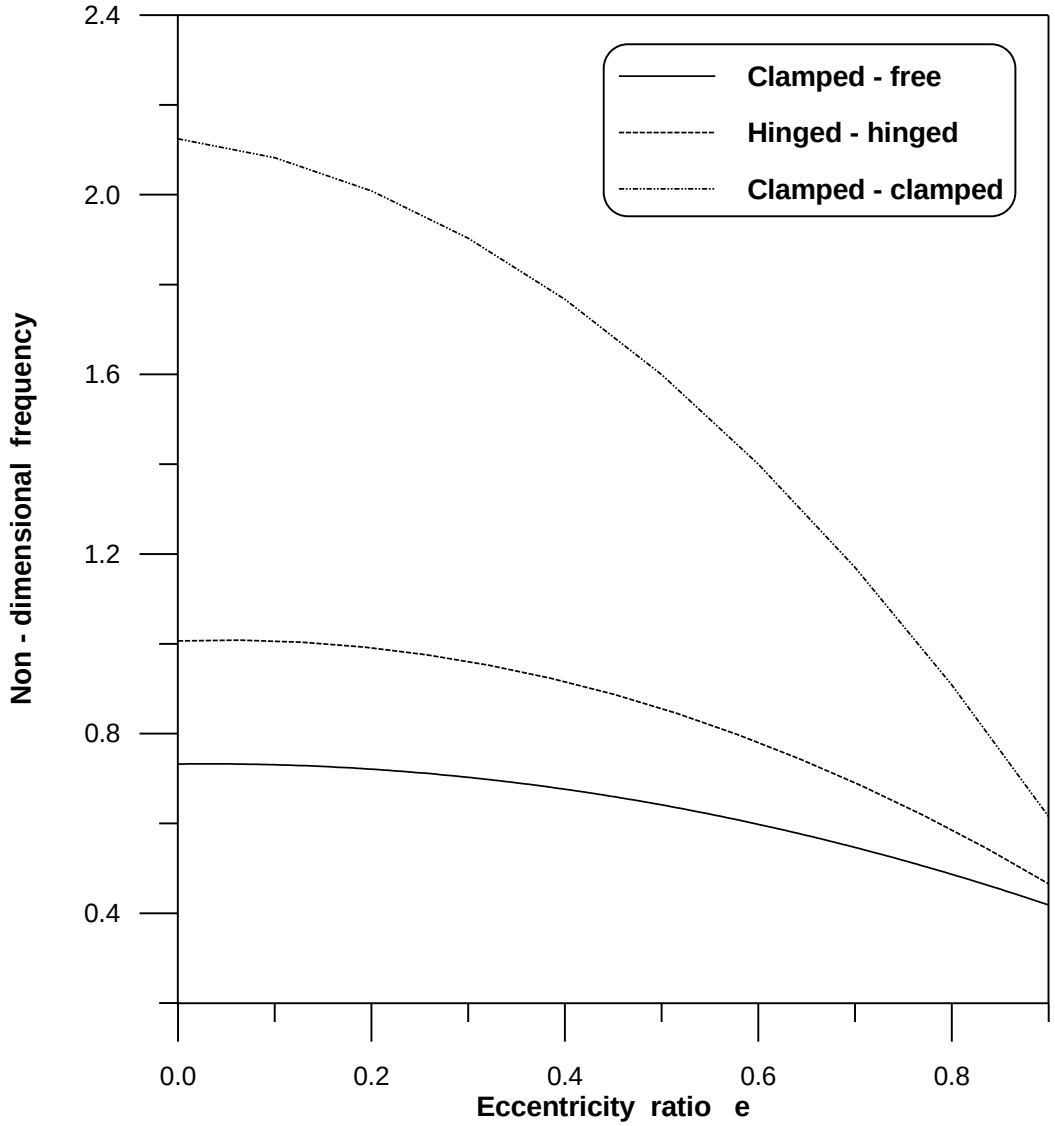

Fig. (4 – 18) Effect of eccentricity on the first bending mode for various boundary conditions

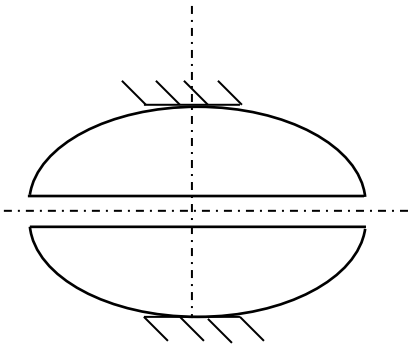

Clamped – clamped

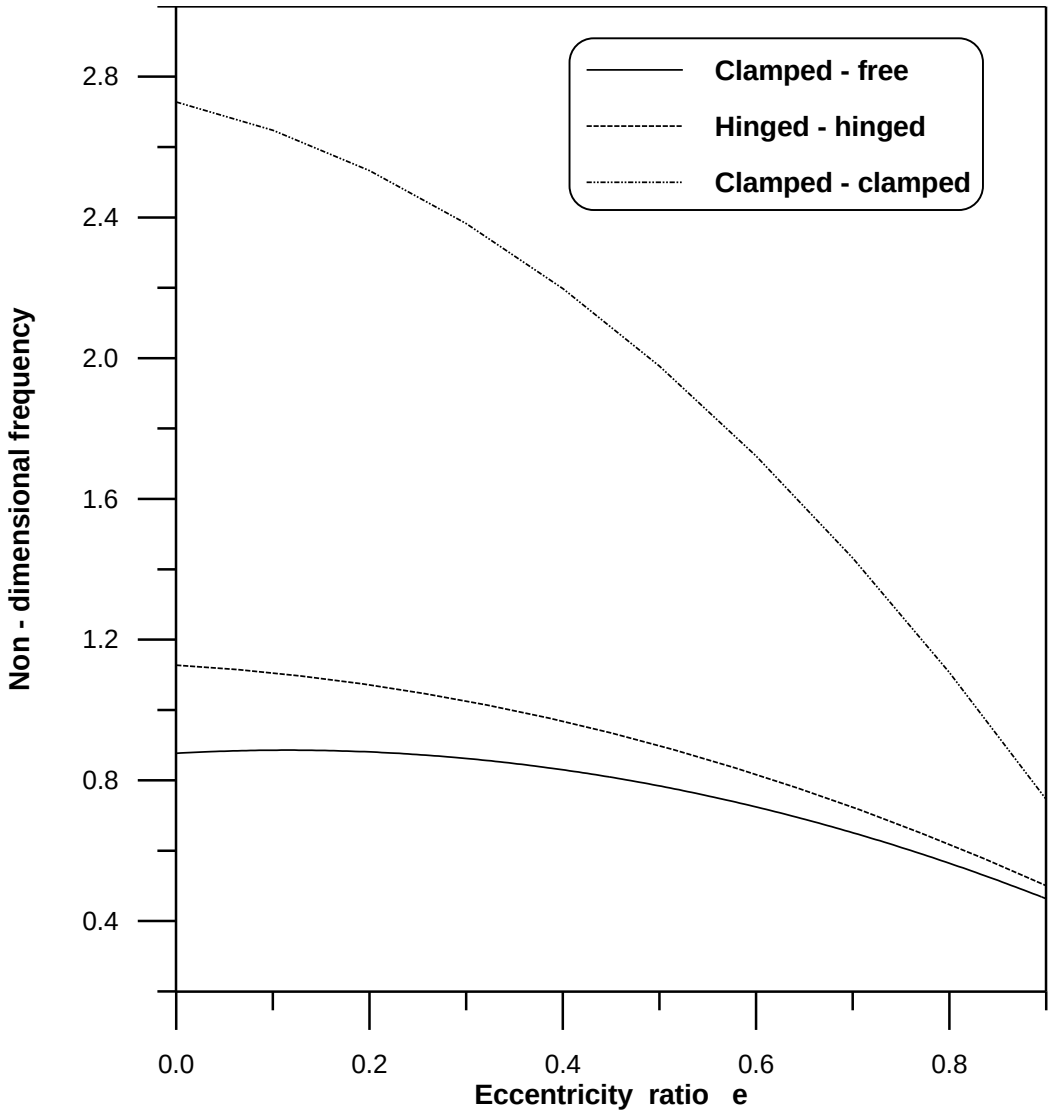

Fig. (4 – 19) Effect of eccentricity on the second bending mode for various boundary conditions

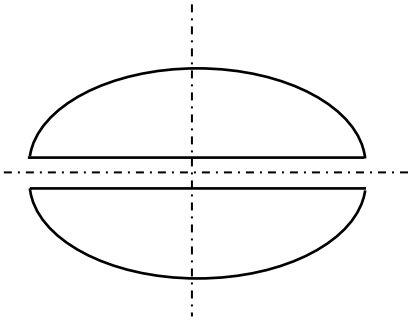

Clamped – free

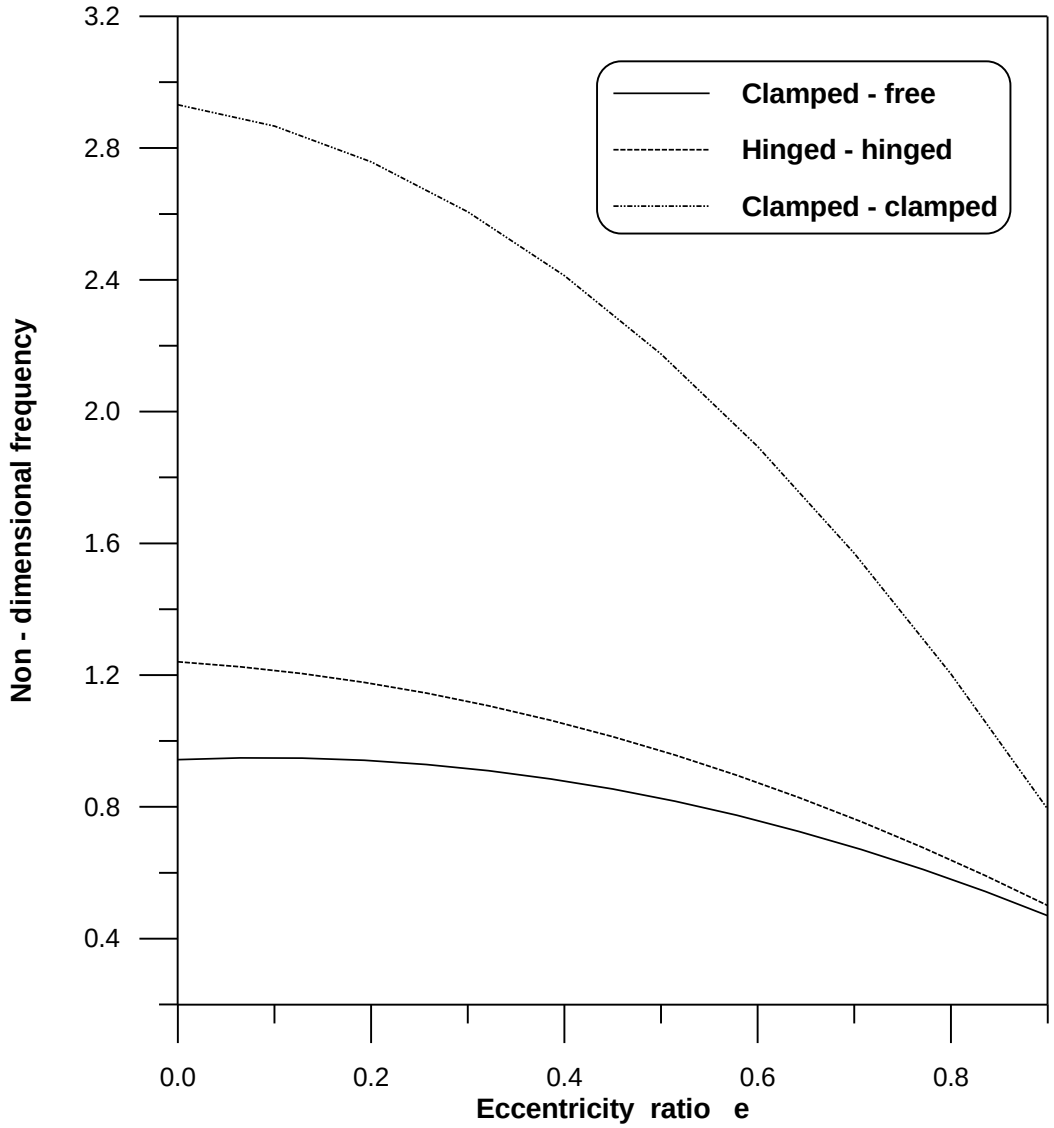

Fig. (4 – 20) Effect of eccentricity on the third bending mode for various boundary conditions

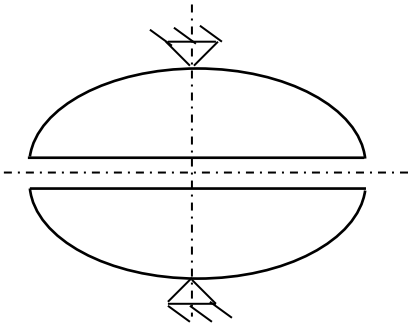

Hinged – hinged

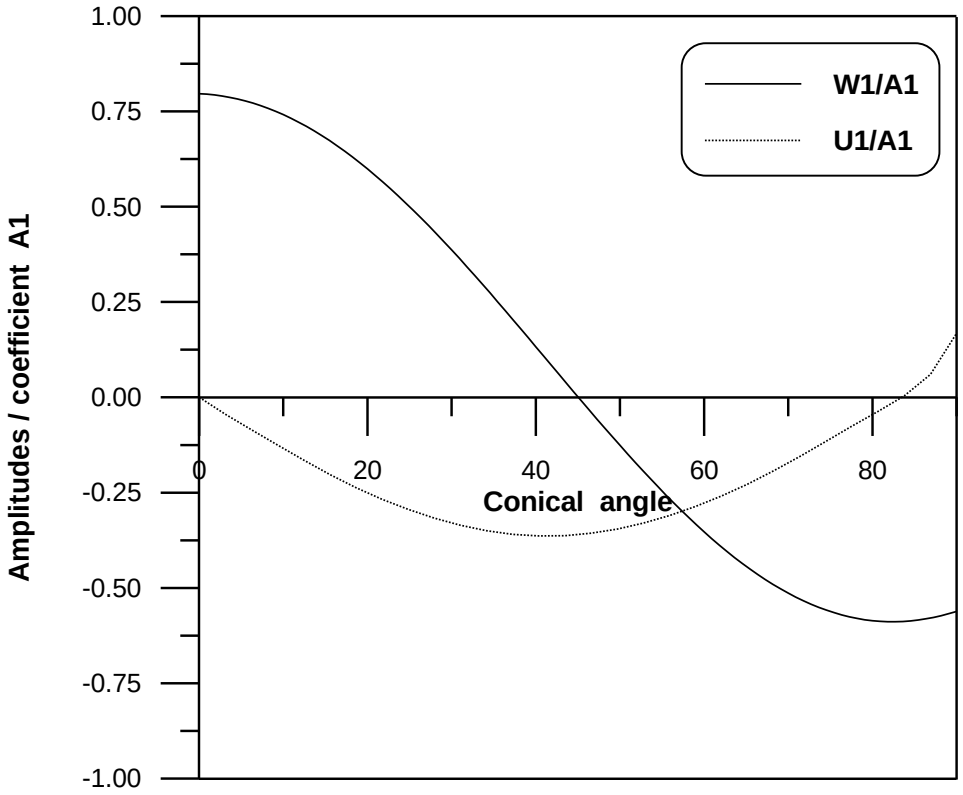

Fig. (4 – 21) Normalized mode shape associated with the first natural frequency of non–shallow spheroidal shell (e = 0.683) obtained by BMM

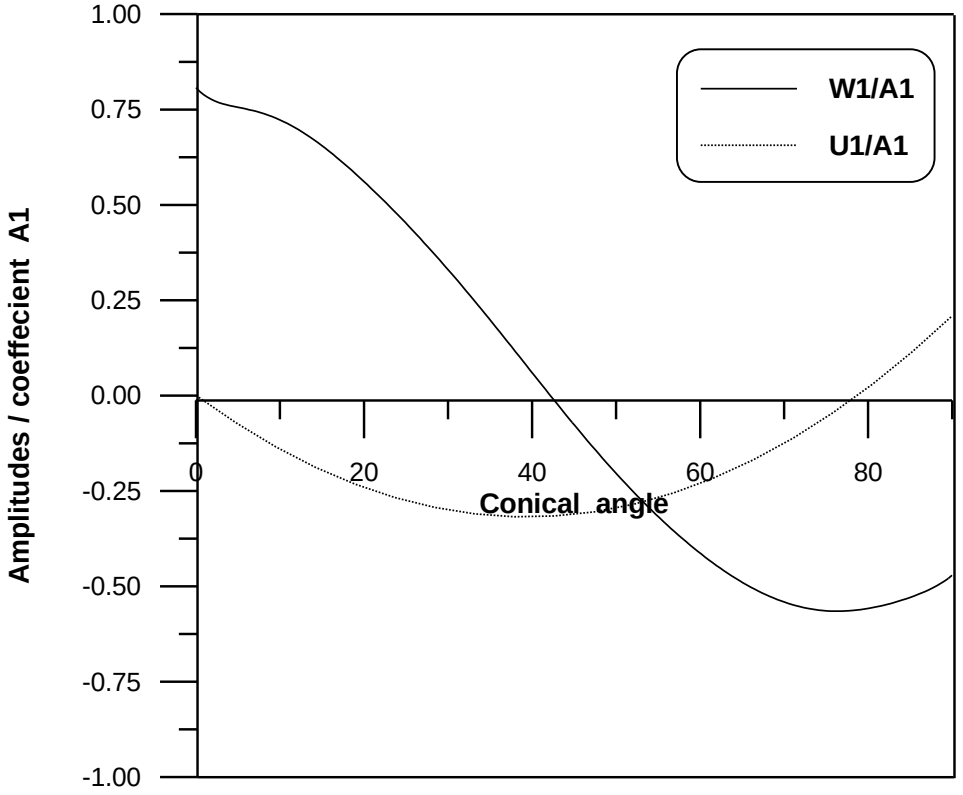

Fig. (4 – 22) Normalized mode shape associated with the first natural frequency of non–shallow spheroidal shell (e = 0.683) obtained by RRM

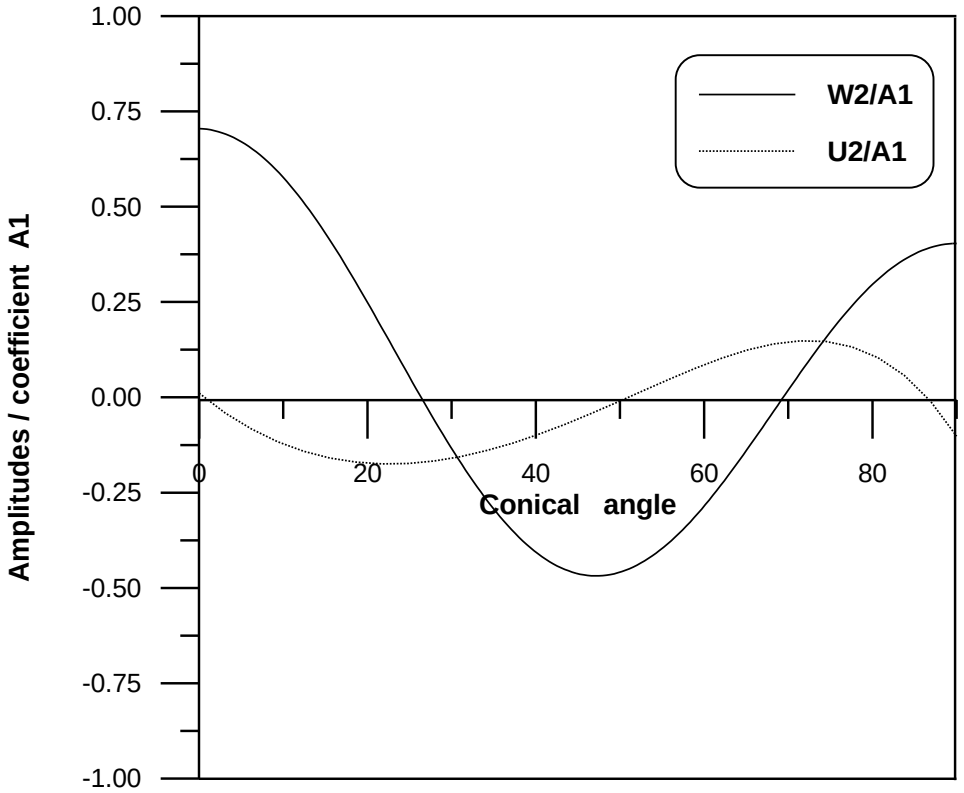

Fig. (4 – 23) Normalized mode shape associated with the second natural frequency of non–shallow spheroidal shell (e = 0.683) obtained by BMM

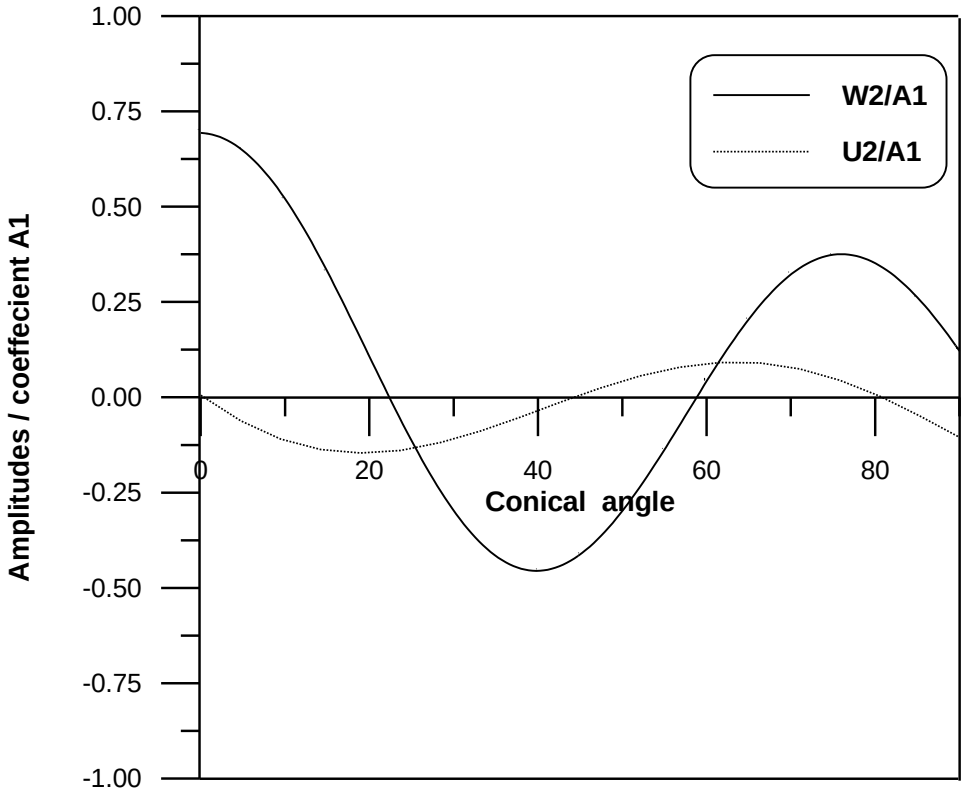

Fig. (4 – 24) Normalized mode shape associated with the second natural frequency of non–shallow spheroidal shell (e = 0.683) obtained by RRM

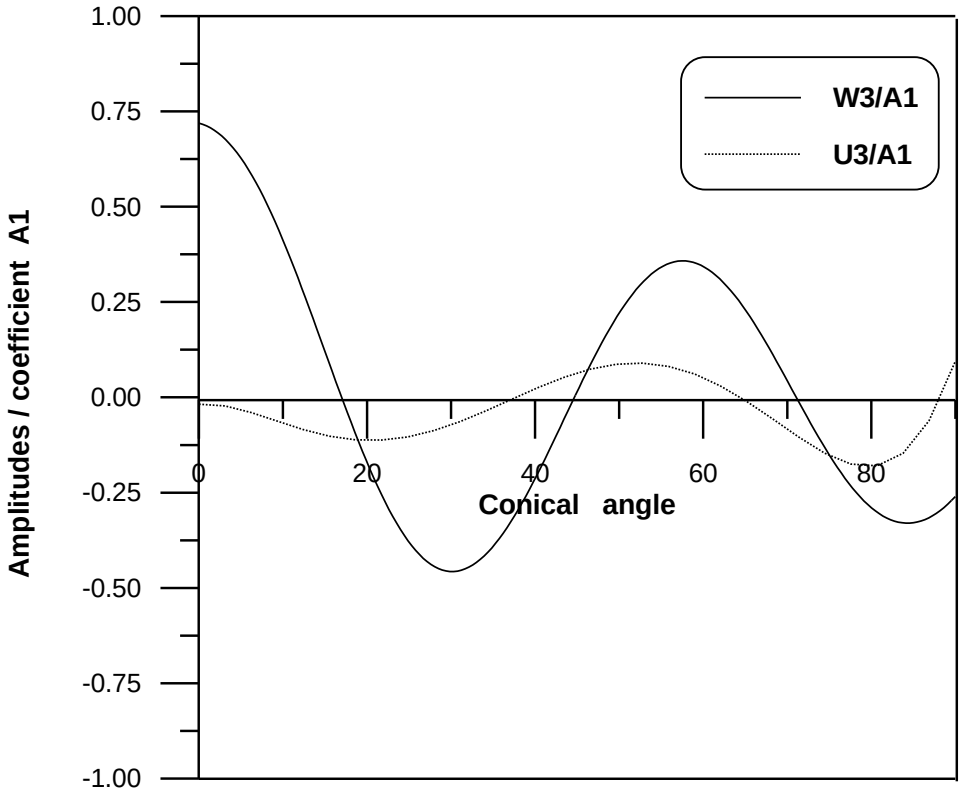

Fig. (4 – 25) Normalized mode shape associated with the third natural frequency of non–shallow spheroidal shell (e = 0.683) obtained by BMM

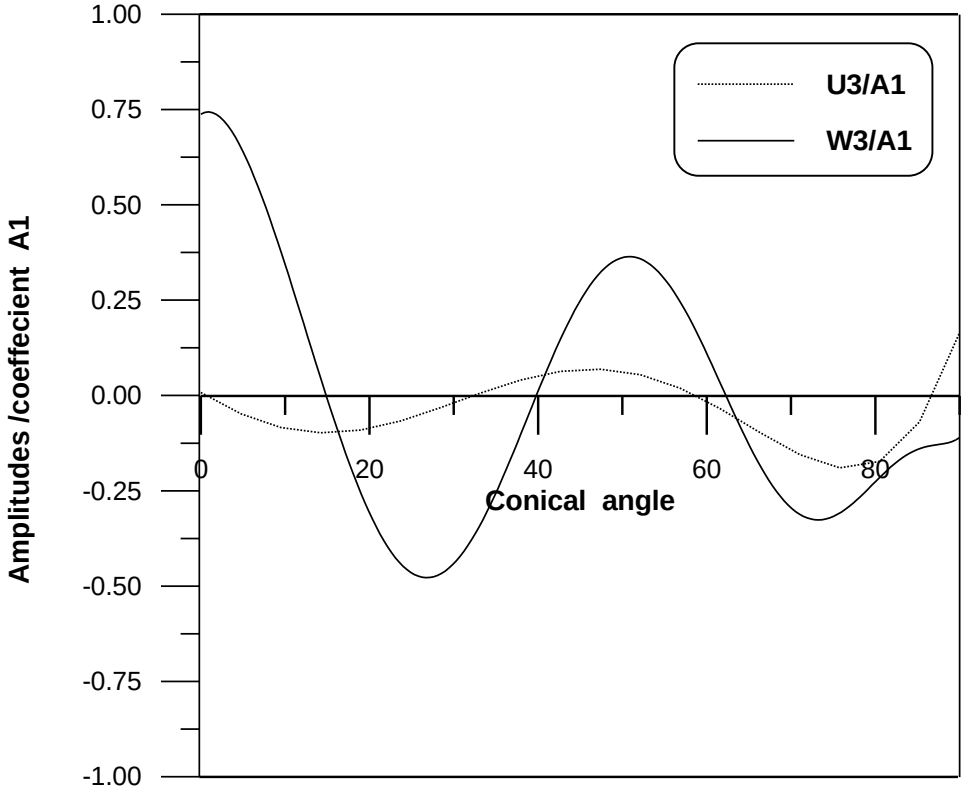

Fig. (4 – 26) Normalized mode shape associated with the third natural frequency of non–shallow spheroidal shell (e = 0.683) obtained by RRM

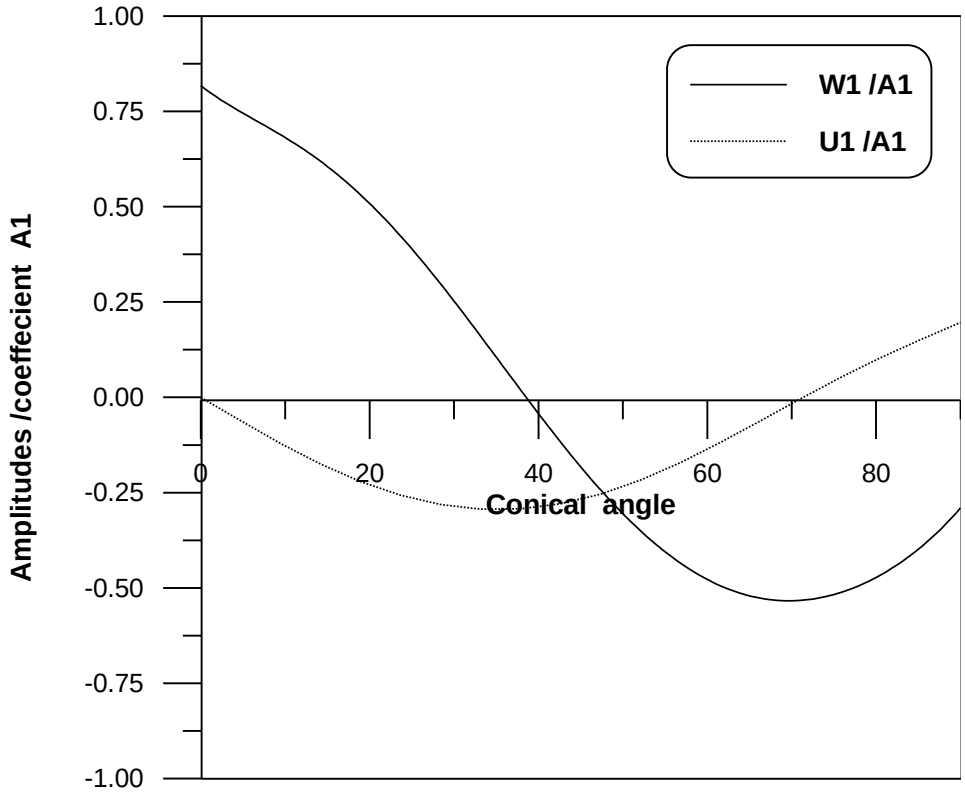

Fig. (4 – 27) Normalized mode shape associated with the first natural frequency of shallow spheroidal shell (e = 0.921) obtained by BMM

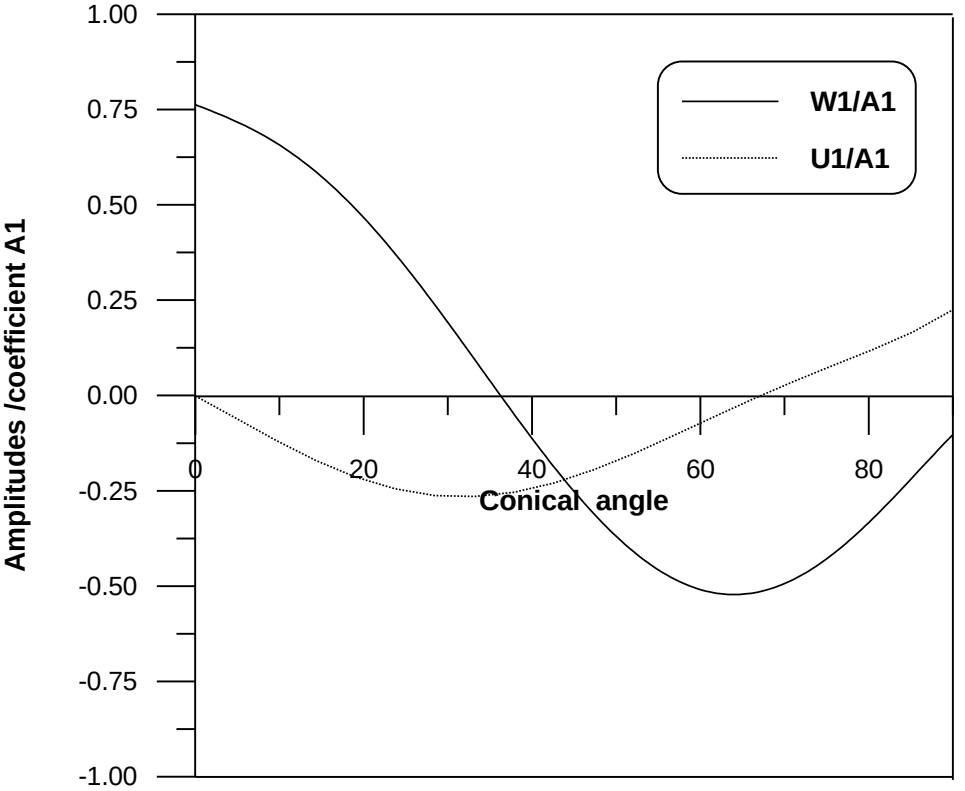

Fig. (4 – 28) Normalized mode shape associated with the first natural frequency of shallow spheroidal shell (e = 0.921) obtained by RRM

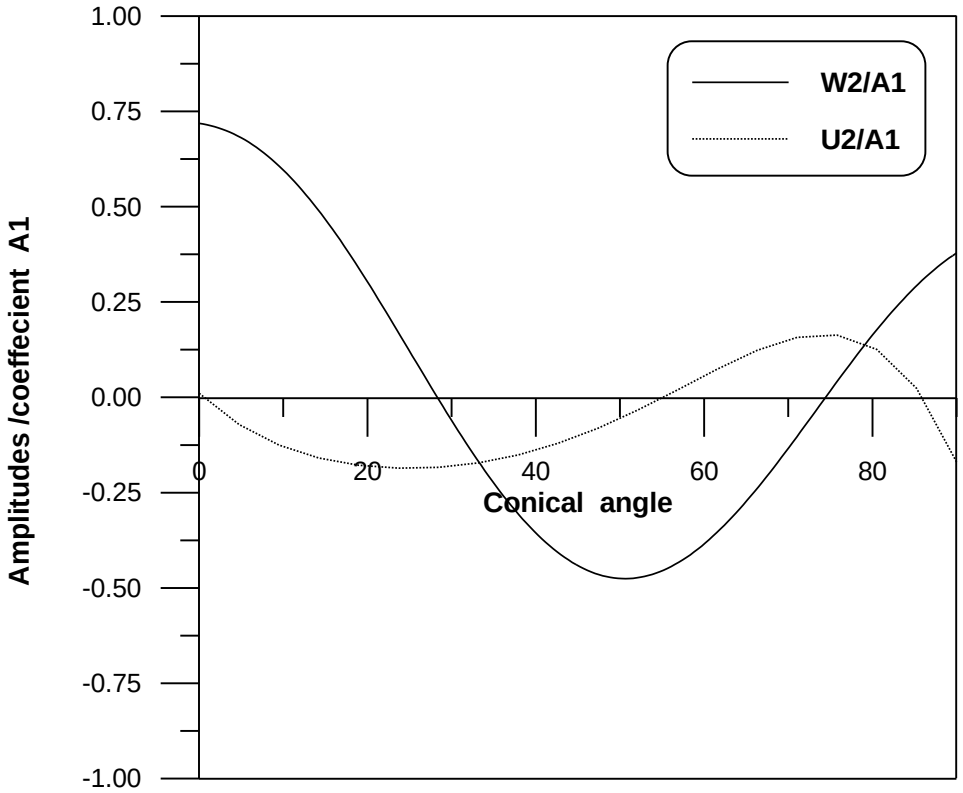

Fig. (4 – 29) Normalized mode shape associated with the second natural frequency of shallow spheroidal shell (e = 0.921) obtained by BMM

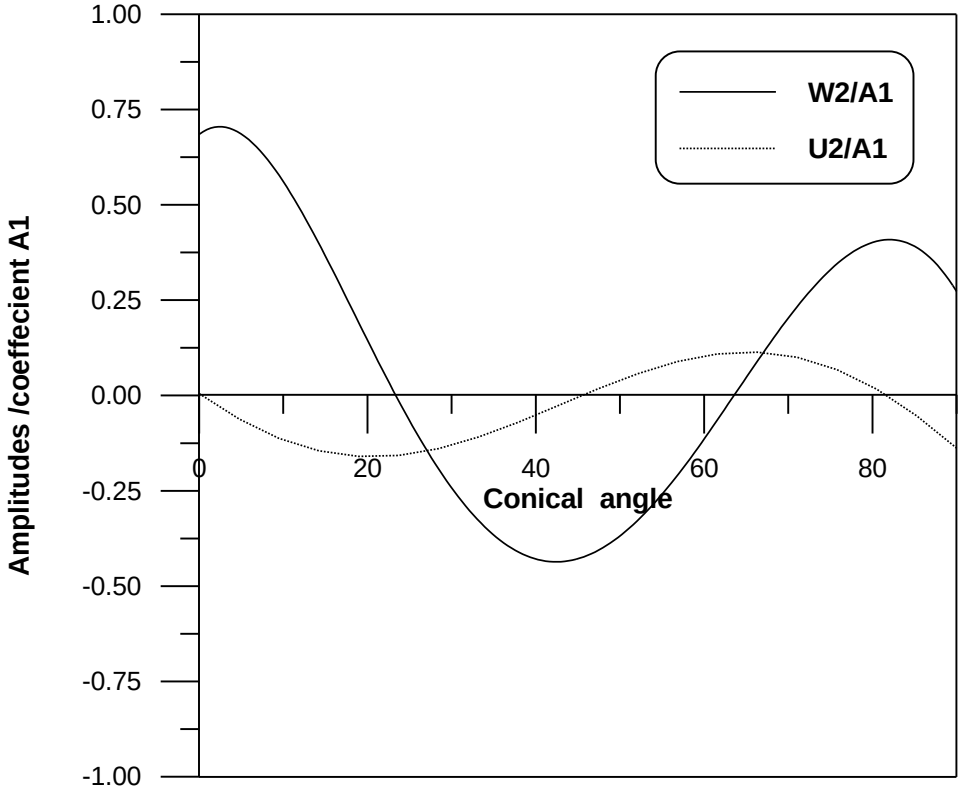

Fig. (4 – 30) Normalized mode shape associated with the second natural frequency of shallow spheroidal shell (e = 0.921) obtained by RRM

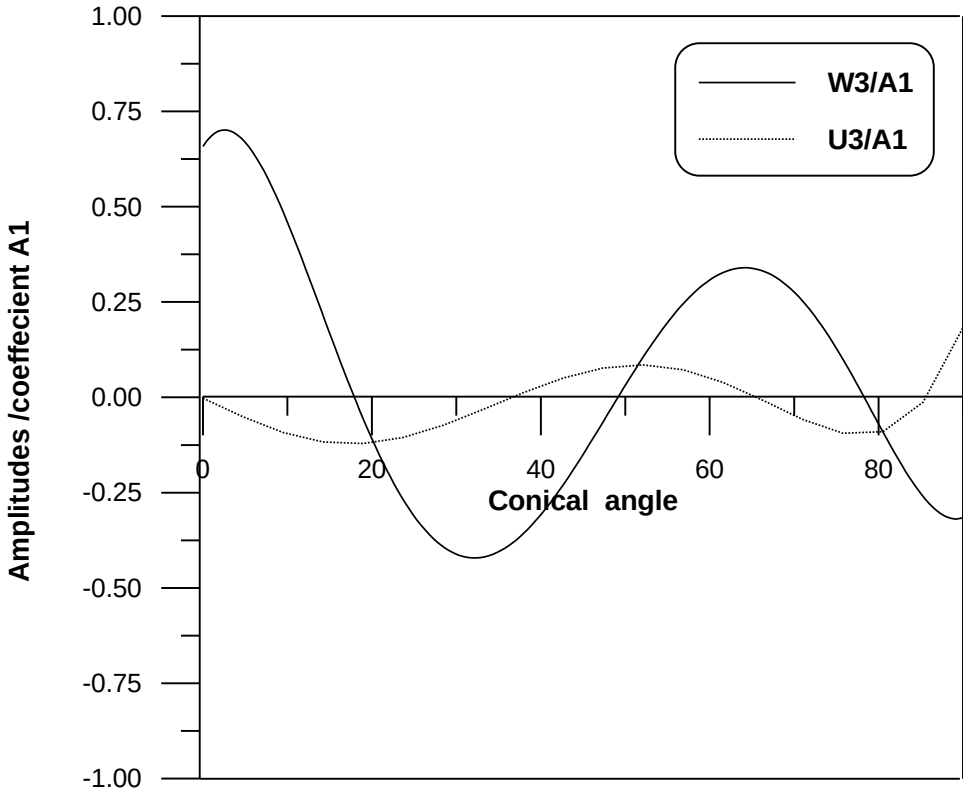

Fig. (4 – 31) Normalized mode shape associated with the third natural frequency of shallow spheroidal shell (e = 0.921) obtained by BMM

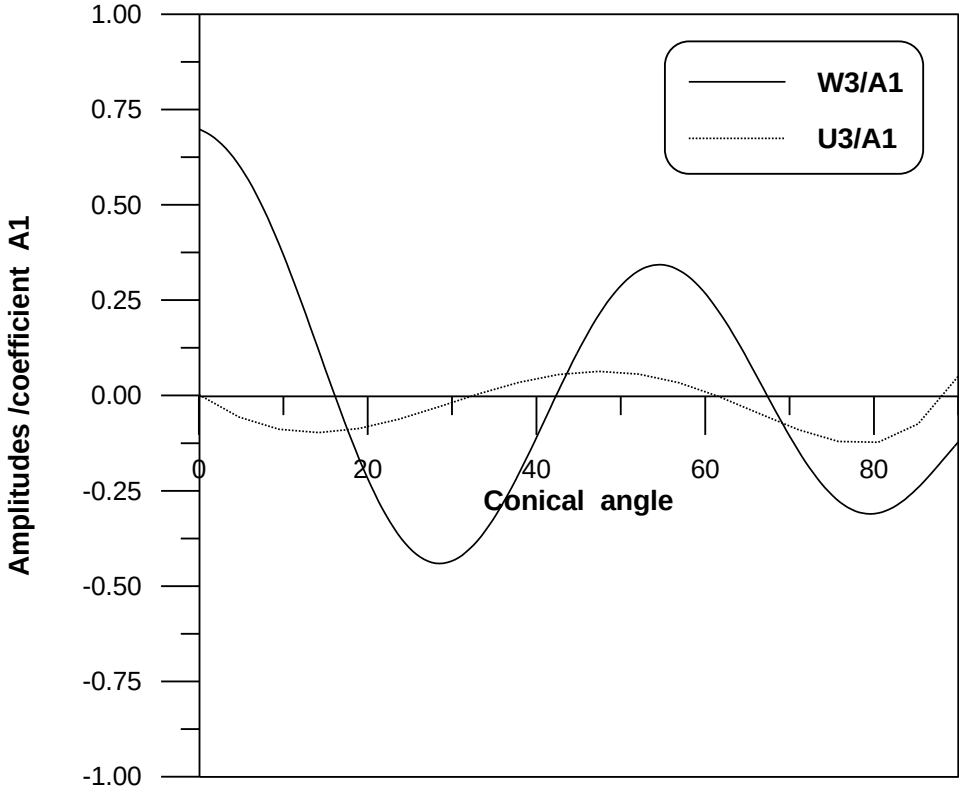

Fig. (4 – 32) Normalized mode shape associated with the third natural frequency of shallow spheroidal shell (e = 0.921) obtained by RRM

CERTIFICATION

We certify that this thesis entitled **"Theoretical Investigation of the Axisymmetric Free Vibration of an Isotropic Thin Oblate Spheroid Shells"** was prepared by **"Nawal Hussein Abdul – Ameer"** under our supervision at **Babylon University**, College of Engineering in partial fulfillment of the requirements for the degree of Master of Science in Mechanical Engineering.

Signature:

Name: Asst. Prof.

Dr. Ahmed A. Al – Rajihy

(Supervisor)

Date: / /2005

Signature:

Name: Asst. Prof.

Dr. Ala M. H. Al – Jesany

(Supervisor)

Date: / /2005

EXAMINING COMMITTEES CERTIFICATE

We certify that we have read this thesis, entitled « **Theoretical Investigation of the Axisymmetric Free Vibration of an Isotropic Thin Oblate Spheroid Shells » ,** and as examining committee, examined the student "**Nawal Hussein Abdul – Ameer"** in its contents and that in our opinion it meets the standard of thesis for the degree of Master of Science in Mechanical Engineering.

Signature:

Name: Asst. Prof.

Dr. Ahmed A. Al – Rajihy

(Supervisor)

Date: / /2005

Signature:

Name: Asst. Prof.

Dr. Ala M. H. Al – Jesany

(Supervisor)

Date: / /2005

Signature:

Name: Asst. Prof.

Dr. Haitham H. Al – Daami

(Member)

Date: / /2005

Signature:

Name: Teacher

Dr. Bassim A. Al - Mousawi

(Member)

Date: / /2005

Name: Asst. Prof.

Dr. Baha I. Kadhim

(Chairman)

Date: / /2005

Approval of the Mechanical Engineering Department

Head of the Mechanical Engineering

Signature:

Name: **Asst. Prof. Dr. Ala M. H. Al – Jesany**

Date: / /2005

Approval of the College Engineering

Dean of the College of Engineering

Signature:

Name: **Asst. Prof. Dr. Haroun A.K. Shaheed**

Date: / /2005

Table (4 – 1) : Natural frequencies of the first three axisymmetric modes of thin sphere,

Hz.

r = 0.1143 m , h = 0.0057 m , E = 207 Gpa , ρ = 7800 Kg/m^3 , υ = 0.3

								Differences with respect to DAS. ٪				
n	**m**	**DAS.[1]**	**SSM.[2]**	**FEM.[3]**	**R.M.[4]**	**RRM.[5]**	**BMM.[6]**	**δ_1٪**	**δ_2٪**	**δ_3٪**	**δ_4٪**	**δ_5٪**
0	**2**	**5281**	**5291**	**5383**	**5335**	**5315**	**5286**	**- 0.2**	**≈ 0.0**	**-1.0**	**-0.6**	**≈ 0.0**
	3	**6321**	**6330**	**6319**	**6510**	**6513**	**6319**	**- 0.1**	**≈ 0.0**	**-3.0**	**-3.0**	**≈ 0.0**
	4	**6883**	**6894**	**6875**	**--------**	**6950**	**6883**	**- 0.1**	**0.1**	**-----**	**-1.0**	**≈ 0.0**

(1) Direct Analytical Solution [31]

(2) State Space Method [31]

(3) Finite Element Method [31]

(4) Rayleigh Method [33]

(5) Rayleigh – Ritz Method [*present work*]

(6) Boundary Conditions Matching Method [*present work*]

δ_1 ٪ = (DAS – SSM) / DAS * 100

δ_2 ٪ = (DAS – FEM) / DAS * 100

δ_3 ٪ = (DAS – R M) / DAS * 100

δ_4 ٪ = (DAS – RRM) / DAS * 100

δ_5 ٪ = (DAS – BMM) / DAS * 100

Table (4 – 2) : Specifications of the tested models

Parameter	Symbol	Value	Units
Major semi axis	a	0.185	m
Minor semi axis	b	0.135	m
Eccentricity	e	0.683	N.D
Normal thickness	h	$1.5 * 10^{-3}$	m
Poisson ratio	υ	0.3	N.D
Modulus of elasticity	E	68	Gpa
Density	ρ	2720	kg / m^3

Shell model (1)

Parameter	Symbol	Value	Units
Major semi axis	a	0.18	m
Minor semi axis	b	0.07	m
Eccentricity	e	0.921	N.D
Normal thickness	h	$1.5 * 10^{-3}$	m
Poisson ratio	υ	0.3	N.D
Modulus of elasticity	E	68	Gpa
Density	ρ	2720	kg / m^3

Shell model (2)

Table (4 – 3) : Theoretical and experimental natural Frequencies for shell model 1 (e = 0.683)
Hz.

	Theoretical			Expt. [33]	Differences with respect to Expt. ٪		
	BMM	**RRM**	**RM[33]**		δ_1٪	δ_2٪	δ_3٪
ω_1	**2430**	**2517**	**3110**	**2400**	**-1.25**	**-5.0**	**-29.0**
ω_2	**2900**	**2973**	**3378**	**2600**	**-11.5**	**-14.0**	**-30.0**
ω_3	**3055**	**3086**	**.....**	**2900**	**-5.0**	**-6.0**	**.....**
ω_4	**3141**	**3180**	**.....**	**3100**	**-1.3**	**-2.6**	**.....**

δ_1 ٪ = (Expt. – BMM) / Expt. * 100

δ_2 ٪ = (Expt. – RRM) / Expt. * 100

δ_3 ٪ = (Expt. – R M) / Expt. * 100

Table (4 – 4) : Theoretical and experimental natural Frequencies for shell model 2 (e = 0.921)
Hz.

	Theoretical			**Expt. [33]**	**Differences with respect to Expt. ٪**		
	BMM	**RRM**	**RM[33]**		**δ_1٪**	**δ_2٪**	**δ_3٪**
ω_1	**1620**	**1673**	**4245**	**1557**	**-4.0**	**-7.5**	**-173.0**
ω_2	**1723**	**1803**	**3243**	**1950**	**11.5**	**7.5**	**-66.0**
ω_3	**1742**	**1813**	**.....**	**2100**	**17.0**	**13.0**	**.....**

δ_1 ٪ = (Expt. – BMM) / Expt. * 100

δ_2 ٪ = (Expt. – RRM) / Expt. * 100

δ_3 ٪ = (Expt. – R M) / Expt. * 100

CHAPTER ONE

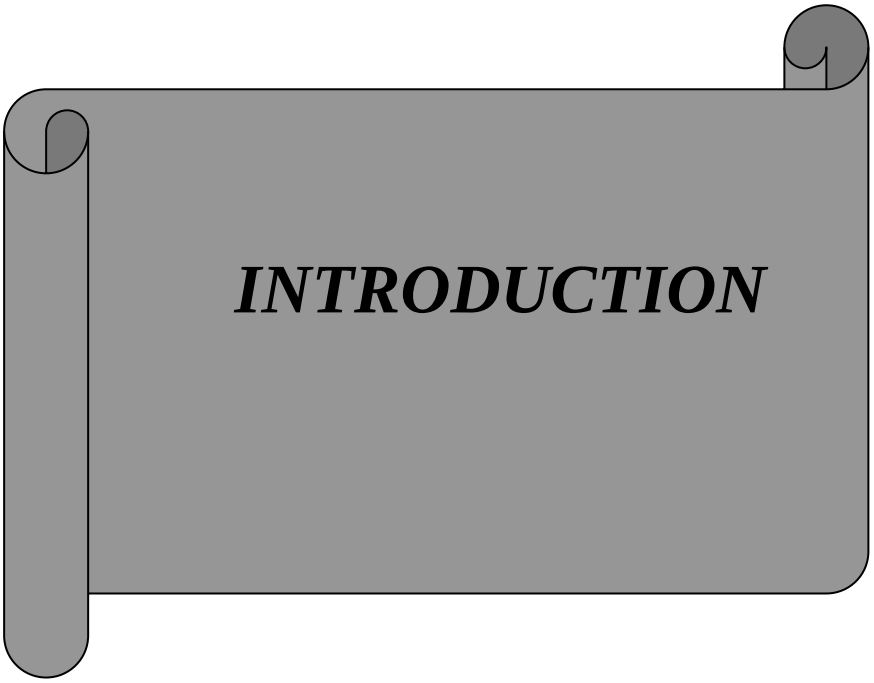

CHAPTER TWO

CHAPTER THREE

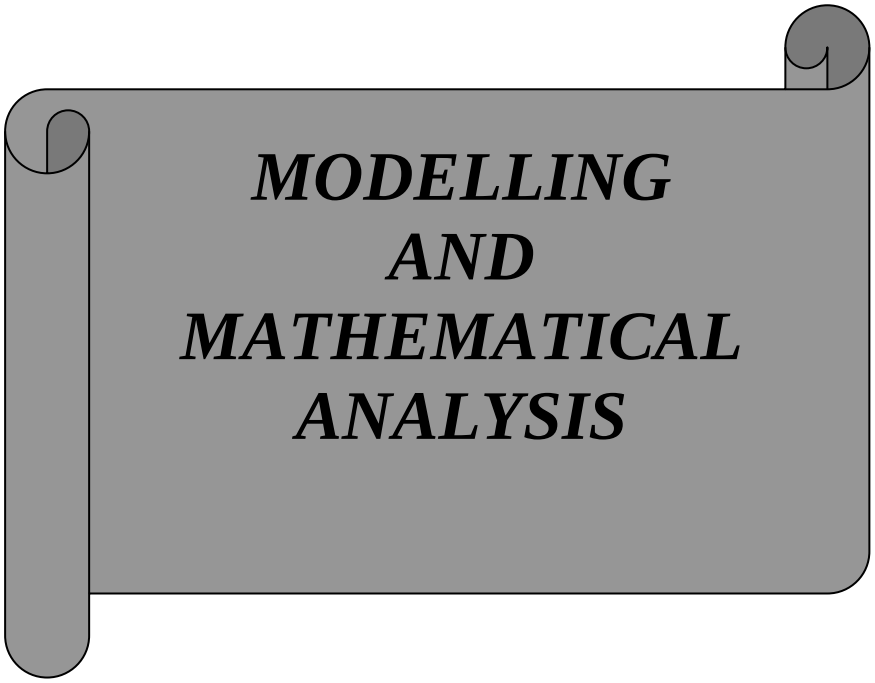

CHAPTER FOUR

CHAPTER FIVE

LIST OF REFERENCES

CHAPTER TWO

LITERATURE REVIEW

2 . 1 Introduction :

While the literature on free and forced vibrations of spherical shells is almost endless, only few papers are published in open literature (according to the author's knowledge) dealing with the free vibration of ellipsoidal shells, and numerical results are lacking. Due to the complexity of the problem it appears that a closed form analytical solution does not exist. Several investigators, using a variety of mathematical techniques, have obtained approximate solutions for the natural frequencies of axisymmetric vibrations of thin prolate spheroidal shells. They following review of Literature is classified into five groups. The subsequence of the authors as arranged according to the historical order.

2 . 2 Spherical Shells :

Sitzungsber [1] numerical solutions of the frequency equations of the complete free – vibration problem began to appear in this paper for spherical shells. With the appearance of these publications, it was recognized that the approximate treatment of shell vibrations, by considering either only the extensional or only the flexural strain energy, could provide useful information in some special cases, but that it covered only a small part of the possible vibration modes.

Wilfred E. Baker [7] presented a detailed study of the theory of free, axisymmetric vibration of thin elastic spherical shell and demonstrate by experiment that the normal modes of vibration predicted do exist. The theory predicts the existence of two infinite sets of normal modes, one of which is bounded in frequency and the other unbounded. The first four modes in each set are identified by experiments on a small steel shell. The author determined the vibration modes of a thin spherical shell, and showed by experiment that these modes physically exist.

Kalnins [11] was concerned with the vibration analysis of spherical shells, closed at one pole and open at the other, by means of the linear classical bending theory of shells. Frequency equations are derived in terms of Legendre function with complex indices, and for axisymmetric vibration the natural frequencies and mode shapes are deduced for opining angles ranging from a shallow to a closed spherical shell. It was found that for all opening angles the frequency spectrum consist of two coupled infinite sets of modes that can be labeled as bending (or flexural) and membrane modes. It was also found that the membrane modes are practically independent of thickness, whereas the bending modes vary with the thickness.

According to the improved theory of shell, **Kallins and Wilkinson [15]** included the effects of transverse shear and rotary inertia. The natural frequencies of closed spherical shell may be obtained from their analysis. It was shown that the five branches appear in the frequency spectrum, whereas only three are known to be predicted by the classical bending theory of shells where govern the torsionless modes while the other two govern the torsional modes.

A series solution for the response of an empty submerged spherical shell excited by a plane step – exponential wave was first presented by **Huang H. et al. [21].** He concluded that the response obtained by

summing the first eight modes (N = 7) is taken as the measured response. This study represents numerical results for steel spherical shells submerged in water that are either empty or filled with water.

Hayek and Dimaggio [22] added perturbation terms to the solution for a spherical shell to determine approximate solutions for the resonance frequencies for submerged prolate spheroidal shell. Numerical results for the first flexural resonance mode were presented for steel shell in water.

Huang H., Lu and Wang Y.F. [23] extended the work done by [21] to include the response due to a spherical step – exponential incident wave.

Concerning related topics, **Irie T., Yamada G., and Marumoto Y., [30]** analyzed the free vibration of an elastically or rigidly point supported spherical shell. The deflection displacements of the shell were written in a series of the Legendre functions and the trigonometric functions. The dynamical energies of the shell were evaluated and the frequency equation was derived by Ritz Method. The natural frequencies and mode shapes were calculated numerically for a closed spherical shell supported at equi – spaced four points located along a parallel of latitude.

Zhang P. and Geer T. L. [35] employed convergence– enhancement techniques to obtain series solutions for the response of a fluid – filled or empty submerged spherical shell excited by a plane step–wave; these techniques are partial series closure at early time. Partial series closure consists of separating the early – time response into a closed – form portion and a complementary mode-sum portion. The closed–form portion invokes the plane–wave approximation for the fluid–structure interaction and neglects stiffness effects in the shell.

Chang Y. C. and Demkowicz L. [37] studied the stability analysis of multilayered vibrating viscoelastic spheres, both in vacuo and in an acoustical fluid. The analysis is done by investigating the effect of viscoelastic damping on the (continuous) Ladyzenskaya – Babuska – Brezzi

(LBB) constants for the related boundary – value problems. The sphere is modeled using both 3–D viscoelasticity and the Kirchho – Love shell theory.

Michael, Sprague and Thomas [39] concluded that Fluid – Structure Interaction, Underwater Shock, Doubly – Asymptotic Approximations, Benchmark Solutions. The title problem is solved through extension of a method previously formulated for plane step-wave excitation, which employs generalized Fourier series augmented by partial closure of those series at early time. The extension encompasses both plane and spherical incident waves with step exponential pressure profiles. The effects of incident–wave curvature and profile decay rate on response behavior are examined. A method previously developed for assessing the discrepancy between calculated and measured response histories is employed to evaluate the convergence of the truncated series solutions. Also studied is the performance of doubly – asymptotic approximations. Finally, the documented computer program that produced the numerical results appearing in this paper.

2 . 3 Prolate Spheroidal Shells :

Dimaggio and Silbeger [5] obtained solutions of differential equation for the mode shapes for the torsional vibration of a prolate spheroid shell by the application of Hamilton's principle was found by single prolate spheroid angle function of the first kind, and the transcendental frequency equation is readily solved with the aid of tabular eigenvalues. Numerical and graphical non–dimensional results are presented for the first eight modes. The same authors in another effort **[6]** used the membrane shell theory, in which the effects of bending resistance were ignored, and the Rayleigh – Ritz variation method was used to obtain approximate solutions for the non – torsional mode shape and natural frequencies.

Shiraishi and Dimaggio [9] obtained perturbation solutions for the modes and frequencies of extensional axisymmetric vibrations of thin elastic prolate spheroidal shells with displacements in the meridian planes. These solutions, which are in the form of infinite series in powers of the square of the eccentricity having as their first term the solution for a spherical shell, converge rapidly for small rations of major to minor axis. The smaller the eccentricity making these series the more convergent.

Nemergut and Brand [13] determined the lower axisymmetric modes of prolate spheroid shell with five values of eccentricity. Their work was distinguished by applying their solution to constant thickness membrane shell by means of integrating numerically the equations of motion while all the others such as [5, 6, 9] have considered prolate spheroid shells with varying thickness. It is found that the frequency associated with higher modes are strongly dependent on the eccentricity.

Dimaggio and Rand [16] applied the finite differences method to obtain approximate solutions for the determination of modes and frequencies for the same problem given in [6 , 9] for two of geometry of middle surface of shell. The first is of constant length of major axis and varying ratio of major axis to minor axis by changing the length of minor axis, the second of constant length of minor axis and varying ratio of major axis to minor axis by changing the length of major axis.

Yen and Dimaggio [18] extended the work of reference [16] to include the influence of fluid loading and an axisymmetric harmonic forcing function. A finite difference method was applied to obtain approximate solutions for radial displacement of the shell surface and the pressure in the fluid both at the shell surface and in the far field. For different frequencies of the harmonic forcing function, numerical results were given for a shell with an eccentricity of 0.986.

Fluid filled prolate spheroid shells were further studied by **Rand and Dimaggio [19]** where a numerical scheme for the problem was developed and extensive numerical results in the form of frequency spectra and mode shapes were displayed.

Bedrosian and Dimaggio [24] used techniques similar to those used by Yen and Dimaggio [18], to obtain the response of a prolate spheroidal shell to transient, uniform forcing function. Numerical results for the radial response were given for steel shell with an eccentricity of 0.986 that was submerged in sea water.

Berger B. S. [26] used Sanders, shell theory to treat a fluid-loaded prolate spheroidal shell of constant thickness subjected to an arbitrary dynamic loading. The infinite region outside the shell was transformed into a finite region before applying a finite difference method to obtain approximate solutions. Numerical results were presented for the acoustic pressure in the fluid at the shell surface and the radial displacement of the shell in response to the application of a spatially uniform ramp – shaped transient forcing function.

In Berger's work the effects of bending resistance were included. and the effects of transverse shear and rotary inertia are not included.

Burtough C. B. and Magrab E. B. [28] derived the displacement equilibrium equations for the non – symmetric dynamic motion of a prolate spheroid shell of constant thickness. They included the effect of bending résistance, transverse shear and rotary inertia and a generalized normal loading applied to the middle shell surface. Galerkin's Method was then used to obtain the natural frequencies for the axisymmetric non – torsional vibrations of the shell for various combinations of physical and geometric parameters.

2 . 4 Oblate Spheroidal Shells :

As for the oblate spheroid shells, **Penzes and Burgin [14]** were the first to solve the problem of the free vibrations of thin isotropic oblate spheroid shells by Galerkin's Method. Membrane theory and harmonic axisymmetric motion were assumed in order to derive the differential equations of motion. It was shown that Galerkin's Method of solution for the oblate spheroid shell yields the exact solution for the closed spherical shell as the eccentricity of the oblate spheroid shell approaches zero. The characteristic mode shapes for spherical shell are described by associated Legendre functions.

Penzes L. [20] extended the solution of reference [14] to include thin orthotropic oblate spheroid shells. He used the same assumptions and equations of motion in [14] except that the principal direction of the elastic compliances was assumed to be a long parallel of latitude and a long meridian. Both of the spheroid and spherical shells were investigated with various orthotropic constants. However, the isotropic case was taken as the limit of the orthotropic problem, and applying the former case to the orthotropic theory yielded the previously published results of the isotropic oblate spheroid shell. The discussion was restricted to the axially symmetric torsionless motion of shells, and entirely neglects the calculations concerning torsion motion. The stiffness was constant through the thickness of the shell.

Fawaz [33] in M.Sc. thesis the Rayliegh variation method was used to obtain natural frequencies and mode shape of axisymmetric vibrations of thin elastic oblate spheroidal shells and presents the results of both theoretical and experimental investigations of the shell. The experimental investigation involves constructing two closed form oblate spheroidal shells with two different eccentricities, and their vibration characteristics

are investigated. Showed that the Rayliegh's Method was found to be suitable only for oblate shells with eccentricities less than 0.6.

2 . 5 Shallow Spherical Shells :

The treatment of transverse vibrations of a shallow spherical shell has been previously given by **Reissner [2]** and by **Johnson and Reissner [3]**, that for transverse vibration the longitudinal inertia terms can be neglected. Starting with this assumption, Reissnere was able to formulate the problem in a simpler way and obtained exact solutions. Analysis for the coupled longitudinal (torsionless) and transverse with axial symmetry was given by **Kalnins A. and Naghdi P. M. [4]**.

The same problem given in [2 , 3] was reconsidered by **Kalnins [10]** with all the inertia terms included. The complete frequency equation was solved and found an additional set of modes that was not considered by Reissner. After the examination of their mode shapes, the additional modes were shown to have tangential displacements larger than the transverse displacement. The results of this paper show that the complete frequency spectrum of a shallow spherical shell consists of two infinite sets of modes with separate increasing node counts in the displacement. They show also that when curvature is diminished indefinitely these two sets of modes reduce to the purely longitudinal and purely transverse modes of a circular plate. The longitudinal modes contain mostly extensional strain energy, while the transverse modes contain mostly flexural strain energy.

Okazaki, A., Urata, Y. and Tatemichi, A. [34] damping properties of three-layered shallow spherical shells have been studied in this paper. Expressing the in–plane displacements in terms of auxiliary functions, the general solution of the equations of motion for non – axisymmetric modes

was given in terms of Bessel's functions. Different shell and plate theories can be used to analyze the sandwich structures.

Antoine Chaign et. al. [41] linear and nonlinear vibrations of shallow spherical shells with free edge are investigated experimentally and numerically and compared to previous studies on percussion instruments such as gongs. The preliminary bases of a suitable analytical model are given. The prime objective of the work is to take advantage of the specific geometry of perfectly isotropic and homogeneous spherical shells in order to isolate the influence of curvature from other possible causes of nonlinearities. Hence, combination resonances due to quadratic nonlinearities are especially studied, for an harmonic forcing of the shell. Identification of excited modes is achieved through systematic comparisons between spatial numerical results obtained from a finite element modeling, and spectral information derived from experiments.

2 . 6 Arbitrary Shells :

Kalnins [12] was concerned with a theoretical investigation of the free vibration of arbitrary shells of revolution by means of the classical bending theory of shell. A method is developed that is applicable to rotationally symmetric shells with meridional variations (including discontinuities) in Young's modulus, poison's ratio, radii of curvature, and thickness. The natural frequencies and the corresponding mode shapes of axisymmetric free vibration of rotationally symmetric shell can be obtained without any limitation on the length of the meridian of the shell. The results of free vibration of spherical and conical shell obtained earlier by means of the bending theory. In addition, parapoloidal shells and sphere–cone shell combination are considered, which have been previously analyzed by means of the inextentional theory of shell, and

natural frequencies and mode shapes predicted by the bending theory are given.

Tavakoli M. S. and Singh R. [31] used a substructure synthesis method based on state space mathematics for the eigen – solution of axisymmetric joined / hermitic thin shell structures. In the state space method (SSM), a system of eight coupled first order differential equations is solved for each shell substructure using the pade approximation for matrix exponentiation. The substructures are then joined by matching all of the displacement and force boundary variables. The authors applied the state space method to the cylindrical, conical, spherical, and toroidal shell. They compared their results to the results obtained previously for the same shells by applying the theoretical analysis and the finite element method. The state space method has strengths lies primarily in its ability to join substructures and match the boundary variables comprehensively.

Zhu F. [36] based upon general thin shell theory and the basic equations of fluid mechanics, the Rayleigh – Ritz Method for coupled fluid – structure free vibrations is developed for arbitrary tanks fully or partially filled inviscid, irrotational and compressible or incompressible fluid, by means of the generalized orthogonality relations of wet modes and the associated Rayleigh quotients.

Aleksandr Korjanik et al. [40] investigated the free damped vibrations of sandwich shells of revolution. As special cases the vibration analysis under consideration of damping of cylindrical, conical and spherical sandwich shells is performed. A specific sandwich shell finite element with 54 degrees of freedom is employed. Starting from the energy method the damping model is developed. Numerical examples for the free vibration analysis with damping based on the proposed finite element approach are discussed. Results for sandwich shells show a satisfactory agreement with various reference solutions.

2 . 7 The Present Study Contributions :

From the above survey of the available literature related to the vibration characteristics of oblate spheroid shells, it can be concluded that none of the references deals directly with the generality of the problem. Furthermore, only certain approaches were attempted to solve special purpose problems. For the sake of generality of the problem as well as for a special purpose investigation, the following two points (which are not found in the literature) are examined;

1. The Rayliegh – Ritz Method is used to show its validity for such shells.
2. The effect of different boundary conditions (such as: clamped – clamped , clamped – free and pined – pined) of the oblate spheroid shells on the free vibration characteristics is investigated.

The free vibration characteristics of a thin elastic oblate spheroid shell will be comprehensively examined.

Two theoretical approaches will be attempted in this work. The first approach is Boundary Matching Method and the second approach is Rayliegh – Ritz Method.

CHAPTER THREE

MODELLING AND MATHEMATICAL ANALYSIS

3 . 1 Introduction

The review of literature reveals that even though the differential equations of motion for general shell of revolution are well spelt out, nevertheless, the formulation of these equations for oblate spheroidal shells are not available. Therefore, the derivation of these equations will be presented in appendix (A). However, the exact solutions of these equations are unobtainable. Hence, an approximate energy approach will be presented in section (3.2) of this chapter.

Furthermore, an exact solution will be tried based on modelling the system under consideration as a structure composed of two open profile spherical shells by matching the continuous boundary conditions. Evidently, the exact solutions for open non – shallow as well as shallow spherical shells are available. This will allow a closed form formulation of the undergoing problem as presented in sections (3.3) and (3.4).

3 . 2 The Rayleigh – Ritz's Energy Method :

Due to the complexity encountered in solving the equations of motion given in appendix (A) analytically, for the undergoing problem, an approximate energy approach based on Rayleigh – Ritz's Method is used in this section.

Rayleigh – Ritz's Method can be used for more complex elastic bodies, such as plates and shells. It will be shown that with these methods, elastic bodies which posses an infinite number of degrees of freedom, are replaced effectively by an approximate multi – degree of freedom system. This method helps to determine the natural frequencies and their associated mode shapes with general boundary conditions in approximate forms. The continuous systems lend to eigenvalue problems that do not lend themselves to closed form solution, owing to non uniform mass or stiffness distributions. Hence, quite often one is forced to seek approximate solution of the eigenvalue problem. The Rayliegh – Ritz's Method may be viewed as an extension of Rayliegh's quotient and is used to obtain more accurate estimate. Therefore, Rayliegh quotient, and its extension, the Rayleigh – Ritz procedure, are essentially statements on the ratio of potential energy to the kinetic energy. Physically, it makes sense that this ratio is related to the frequency of oscillation [38]. At the natural frequency (ω), and assuming separation of variables, the shell displacement may be written in the following forms [33] :-

$$\left.\begin{aligned} w(\Phi', t) &= W(\Phi') \, . \, e^{i\omega t} \\ \text{and} \\ u_{\Phi}(\Phi', t) &= U_{\Phi}(\Phi') \, . \, e^{i\omega t} \end{aligned}\right\} \qquad \ldots (3 . 2 . 1)$$

Substituting these in the strain energy expression gives :

$$U = \int_{-h/2}^{h/2} \int_{0}^{2\pi} \int_{0}^{2\pi} \frac{1}{2} [\sigma_{\Phi'} \, \varepsilon'_{\Phi'} + \sigma_{\theta} \, \varepsilon'_{\theta}] \, R_{\Phi} \, R_{\theta} \sin \Phi' \, d\Phi \, d\theta \, dz \qquad (3 . 2 . 2)$$

where,

The stress in terms of strain are defined

$$\left.\begin{aligned} &\sigma_{\Phi'} = \frac{E}{(1-\nu^2)}\left[\varepsilon'_{\Phi'} + \upsilon\,\varepsilon'_{\theta}\right],\ \sigma_{\theta} = \frac{E}{(1-\nu^2)}\left[\varepsilon'_{\theta} + \upsilon\,\varepsilon'_{\Phi'}\right] \\ &\text{and} \\ &\varepsilon'_{\Phi'} = \varepsilon^{\circ}_{\Phi} + z k_{\Phi} \quad , \quad \varepsilon'_{\theta} = \varepsilon^{\circ}_{\theta} + z k_{\theta} \end{aligned}\right\} \qquad (3.2.3)$$

An expression for the maximum potential energy [Umax] may be obtained upon taking $e^{i\omega t}$ to be unity and applying the appropriate expressions for $б_{\Phi'}$, $б_{\theta}$, $Є'_{\Phi'}$ and $Є'_{\theta}$ as derived in appendix (A), we get,

$$\begin{aligned} U_{max} = \frac{E h}{2(1-\upsilon^2)} \int_0^{2\pi}\int_0^{2\pi} \Bigg\{ & \frac{h^2}{12}\left[\frac{1}{R_{\Phi}^2}\left[\frac{\partial}{\partial\Phi'}\left[\frac{U_{\Phi}}{R_{\Phi}} - \frac{\partial W}{R_{\Phi}\,\partial\Phi'}\right]\right]\right. \\ & + \frac{\cos^2\Phi'}{R_{\Phi}^2\,R_{\theta}^2\,\sin^2\Phi'}\left[U_{\Phi} - \frac{\partial W}{\partial\Phi'}\right]^2 + 2\,\upsilon\,\frac{\cos\Phi'}{R_{\theta}\,R_{\Phi}^2\,\sin\Phi'}\left[U_{\Phi} - \frac{\partial W}{\partial\Phi'}\right]. \\ & \left.\cdot\frac{\partial}{\partial\Phi'}\left[\frac{U_{\Phi}}{R_{\Phi}} - \frac{\partial W}{R_{\Phi}\,\partial\Phi'}\right]\right] + \frac{1}{R_{\Phi}^2}\left[\frac{\partial U_{\Phi}}{\partial\Phi'} + W\right]^2 \\ & + \frac{1}{(R_{\theta}\sin\Phi')^2}\left(U_{\Phi}\cos\Phi' + W\sin\Phi'\right)^2 \\ & + \frac{2\,\upsilon}{R_{\theta}\,R_{\Phi}\sin\Phi'}\left[\frac{\partial U_{\Phi}}{\partial\Phi'} + W\right].\left(U_{\Phi}\cos\Phi' + W\sin\Phi'\right)\Bigg\}. \\ & R_{\Phi}\,R_{\theta}\sin\Phi'\,d\Phi'\,d\theta \end{aligned} \qquad \ldots (3.2.4)$$

The kinetic energy expression is :

$$K = \int_{-h/2}^{h/2}\int_0^{2\pi}\int_0^{2\pi} \tfrac{1}{2}\,\rho\left[\left[\frac{\partial U_{\Phi}}{\partial t}\right]^2 + \left[\frac{\partial W}{\partial t}\right]^2\right] R_{\Phi}\,R_{\theta}\sin\Phi'\,d\Phi'\,d\theta\,dz \qquad (3.3.5)$$

After integrating with respect to (z) and substituting for the appropriate expressions, the maximum kinetic energy will take the form :

$$K_{max} = \frac{\omega^2 \rho h}{2} \int_0^{2\pi} \int_0^{2\pi} (U_\Phi^2 + W^2) R_\Phi R_\theta \sin\Phi' \, d\Phi' \, d\theta \quad \ldots (3 . 2 . 6)$$

The kinetic energy for ω=1 rad/sec is customarily define as K^*_{max}, and, therefore,

$$K_{max} = \omega^2 K^*_{max}$$

For a system with no dissipation losses, such as those due to friction or damping, the maximum potential energy equals the maximum kinetic energy,

$$U_{max} = \omega^2 K^*_{max}$$

Equating the maximum kinetic energy to the maximum potential energy, an expression for the natural frequency may be written as :

$$\omega_r^2 = \frac{U_{max}}{K^*_{max}} = \frac{N}{D} \qquad r = 1, 2, 3, ..., n \qquad \ldots (3 . 2 . 7)$$

where N and D represent the equations in the numerator and denominator, respectively. Following the procedure of Rayleigh–Ritz's Method, the radial (or transverse) and tangential displacements can be written in power series form as :

$$w(\Phi') = \sum_{i=1}^{n} a_i . W_i(\Phi') \quad , \quad u_\Phi(\Phi') = \sum_{i=1}^{n} b_i . U_{\Phi i}(\Phi') \quad \ldots (3 . 2 . 8)$$

where a_i and b_i are coefficients to be determined. The functions $W_i (\Phi')$, $U_\Phi (\Phi')$ satisfy all the geometry boundary conditions of the system. Equation (3 . 2 . 7) is an exact expression for the frequency according to Rayleigh quotient. In order to use the procedure of Rayleigh–Ritz's

method, equation (3 . 2 . 8) is substituted into equation (3 . 2 . 4), and (3 . 2 . 6), then the results is used in equation (3 . 2 . 7).

Now substituting equation (3 . 2 . 8) into equations (3 . 2 . 4) and (3 . 2 . 6), and after some mathematical manipulations, the following equation will result [see appendix B] :

$$\omega_r^2 = \frac{\alpha}{\Psi} \qquad r = 1, 2, 3, ..., n \qquad \ldots (3 . 2 . 9)$$

where

$$\begin{aligned}\alpha = \sum_{i=1}^{n}\sum_{j=1}^{n} c_i c_j \frac{E h \pi}{(1-\upsilon^2)} \int_0^{2\pi} \Big\{ & \frac{h^2}{12 R_\Phi^4}\left[U'_{\Phi i} U_{\Phi j}' - 2U_{\Phi i}' W_i'' + W_i'' W_j''\right]\sin\Phi' \\ & + \frac{\upsilon h^2}{6 R_\theta R_\Phi^3}\left[U_{\Phi i} U_{\Phi i}' - U_{\Phi i} W_i'' - U_{\Phi i}' W_i' + W_i' W_i''\right]\cos\Phi' \\ & + \frac{h^2}{12 R_\Phi^2 R_\theta^2}\left[U_{\Phi i} U_{\Phi j} - 2U_{\Phi i} W_i' + W_i' W_j'\right]\frac{\cos^2\Phi'}{\sin\Phi'} \\ & + \frac{1}{R_\Phi^2}\left[U_{\Phi i}' U_{\Phi j}' + 2U_{\Phi i}' W_i + W_i W_j\right]\sin\Phi' \\ & + \frac{1}{R_\theta^2}\left[U_{\Phi i} U_{\Phi j} \frac{\cos^2\Phi'}{\sin\Phi'} + 2U_{\Phi i} W_i \cos\Phi' + W_i W_j \sin\Phi' \right] \\ & + \frac{2\upsilon}{R_\Phi R_\theta}\left[U_{\Phi i} U_{\Phi i}'\cos\Phi' + U_{\Phi i}' W_i \sin\Phi' + U_{\Phi i} W_i \cos\Phi' + W_i W_i \sin\Phi'\right] \Big\}. \\ & . R_\Phi R_\theta \, d\Phi' \qquad \ldots (3 . 2 . 9a)\end{aligned}$$

$$\Psi = \sum_{i=1}^{n}\sum_{j=1}^{n} c_i c_j \int_0^{2\pi} \rho h \pi \left[U_i U_j + W_i W_j\right] R_\Phi R_\theta \sin\Phi' \, d\Phi' \qquad \ldots (3 . 2 . 9b)$$

An n – term finite sum leads to the estimation of the first frequencies. Equations (3 . 2 . 9a) and (3 . 2 . 9b) give the physical properties of the shell from the stiffness and mass distribution point of view.

The stiffness and mass of the shell are given by the following two equations respectively:

$$k_{ij} = \frac{E h \pi}{(1-\upsilon^2)} \int_0^{2\pi} \{ \frac{h^2}{12 R_\Phi^4} \left[U_{\Phi i}' \; U_{\Phi j}' - 2 U_{\Phi i}' W_i'' + W_i'' W_j'' \right] \sin\Phi'$$
$$+ \frac{\upsilon h^2}{6 R_\theta R_\Phi^3} \left[U_{\Phi i} U_{\Phi i}' - U_{\Phi i} W_i'' - U_{\Phi i}' W_i' + W_i' W_i'' \right] \cos\Phi'$$
$$+ \frac{h^2}{12 R_\Phi^2 R_\theta^2} \left[U_{\Phi i} U_{\Phi j} - 2 U_{\Phi i} W_i' + W_i' W_j' \right] \frac{\cos^2\Phi'}{\sin\Phi'}$$
$$+ \frac{1}{R_\Phi^2} \left[U_{\Phi i}' U_{\Phi j}' + 2 U_{\Phi i}' W_j + W_i \; W_j \right] \sin\Phi'$$
$$+ \frac{1}{R_\theta^2} \left[U_{\Phi i} U_{\Phi j} \frac{\cos^2\Phi'}{\sin\Phi'} + 2 U_{\Phi i} \; W_i \cos\Phi' + W_i W_j \sin\Phi' \right]$$
$$+ \frac{2\upsilon}{R_\Phi R_\theta} \left[U_{\Phi i} U_{\Phi i}' \cos\Phi' + U_{\Phi i}' W_i \sin\Phi' + U_{\Phi i} W_i \cos\Phi' + W_i W_i \sin\Phi' \right] \}.$$
$$. R_\Phi R_\theta \, d\Phi' \qquad \ldots (3.2.10)$$

and

$$m_{ij} = \int_0^{2\pi} \rho \, h \pi \left[U_i U_j + W_i W_j \right] R_\Phi R_\theta \sin\Phi' d\Phi' \qquad \ldots (3.2.11)$$

Then

$$\omega_r^{\,2} = \frac{N}{D} = \frac{\sum_{i=1}^{n} \sum_{j=1}^{n} c_i c_j \; k_{ij}}{\sum_{i=1}^{n} \sum_{j=1}^{n} c_i c_j m_{ij}} \qquad \ldots (3.2.12)$$

The exact frequency is always smaller than the approximate value. In order to minimize the approximate value, which is given by equation (3 .

2 . 12), it should be differentiated with respect to c_i and equating the resulting expression to zero, that is :

$$\frac{\partial}{\partial c_i}\left(\frac{N}{D}\right) = \frac{D\,\partial N/\partial c_i - N\,\partial D/\partial c_i}{D^2} = 0 \qquad \text{i = 1, 2, 3, ..., n} \quad \ldots (3 . 2 . 13)$$

This equation can be satisfied if and only if the numerator equals zero, since D is never equal to zero. The numerator can be written in a more useful form as :

$$\frac{\partial N}{\partial c_i} - \frac{N}{D}\frac{\partial D}{\partial c_i} = 0 \qquad \text{i = 1, 2, . . . , n} \qquad \ldots (3 . 2 . 14)$$

It is as given by equation (3 . 2 . 7) $\omega_r^2 = N / D$, and n is the number of terms in the approximate solution. The infinite degrees of freedom system has been replaced by an n degree of freedom system. Therefore, Equation (3 . 2 . 13) for i = 1, 2, can be written in matrix form as :

$$\begin{bmatrix} k_{11} - \omega^2 m_{11} & k_{12} - \omega^2 m_{12} \\ k_{12} - \omega^2 m_{12} & k_{22} - \omega^2 m_{22} \end{bmatrix} \begin{Bmatrix} c_1 \\ c_2 \end{Bmatrix} = \begin{Bmatrix} 0 \\ 0 \end{Bmatrix} \qquad \ldots (3 . 2 . 15)$$

or in general matrix notation as :

$$\left[\{K\} - \omega^2 \{M\}\right]\{c\} = \{0\} \qquad \ldots (3 . 2 . 16)$$

The evaluation of this determinant provides the estimation of the first two natural frequencies ω_1^2 and ω_2^2. Since we have used a two–term approximate solution, it results in a two degree of freedom approximated system [38].

In the present work, the same argument of Penzes and Burgin [14] that the mode shapes of a spherical shell satisfies the boundary conditions

of an oblate spheroid shell has been adopted, the assumed mode shapes were chosen to represent the first two modes of a closed spherical shell as illustrated by Kalnins [11].

3 . 3 Engineering Model By Non – Shallow Shell Theory :

3 . 3 . 1 Problem Formulation :

The problem of vibration of oblate spheroid shells will be treated in an engineering modeling approach where the oblate spheroid shell is modeled as a structure composed of two spherical shells joined rigidly at their ends. Centers of curvature of the two spherical shell elements fall along the minor axis of the proposed oblate spheroid [Fig. (3 – 1) for details].

Such approximation is not far from reality, as the oblate spheroidal tanks are produced by joining, either by welding or riveting, two spherical shell elements through a toroidl shell element.

The effective radius (R_r) of the spherical shell model represents the radius of curvature at the apex of the shell. This radius can be obtained from the geometrical relation.

$$R_{\Phi} = \frac{a(1-e^2)}{(1-e^2\cos^2\Phi')^{3/2}} \qquad \ldots (3 . 3 . 1)$$

Setting (Φ') to zero results the radius of the shell at the apex as :

$$R_r = \frac{a}{(1-e^2)^{1/2}} \qquad \ldots (3 . 3 . 2)$$

where,

e = 0 for sphere.

e = 1 for plate.

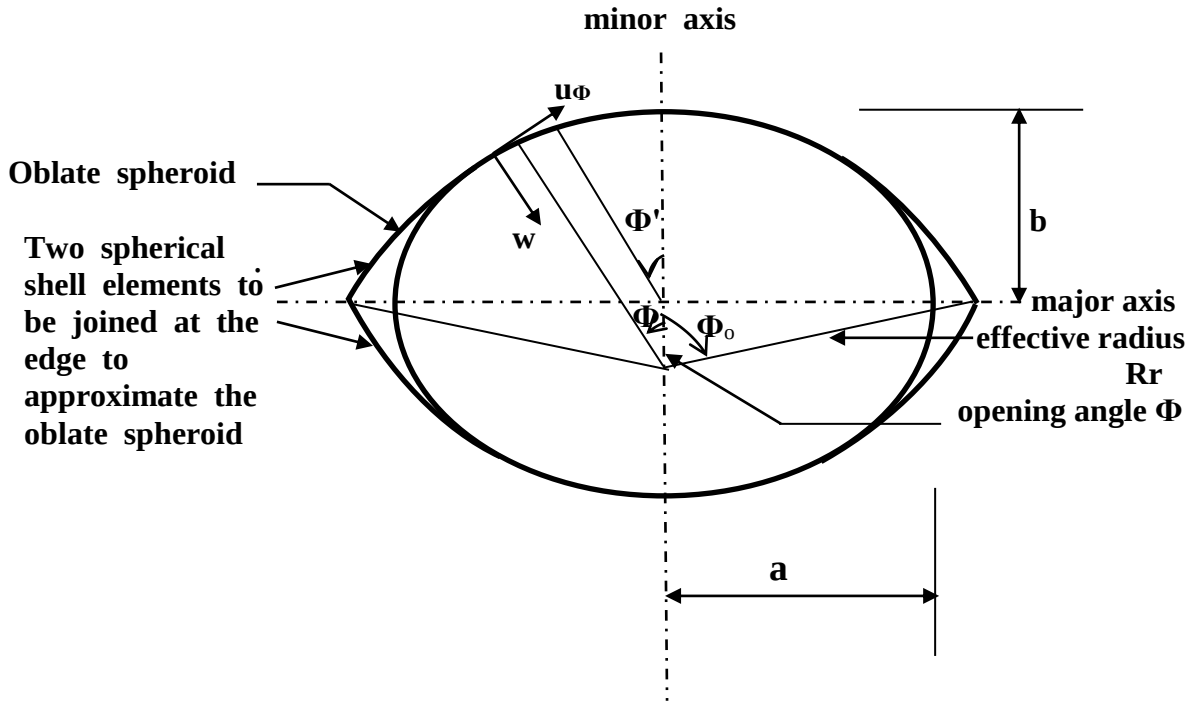

Fig. (3 – 1) An oblate spheroid and its approximate of two spherical shell elements joined at the edge

An approximate opening angle (Φ_0) may be obtained by using the following formula:

$$\Phi_o = \cos^{-1}\frac{R_r - b}{R_r} \qquad \ldots (3.3.3)$$

Figures (3 – 2 , 3 – 3) show the values of the effective radius and opening angle versus the eccentricity. Contemplating through figure (3 – 4) which resembles the approximate oblate model indicate that the geometries of the oblate and the model are almost the same in the region (a – b) however, divergence exists between the regions (b – c). Closer approximate is expected for the exact spheroid and the model at small values of eccentricities. The separable homogeneous solutions to the axisymmetric vibration problem of thin elastic spherical shells including the effects of bending can be obtained from the equations derived in appendix (A) for an oblate spheroid shell by setting the eccentricity ratio to zero. Dividing equations (A . 2 . 12 – A . 2 . 14) by R_r sin Φ' results the following equations of motion.

$$\frac{\partial N_\Phi}{\partial \Phi} + \left(N_\Phi - N_\theta . \cot\Phi + Q_\Phi \right) = R_r . \rho . h \frac{\partial^2 U_\Phi}{\partial t^2} \qquad \ldots (3.3.4)$$

$$\frac{\partial Q_\Phi}{\partial \Phi} + Q_\Phi \cot\Phi - \left(N_\Phi + N_\vartheta \right) = R_r . \rho . h \frac{\partial^2 W}{\partial t^2} \qquad \ldots (3.3.5)$$

$$\frac{\partial M_\Phi}{\partial \Phi} + \left(M_\Phi - M_\theta \right) \cot\Phi - R_r . Q_\Phi = 0 \qquad \ldots (3.3.6)$$

(In this case $R_\Phi = R_\theta = R_r$ and $\Phi = \Phi'$)

The same equations were derived by Naghdi and Kalnins [8], as the equations of motion of spherical shells.

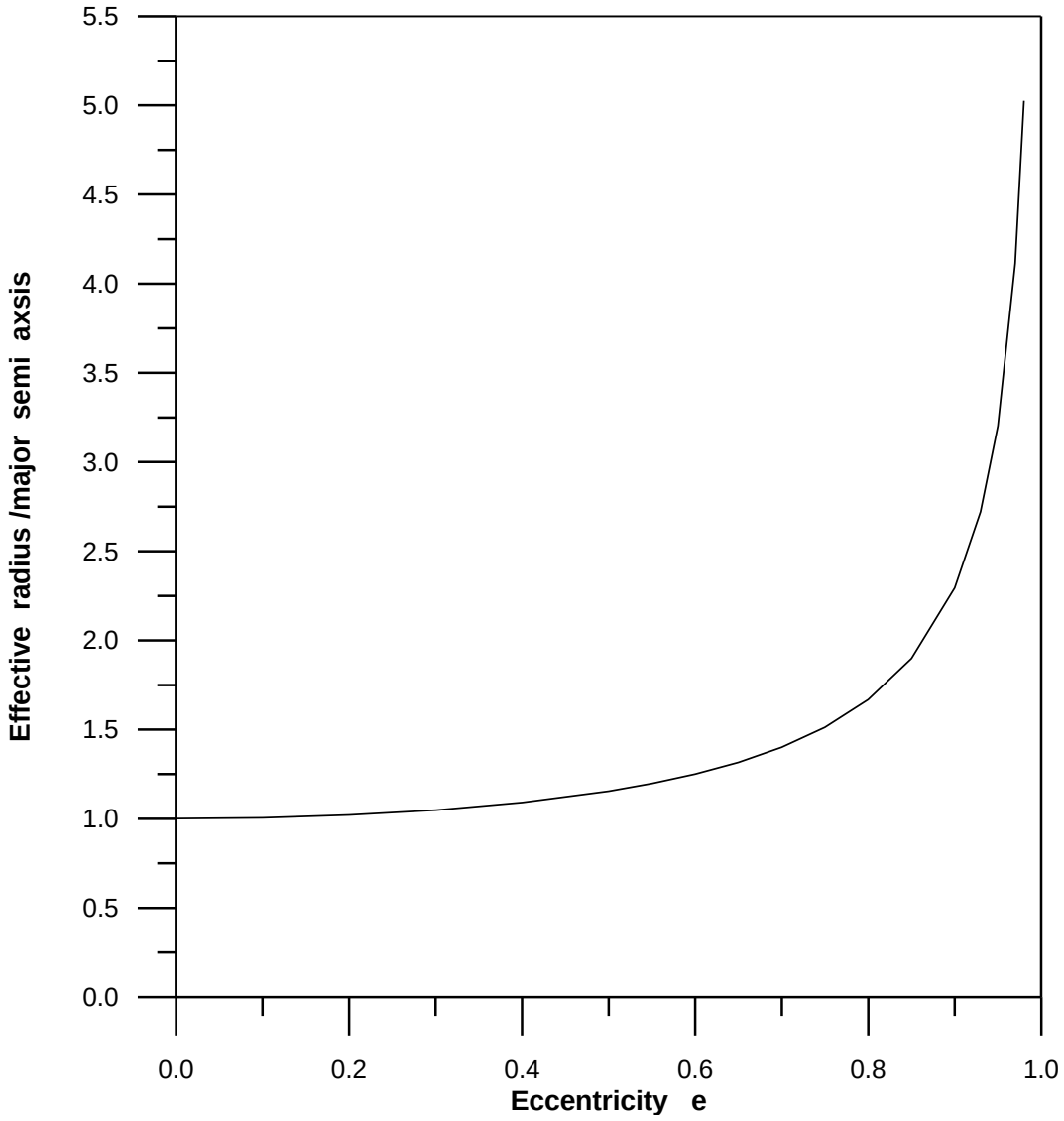

Fig. (3 – 2) The effective radius / major semi – axis vs. eccentricity

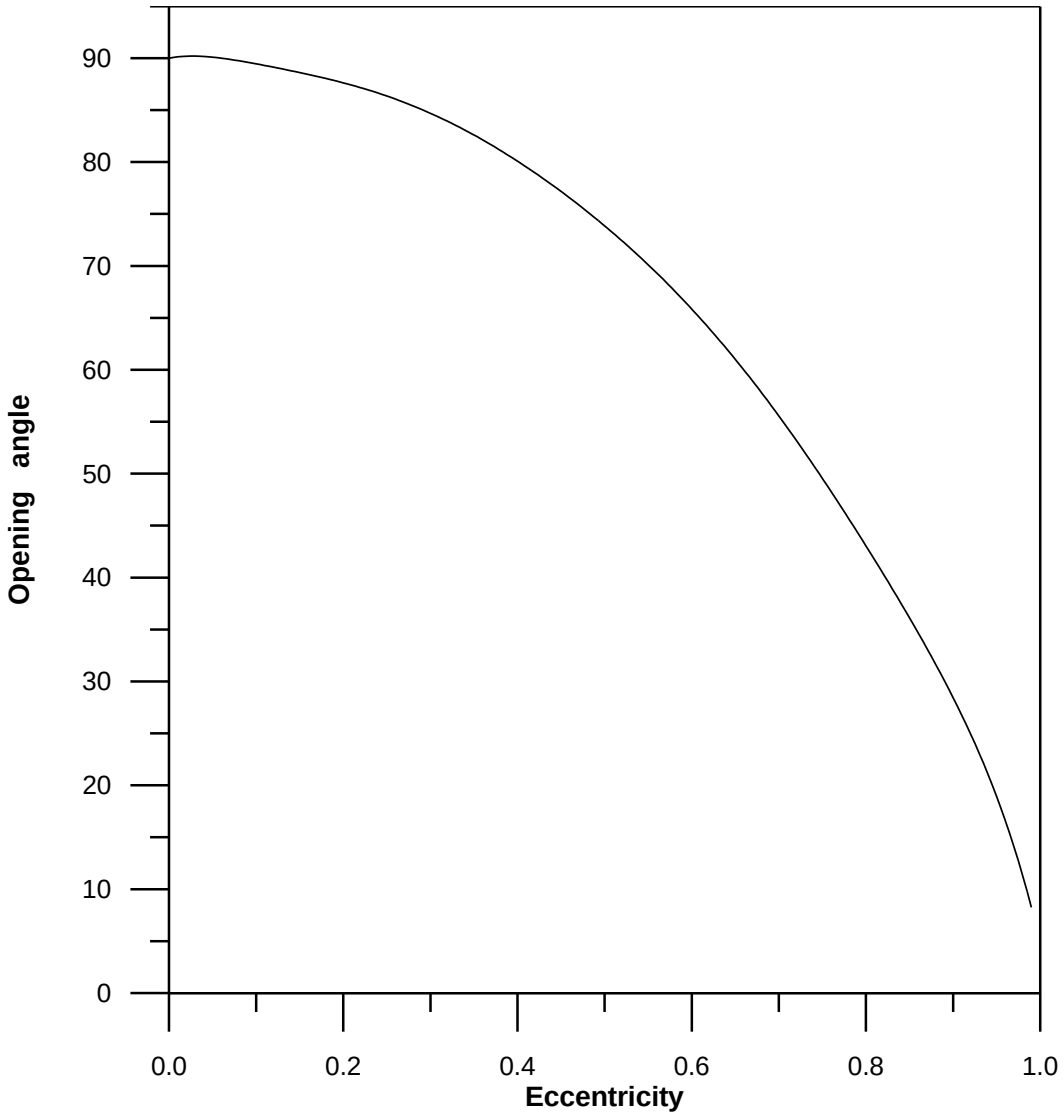

Fig. (3 – 3) The opening angle (Φ_o) of the approximate spherical shells vs. eccentricity

Assuming that the temporal and spatial dependence of the free vibration are separable, the displacements may be assumed as [33]:

$$\left.\begin{aligned} u_{\Phi}(\Phi, t) &= U(\Phi) \cdot \cos \omega t \\ w(\Phi, t) &= W(\Phi) \cdot \cos \omega t \end{aligned}\right\} \quad \ldots (3.3.7)$$

where (ω) denotes the circular frequency, t : time and Φ denotes the angle measured from the (vertical axis).

The stress resultants and couples are related to the displacements of the reference surface by the same expressions derived in appendix A of the thesis with the eccentricity set equal to zero.

The free vibration of spherical shells was solved analytically by [11]. In this work considering the actual Φ – dependent coefficient of the variable as those derived in the latter reference which are :

$$W = \sum_{i=1}^{3} \left[A_i P_{ni}(x) + B_i Q_{ni}(x) \right] \quad \ldots (3.3.8a)$$

$$U_{\Phi} = \sum_{i=1}^{3} -(1+\upsilon) C_i \left[A_i P_{ni}'(x) + B_i Q_{ni}'(x) \right] \quad \ldots (3.3.8b)$$

$$N_{\Phi} = \frac{E.h}{(1-\upsilon) R_r} \sum_{i=1}^{3} \left\{ (1 + C_i \beta_i). \left[A_i P_{ni}(x) + B_i Q_{ni}(x) \right] \right.$$

$$\left. + (1-\upsilon) C_i \cot\Phi \left[A_i P_{ni}'(x) + B_i Q_{ni}'(x) \right] \right. \quad \ldots (3.3.8c)$$

$$N_{\theta} = \frac{E.h}{(1-\upsilon) R_r} \sum_{i=1}^{3} \left\{ (1 + \upsilon C_i \beta_i). \left[A_i P_{ni}(x) + B_i Q_{ni}(x) \right] \right.$$

$$\left. - (1-\upsilon) C_i \cot\Phi \left[A_i P_{ni}'(x) + B_i Q_{ni}'(x) \right] \right. \quad \ldots (3.3.8d)$$

$$M_{\Phi} = \frac{D_b}{R_r^{\,2}} \sum_{i=1}^{3} \left[1 + (1+\upsilon) C_i \right] \left\{ \beta_i \left[A_i P_{ni}(x) + B_i Q_{ni}(x) \right] \right.$$

$$\left. + (1-\upsilon) C_i \cot\Phi \left[A_i P_{ni}'(x) + B_i Q_{ni}'(x) \right] \right. \quad \ldots (3.3.8e)$$

$$M_\theta = \frac{D_b}{R_r^{\,2}} \sum_{i=1}^{3} \left[\, 1+(1+\upsilon)C_i \,\right] \left\{ \upsilon\, \beta_i \left[A_i P_{ni}(x) + B_i Q_{ni}(x) \right] \right.$$

$$\left. -(1-\upsilon)\cot\Phi \left[A_i P_{ni}'(x) + B_i Q_{ni}'(x) \,\right] \right\} \qquad \ldots (3.3.8f)$$

$$Q_\Phi = \frac{D_b}{R_r^{\,2}} \sum_{i=1}^{3} \left[\, 1+(1+\upsilon)C_i \,\right] (\upsilon + \beta_i - 1) \left[A_i P_{ni}'(x) + B_i Q_{ni}'(x) \right] \qquad \ldots (3.3.8g)$$

where,

$$C_i = \frac{1+(\beta_i - 2)/\left[(1+\upsilon)(1+\xi\,)\right]}{1-\upsilon-\beta_i+\xi\left(1-\upsilon^2\right)\Omega^2/\left(1+\xi^{\,2}\right)}$$

$$\xi = 12R_r^{\,2}/h^2$$

$$n_i = -\tfrac{1}{2} + \sqrt{1/4+\beta_i}$$

$x = \cos\Phi$

The parameters β_i's are the three roots of the cubic equation:-

$$\beta^{\,3} - \left[4+\left(1-\upsilon^{\,2}\right)\Omega^2\,\right]\beta^{\,2} + \left[4+(1-\upsilon)\left(1-\upsilon^{\,2}\right)\Omega^2+(1+\xi)\left(1-\upsilon^{\,2}\right)\right]$$

$$\left(1-\Omega^{\,2}\right)\beta + (1-\upsilon)\left(1-\upsilon^{\,2}\right)\left[\,\Omega^{\,2}-\frac{2}{1-\upsilon}\right]\left[\,1+(1+\upsilon)\left[\,\Omega^{\,2}-\frac{1}{1+\upsilon}\right]\right] = 0 \qquad \ldots (3.3.9)$$

and $\Omega^2 = \dfrac{\rho\,\omega^{\,2} R_r^2}{E}$

$$D_b = \frac{E\,h^3}{12\,(1-\upsilon^{\,2})}$$

$P_n(x)$, $Q_n(x)$ are Legendre functions of the first and the second kinds, respectively $P_n'(x)$, $Q_n'(x)$ are the derivatives with respect to (Φ) of the Legendre functions of the first and the second kinds, respectively. A_i & B_i are arbitrary constants.

The above solutions can be applied to the study of free vibration of an elastic spherical shell bounded in general by any two concentric openings.

As we are dealing with shells closed at the apex ($\Phi = 0$), and since the Legendre function of the second kind is singular at that point, then the arbitrary constants (B_i's) are set equal to zero. For this reason, in the remainder of this section all terms involving $Q_n(x)$ are omitted.

The character of the solution given by equations (3 . 3 . 8) is strongly dependent on the character of the three indices n_1, n_2, n_3. For the purpose of illustration of the various combinations of complex and real values that the indices may assume, figure (3 – 5) which is extracted from reference [11] shows a plot of n_i (i =1, 2, 3) vs. Ω for a given constant value of υ and h / R, the character of n_i varies little with the latter two parameters.

The variation of the characters n_1, n_2, and n_3 are given by [11] :

Zone I
$$n_1 = b_1$$
$$n_2 = b_2 + i\,b_3$$
$$n_3 = b_2 - i\,b_3$$

Zone II
$$n_1 = b_1$$
$$n_2 = -\tfrac{1}{2} + i\,b_3$$
$$n_3 = -\tfrac{1}{2} - i\,b_2$$

Zone III
$$n_1 = b_1$$
$$n_2 = b_2$$
$$n_3 = -\tfrac{1}{2} + i\,b_3$$

Here b_1, b_2, and b_3 are real numbers.

It is clear that for zone I it is appropriate to observe that a pair of Legendre functions have indices which are complex conjugates, they can be written in the form;

$$P_{a\pm b}(\cos\Phi)=R_e\left\lfloor P_{a+ib}(\cos\Phi)\right\rfloor \pm \mathrm{Im}\left\lfloor P_{a+ib}(\cos\Phi)\right\rfloor$$

Now, according to the fact that the deflections (W) and (U_Φ) must be real quantities, we must insure that the right side of equation (3 . 3 . 8a and b) will also be real. This is accomplished by defining the arbitrary constants according to the scheme.

$$A_2 + A_3 = C_2 \quad , \quad i\,(A_2 - A_3) = C_3$$

Hence the solution takes the form :

$$W = \sum_{i=1}^{3} C_1 P_{b1}(\cos\Phi) + C_2[\,\mathrm{Re}\,P_{b2+ib3}(\cos\Phi)\,] + C_3[\,I_m P_{b2-ib3}(\cos(\Phi)\,] \qquad \ldots (3.3.10)$$

In this way, the solution in zone I can be expressed in terms of real functions.

As for zones II and III it is appropriate to recall that the Legendre functions of the index -1/2 + ib are called conical functions which are always real quantities.

Also the corresponding values of β_2 and β_3 are real, thus the solution given in the form of equation (3 . 3 . 8a and b) is directly applicable.

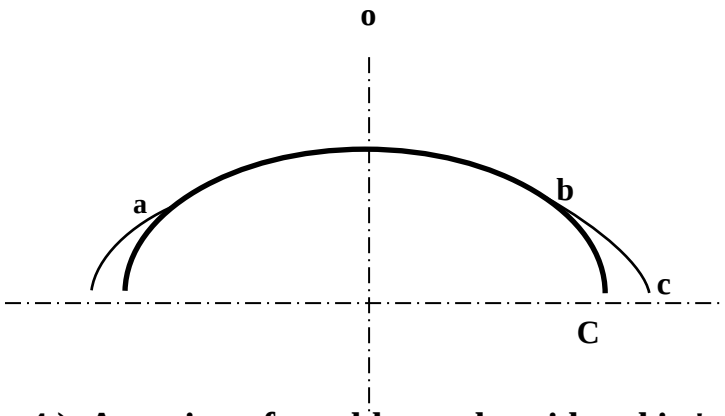

Fig. (3 – 4) A section of an oblate spheroid and its' approximate spherical shell element

Fig. (3 – 5) The value of the index (n) vs. the non - dimensional frequency (Ω) extracted from [11]

3 . 3 . 2 The Frequency Equation :

As stated before the two spherical shell elements are assumed to be rigidly connected along their edge $\Phi=\Phi_o$. To guarantee that the continuity of all deflections, slopes, moments and forces along the function is insured, (selecting the coordinates of the top shell as the reference coordinates) the boundary conditions at the junctions may be written as follows [(Fig. 3 – 6)]:

1 – kinematics :

$$W_1 - U_{\Phi 2} \sin 2\Phi_0 + W_2 \cos 2\Phi_0 = 0 \qquad \ldots (3 . 3 . 11)$$

$$U_{\Phi 1} - U_{\Phi 2} \cos 2\Phi_0 - W_2 \sin 2\Phi_0 = 0 \qquad \ldots (3 . 3 . 12)$$

$$\frac{\partial W_1}{\partial \Phi_1} + \frac{\partial W_2}{\partial \Phi_2} = 0 \qquad \ldots (3 . 3 . 13)$$

2 - equilibrium :

$$- Q_1 - Q_2 \cos 2\Phi_0 - N_{\Phi 2} \sin 2\Phi_0 = 0 \qquad \ldots (3 . 3 . 14)$$

$$N_{\Phi 1} - Q_2 \sin 2\Phi_0 - N_{\Phi 2} \cos 2\Phi_0 = 0 \qquad \ldots (3 . 3 . 15)$$

$$M_1 - M_2 = 0 \qquad \ldots (3 . 3 . 16)$$

Substituting the terms of equation. (3.3.8a – g) into the boundary conditions results in six homogenous simultaneous equations in terms of the constants which can be written as follows : -

$$\sum_{i=1}^{6} C_{i,K}(\Omega).A_{i.K} = 0 \qquad , \qquad k=1, ...,6$$

where the elements $C_{i,k}$ are functions of Ω. These elements are generated from the applications. For non trivial solution of the simultaneous equations, the determinant of the coefficients $C_{i,k}$ must vanish, thus

$$\begin{vmatrix} C_{11} & & C_{16} \\ & & \\ C_{61} & & C_{66} \end{vmatrix} = 0 \qquad \ldots (3.3.17)$$

The resulting determinant equation is the intended frequency equation.

The calculation of the natural frequency is carried out by specifying an initial guessed then evaluating the determinant $|C_{i,j}|$. Increasing the frequency by small increments and repeating the same procedure until the value of the determinant changes its sign. This indicates that a natural frequency is expected in the new value. The frequency increment is then minimized and the operation is repeated until the desired accuracy of the natural frequency is obtained when the determinant is vanished. The mode shape associated with any natural frequency is then derived by substituting the value of the natural frequency obtained above in equation. (3 . 3 . 17) and normalizing the $[A]$ coefficients and determining the eigenvectors.

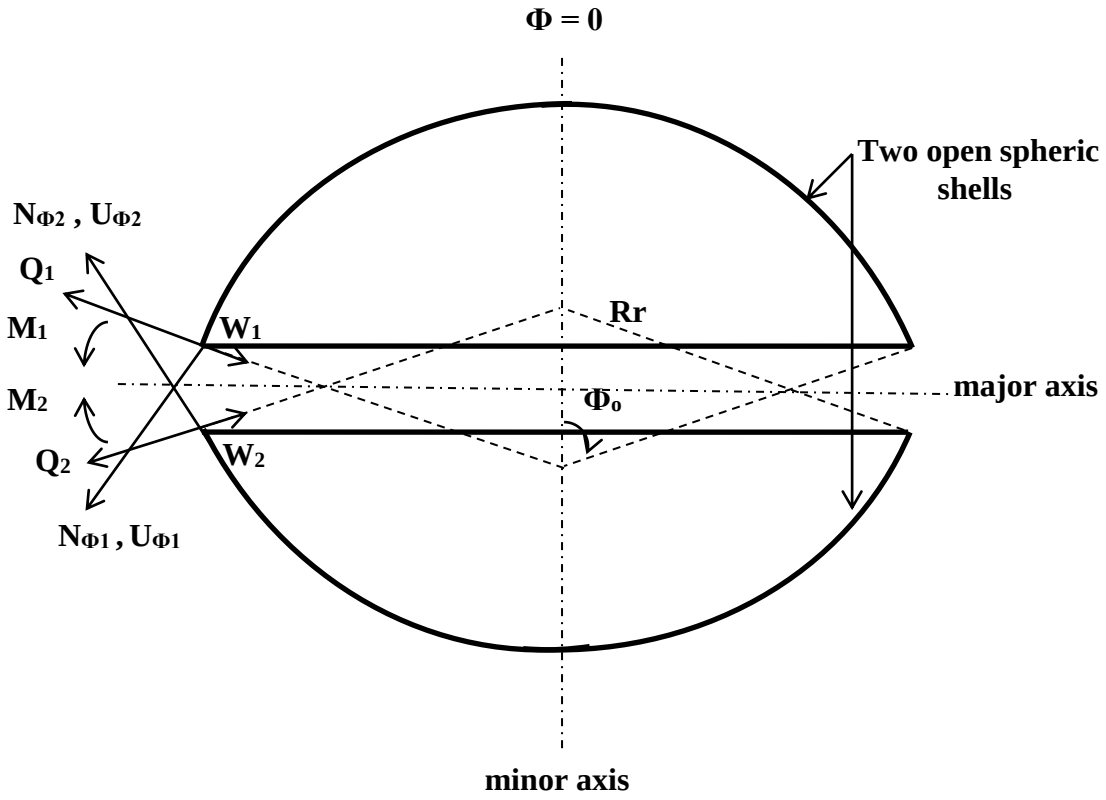

Fig . (3 – 6) Matching boundary conditions of two non – shallow spherical shells elements

3 . 4 Engineering Model By Shallow Shell Theory :

3 . 4 . 1 Problem Formulation :

As the eccentricity of the oblate spheroidal shell approaches values greater than (0.93), the opening angle (Φ_o) of the approximate spherical shells reaches the value of (25°). For such an angle, the assumption of " Reissner " for shallow spherical shell is valid. Adopting the Gauss condition :

$$d\,r = R\,d\Phi \qquad \ldots (3 . 4 . 1)$$

As Φ_o is less than 25°, and Reissner's argument of the transverse shearing stress resultants to the equilibrium of forces in the meridian and tangential directions are neglecting the contribution of stretching displacement to the change of curvatures expressions, the equations of motion of axisymmetric free vibration may be written as : -

$$\frac{\partial}{\partial r}\left(rN_r\right) - N_\theta = \rho.h.r\frac{\partial^2 U_r}{\partial t^2} \qquad \ldots (3 . 4 . 2)$$

$$\frac{\partial}{\partial r}\left(r\,Q_r\right) - \frac{r}{R_r}\left(N_r + N_\theta\right) = \rho.h.r\frac{\partial^2 W_r}{\partial t^2} \qquad \ldots (3 . 4 . 3)$$

$$\frac{\partial}{\partial r}\left(r\,M_r\right) - M_\theta - r\,Q_r = 0 \qquad \ldots (3 . 4 . 4)$$

The strain – displacement relations are given by :

$$\varepsilon_r{}^\circ = \frac{\partial U_r}{\partial r} + \frac{W_r}{R_r} \qquad \ldots (3 . 4 . 5)$$

$$\varepsilon_\theta{}^\circ = \frac{1}{r}\left(U_r\right) + \frac{W_r}{R_r} \qquad \ldots (3 . 4 . 6)$$

$$k_r = \frac{\partial}{\partial r}\left[-\frac{\partial W_r}{\partial r}\right] \qquad \ldots (3.4.7)$$

$$k_\theta = \frac{1}{r}\left[-\frac{\partial W_r}{\partial r}\right] \qquad \ldots (3.4.8)$$

The displacement parallel to the horizontal and the vertical axis of a freely vibrating shell may be expressed as :

$$U_r(r,t) = U(r)\cos\omega t \qquad \ldots (3.4.9a)$$

$$W_r(r,t) = W_r(r)\cos\omega t \qquad \ldots (3.4.9b)$$

The free vibration of shallow shells were solved by Kalnin's and Naghdi [8].

The general solution for the equations may be written as :

$$W_r(r) = \sum_{i=1}^{3} A_i J_0\left[\mu_i \frac{r}{d}\right] + B_i Y_0\left[\mu_i \frac{r}{d}\right] \qquad \ldots (3.4.10a)$$

and

$$U_r(r) = 2\frac{H}{d}\left[\frac{r}{d}W_r(r) + (1+\upsilon)\sum_{i=1}^{3}\left[(1-\upsilon^2)(h/d)^2(\omega/\omega_0)^2 - \mu_i^2\right]^{-1} \cdot\left[\mu_i A_i J_1\left[\mu_i \frac{r}{d}\right] + \mu_i B_i Y_1\left[\mu_i \frac{r}{d}\right]\right]\right] \qquad \ldots (3.4.10b)$$

where the parameters μ_i's are the roots of the equation :

$$\mu^6 - (1-\upsilon^2)(h/d)^2(\omega/\omega_0)\mu^4 - 12(1-\upsilon^2).\left[(\omega/\omega_0)^2 - 4(H/h)^2\right]\mu^2 + 12(1-\upsilon^2)(h/d)^2(\omega/\omega_0)^2.\left[(1-\upsilon^2)(\omega/\omega_0)^2 - 8(1+\upsilon)(H/h)^2\right] = 0 \qquad \ldots (3.4.11)$$

where,

A_i's & B_i's are arbitrary constants,

$\omega_0 = \sqrt{E h^2 / \rho\, d^2}$,

J_o and Y_o are the Bessel functions of the first and second kind of zero order respectively.

J_1 and Y_1 are Bessel functions of the first and second kind of order one.

H – hieght of shell.

d – base raduis of the shell.

3 . 4 . 2 The Frequency Equation

The model is considered as two shallow spherical shells joined together at their edges and closed at the apex. As in the approximate model for an oblate spheroidal shell, and since the solutions $Y_o (\mu_i(r/d))$ and $Y_1 (\mu_i(r/d))$ are singular at the apex (r = 0) point, they have to be omitted from the solution by setting $B_i = 0$. Now, there are six arbitrary constants (A_i), three constants for the upper shell and three others for the lower shell, which are to be determined from the available boundary conditions at (r = d), [Fig. (3 – 7)]. These conditions may be written as :

$$(U_r)_1 + (U_r)_2 = 0 \qquad \ldots (3 . 4 . 12)$$

$$(W_r)_1 - (W_r)_2 = 0 \qquad \ldots (3 . 4 . 13)$$

$$\left(\frac{\partial W_r}{\partial r}\right)_1 - \left(\frac{\partial W_r}{\partial r}\right)_2 = 0 \qquad \ldots (3 . 4 . 14)$$

$$(N_r)_1 + (N_r)_2 \cos (2\Phi_o) - (Q_r)_2 \sin (2\Phi_o) = 0 \qquad \ldots (2 . 4 .15)$$

$$(Q_r)_1 - (N_r)_2 \sin (2\Phi_o) - (Q_r)_2 \cos (2\Phi_o) = 0 \qquad \ldots (2 . 4 .16)$$

$$(M_r)_1 - (M_r)_2 = 0 \qquad \ldots (2 . 4 .17)$$

Here the r – dependent variables are

$$N_r = \frac{hE}{R_r}\sum_{i=1}^{3}\left[\frac{\mu_i J_1(\mu_i)+(1+\upsilon)(h/d)^2(\omega/\omega_0)^2 J_0(\mu_i)}{(1-\upsilon^2)(h/d)^2(\omega/\omega_0)^2-\mu_i^2}\right] \qquad \ldots (3.4.18)$$

$$Q_r = -\frac{E h^3}{12(1-\upsilon^2)d^3}\sum_{i=1}^{3}\mu_i^3 J_1(\mu_i) \qquad \ldots (3.4.19)$$

$$M_r = -\frac{E h^3}{12(1-\upsilon^2)d^2}\sum_{i=1}^{3}\mu_i\left[(1-\upsilon)J_1(\mu_i)-\mu_i J_0(\mu_i)\right] \qquad \ldots (3.4.20)$$

Substituting the equations which give (W_r), (U_r), and $\left(\frac{\partial W}{\partial r}\right)$ in the boundary conditions with the appropriate terms results in six homogenous simultaneous equations in terms of (A_i). The same procedure described for the non – shallow shell may be used here to find the natural frequencies of model according to the shallow shell theory.

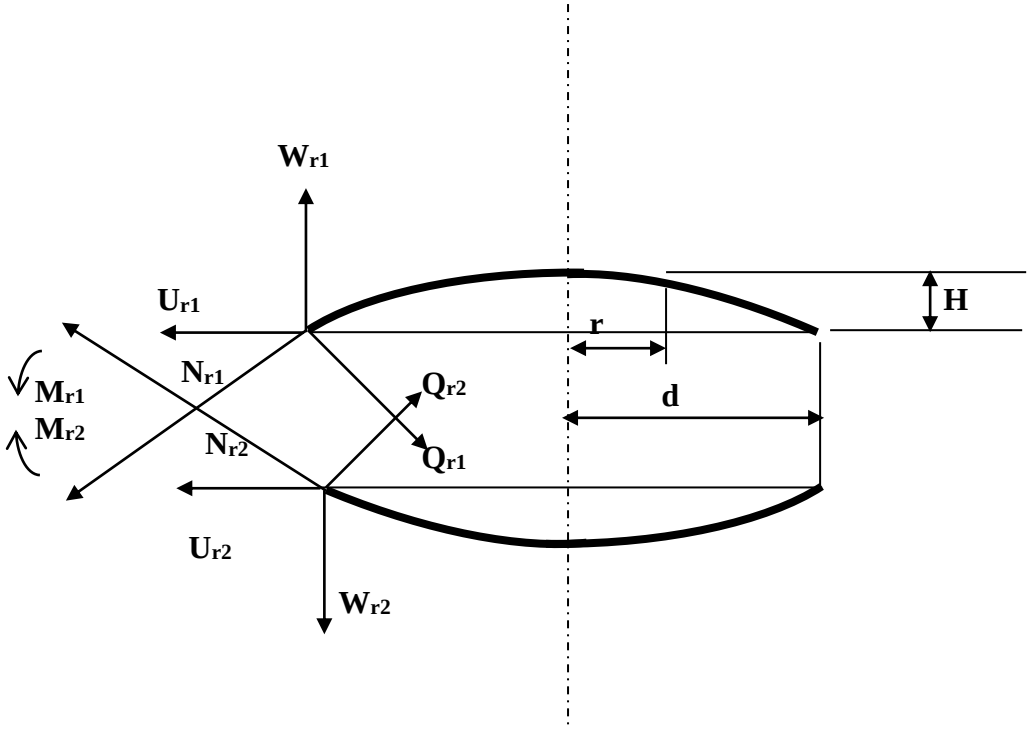

Fig. (3 – 7) Matching boundary conditions of two shallow spherical shell elements

3 . 5 Computational Procedure

The main purpose of this section is to present the computer programs used in this thesis to obtain the natural frequencies. The programs are written in Quick Basic Language.

3 . 5 . 1 Matching Boundary Conditions of Two Non – Shallow Spherical Shells :

In this section the main program for finding the natural frequencies of an oblate spheroidal shell through modelling it by two non – shallow spherical shells joined rigidly at the edge is presented.

Input data to the program includes starting the non – dimensioned frequency parameter (λ_{st}), by which the iterations will start at number of decimal digits of the natural frequency to be found, eccentricity, major axis, thickness and poison ratio of the material.

The first step is to calculate the effective radius and opening angle of the relative spherical shells model. Then the non – dimensional frequency parameter (λ_{st}) is changed to (Ω_{st}) parameter to be used in the in the process of calculations. The iteration then starts with the starting value of (Ω_{st}) that corresponds to the input parameter (λ_{st}) in the following procedure :-

1. The coefficients of the indicial third order polynomial which are functions of the non dimensional frequency parameter Ω, the poisson ratio υ, the effective radius R_r , and the thickness h, are first computed:-
2. Calling Siljak subprogram, the real and imaginary roots of the polynomial are calculated. Once these roots are found, the real and imaginary parts of the Legendre functions indices are calculated.

3. Introducing the values of the real and the imaginary parts of the index, along with the value of the opening angle, into the Legendre and the derivative Legendre subprograms, the Legendre function of the first kind and its derivative with respect to the angle (Φ) are calculated using the definition

$$P_n (\cos\Phi) = F(-n,\ n+1,\ 1,\ \sin^2\Phi/ 2) \qquad \ldots (3 . 5 . 1)$$

where, F(. . .) is the hypergeometric function, which is evaluated by using the representation : -

$$F(a, b, c, z) = \frac{\Gamma(c)}{\Gamma(a)\Gamma(b)} \sum_{k=0}^{\infty} \frac{\Gamma(a+k)\,\Gamma(b+k)}{\Gamma(c+k)} \frac{z^k}{k!} \qquad \ldots (3 . 5 . 2)$$

Here Γ (. . .) denotes the Gamma function. The derivative of the Legendre function is determined by differentiating (3.5.1) with respect to (Φ).

4. The displacements, slopes, forces and moments are then determined at the edge ($\Phi=\Phi_o$) of the spherical shells using (Eqs. 3 . 3 . 8)
5. The values equated in (4) above are then substituted in the following determinant of the boundary matched conditions :-

$$\begin{bmatrix}
C_{1,1} & .. & .. & . -C_{2,1}\sin 2\Phi_0 + C_{1,1}\cos 2\Phi_0 & .. & .. \\
C_{2,1} & .. & .. & . -C_{2,1}\cos 2\Phi_0 - C_{1,1}\sin 2\Phi_0 & .. & .. \\
C_{3,1} & .. & .. & . \ C_{3,1} & .. & .. \\
C_{4,1} & .. & .. & . -C_{4,1}\cos 2\Phi_0 - C_{5,1}\sin 2\Phi_0 & .. & .. \\
-C_{5,1} & .. & .. & . \ C_{4,1}\sin 2\Phi_0 - C_{5,1}\cos 2\Phi_0 & .. & .. \\
C_{6,1} & .. & .. & . -C_{6,1} & .. & ..
\end{bmatrix}$$

where

$C(1 , I) = P_{nI} (\cos\Phi_o)$

$C(2 , I) = -(1+\upsilon) * C_I * P_{nI}' (\cos\Phi_o)$

$C(3 , I) = P_{nI}' (\cos\Phi_o)$

$$C(4,I) = \frac{h^3}{12(1-\upsilon^2).R_r^3}\left[1+\left((1+\upsilon)C_I\right).(\upsilon+\beta_I-1).\left(P_{nI}'(\cos\Phi)\right)\right]$$

$$C(5,I) = \frac{h}{(1-\upsilon).R_r}\left[(1+C_I.\beta_I).P_{nI}(\cos\Phi_o)+(1-\upsilon).\cot\Phi.C_I .P_{nI}'(\cos\Phi)\right]$$

$$C(6,I) = \frac{h^3}{12(1-\upsilon^2).R_r^2}\left(1+(1+\upsilon)C_I\right)\left[\beta_I\left(P_{nI}(\cos\Phi)\right)+(1-\upsilon).\cot\Phi_o .P_{nI}'(\cos\Phi_o)\right]$$

where all the above symbols are the same as mentioned in section (3 . 3), I= 1, 2, 3

6. The value of the determinant is then evaluated, and recorded using the hardware of the computer. Then the computations are repeated for next value of (Ω) and the value of the determinant is compared to the value of the previous run. If, however, the sign of the value changes i.e. , from positive to negative sign, a natural frequency is expected to occur between the two successive values of (Ω). Thus the step of iteration is divided by ten and the operation is repeated until the non dimensional natural frequency with the needed accuracy is found.

3 . 5 . 2 Matching Boundary Conditions of Two Shallow Spherical Shells :

The computation process in this section is nearly identical to the previous section obviously, the calculation here follows the solution of section (3 . 4).

In order to formulate the determinant of boundary conditions, it is necessary to obtain the Bessel function of the first kind of order zero with its derivative and the Bessel function of the first kind of order one.

To do so, the (Bs1) and (MBs1) subprogram's were written using the following integral representations

$$J_n(x) = \frac{1}{\pi} \int_0^{\pi} \cos\left(n\Phi - x \cdot \sin(\Phi)\right) d\Phi \qquad \ldots (3.5.3)$$

$$I_n(Y) = \frac{1}{\pi} \int_0^{\pi} \exp\left(Y \cdot \cos(\Phi)\right) \cdot \cos(n.\Phi)\, d\Phi \qquad \ldots (3.5.4)$$

The real and imaginary parts of the Bessel function of the first kind of zero order and a complex parameter are:-

$$\mathrm{Re}\,(J_o(z)) = -J_o(x) \cdot I_o(y) - 2 \cdot J_2(x) \cdot I_2(y) + 2 \cdot J_4(x) \cdot I_4(y) \qquad \ldots (3.5.5)$$

$$\mathrm{Im}\,(J_o(z)) = -2 \cdot J_1(x) \cdot I_1(y) + 2 \cdot J_3(x) \cdot I_3(y) - 2 \cdot J_5(x) \cdot I_5(y) \qquad \ldots (3.5.6)$$

Here $z = x + iy$

also the real and imaginary parts of the Bessel function of the first kind and the first order with complex parameter are:

$$\mathrm{Re}(J_1(z)) = J_1(x) \cdot I_o(y) - J_1(x) \cdot I_2(y) + 2 \cdot J_3(x) \cdot I_2(y) - J_3(x) \cdot I_4(y) - J_5(x) \cdot I_4(y) \qquad \ldots (3.5.7)$$

$$\mathrm{Im}(J_1(z)) = J_o(x) \cdot I_1(y) - J_2(x) \cdot I_1(y) - J_2(x) \cdot I_3(y) + J_4(x) \cdot I_3(y) + J_4(x) \cdot I_5(y) \qquad (3.5.8)$$

Now, the displacements, slopes , forces and moments are computed using equations (3 . 4 . 12 – 3 . 4 . 17) and the following determinant will result :

$$\begin{bmatrix} C_{1,1} & \cdots & \cdots & \cdot & C_{1,1} & \cdots & \cdots \\ C_{2,1} & \cdots & \cdots & \cdot & -C_{2,1} & \cdots & \cdots \\ C_{3,1} & \cdots & \cdots & \cdot & -C_{3,1} & \cdots & \cdots \\ C_{4,1} & \cdots & \cdots & \cdot & C_{4,1}\cos 2\Phi_0 - C_{5,1}\sin 2\Phi_0 & \cdots & \cdots \\ C_{5,1} & \cdots & \cdots & \cdot & -C_{4,1}\sin 2\Phi_0 - C_{5,1}\cos 2\Phi_0 & \cdots & \cdots \\ C_{6,1} & \cdots & \cdots & \cdot & -C_{6,1} & \cdots & \cdots \end{bmatrix}$$

where,

$$C(1,I) = J_o(\mu_I) + \frac{(1+\upsilon).\mu_I.J_1(\mu_I)}{(1-\upsilon^2)(h/d)^2(\omega/\omega_o)^2 - \mu_I^2}$$

$$C(2,I) = J_o(\mu_I)$$

$$C(3,I) = \mu_I.J_1(\mu_I)$$

$$C(4,I) = \frac{h}{R_r}\left[\frac{-\mu_I.J_1(\mu_I) + (1+\upsilon)(h/d)^2(\omega/\omega_o)^2 J_o(\mu_I)}{(1-\upsilon^2)(h/d)^2(\omega/\omega_o)^2 - \mu_I^2}\right]$$

$$C(5,I) = -\frac{h^3}{12(1-\upsilon^2)d^3}\left[\mu_I^3.J_1(\mu_I)\right]$$

$$C(6,I) = -\frac{h^3}{12(1-\upsilon^2)d^2}\left[\mu_I\left((1-\upsilon).J_1(\mu_I) - \mu_I.J_o(\mu_I)\right)\right]$$

where all symbols are as in section (3 . 4) , I = 1 , 2 , 3

The same procedure of point (6) in the previous section is repeated until a natural frequency is found.

3 . 5 . 3 The Rayliegh Ritz's Energy Method of Two Non – Shallow Spherical Shell :

The computation process in this section is nearly identical to the section (3 . 5 . 2) obviously, the calculation here follows the solution of section (3 . 2).

The stiffness and mass are then determined at the edge ($\Phi=\Phi_o$) of the spherical shells using (Eqs. 3 . 2 . 10 , 3 . 2 .11) respectively.

The values equated in the above equations are then substituted in the following determinant :

$$\begin{vmatrix} k_{11}-\Omega^2 m_{11} & k_{12}-\Omega^2 m_{12} & k_{13}-\Omega^2 m_{13} \\ k_{21}-\Omega^2 m_{21} & k_{22}-\Omega^2 m_{22} & k_{23}-\Omega^2 m_{23} \\ k_{31}-\Omega^2 m_{31} & k_{32}-\Omega^2 m_{32} & k_{33}-\Omega^2 m_{33} \end{vmatrix} = 0$$

The same procedure of point (6) in the section (3 . 5 . 2) is repeated until a natural frequency is found.

3 . 5 . 4 The Rayliegh Ritz's Energy Method of Two Shallow Spherical Shell :

The computation process in this section is nearly identical to the previous section obviously, the calculation here follows the equations (3 . 2 . 4) , (3 . 2 . 6) and (3 . 4 . 5 – 3 . 4 . 8). However, the stiffness and the mass of shallow shell are shown below respectively :

$$k_{ij} = \int_0^d \frac{E h \pi}{(1-\upsilon^2)} \left[\frac{1}{r^2} U_{ri} U_{rj} + \frac{2}{R_r . r} U_{ri} W_{ri} + \frac{1}{R_r{}^2} W_{ri} W_{rj} + 2\upsilon \left(\frac{1}{r} U_{ri} U_{ri}' + \frac{1}{R_r . r} U_{ri} W_{ri} + \frac{1}{R_r} W_{ri} U_{ri}' + \frac{1}{R_r{}^2} W_{ri} W_{rj} \right) + U_{ri}' U_{rj}' + \frac{2}{R_r} U_{ri}' W_{ri} + \frac{1}{R_r{}^2} W_{ri} W_{rj} + \frac{h^2}{12} \left(\frac{1}{r^2} W_{ri}' W_{rj}' + 2\upsilon \frac{1}{r} W_{ri}' W_{rj}'' + W_{ri}'' W_{rj}'' \right) \right] r\, dr \qquad \ldots (3 . 5 . 9)$$

$$m_{ij} = \int_0^d \rho h \pi \left[U_i U_j + W_i W_j \right] r\, dr \qquad \ldots (3 . 5 . 10)$$

The stiffness and mass are then determined at the edge ($\Phi=\Phi_o$) of the spherical shells using (Eqs. 3 . 5 . 9 , 3 . 5 .10) respectively.

The values equated in the above equations are then substituted in the following determinant :

$$\begin{vmatrix} k_{11} - \Omega^2 m_{11} & k_{12} - \Omega^2 m_{12} & k_{13} - \Omega^2 m_{13} \\ k_{21} - \Omega^2 m_{21} & k_{22} - \Omega^2 m_{22} & k_{23} - \Omega^2 m_{23} \\ k_{31} - \Omega^2 m_{31} & k_{32} - \Omega^2 m_{32} & k_{33} - \Omega^2 m_{33} \end{vmatrix} = 0$$

The same procedure of point (6) in the section (3.5.2) is repeated until a natural frequency is found.

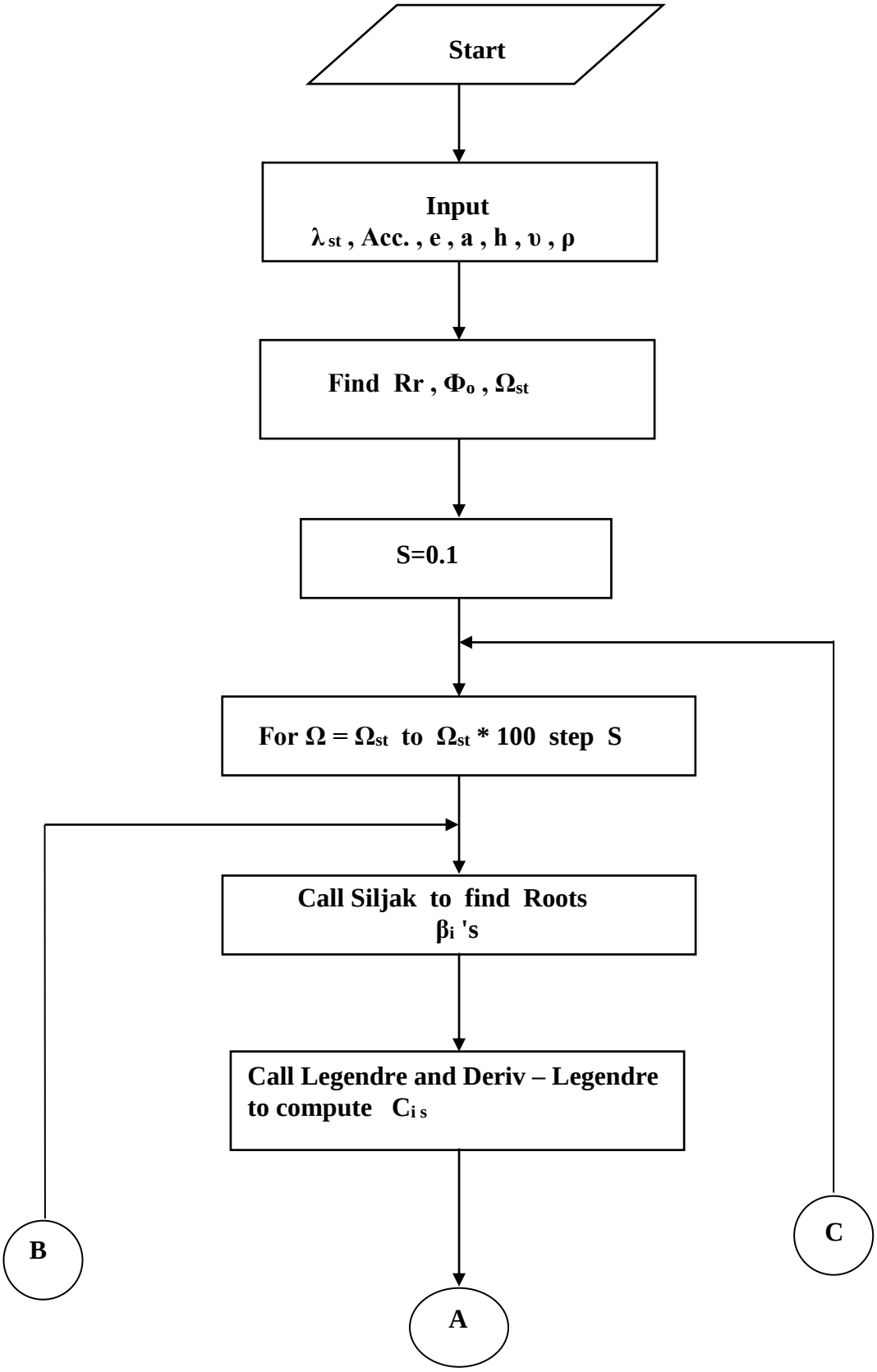

Fig. (3 – 8) Flow chart of non – shallow spheroidal shell. . . . Continue

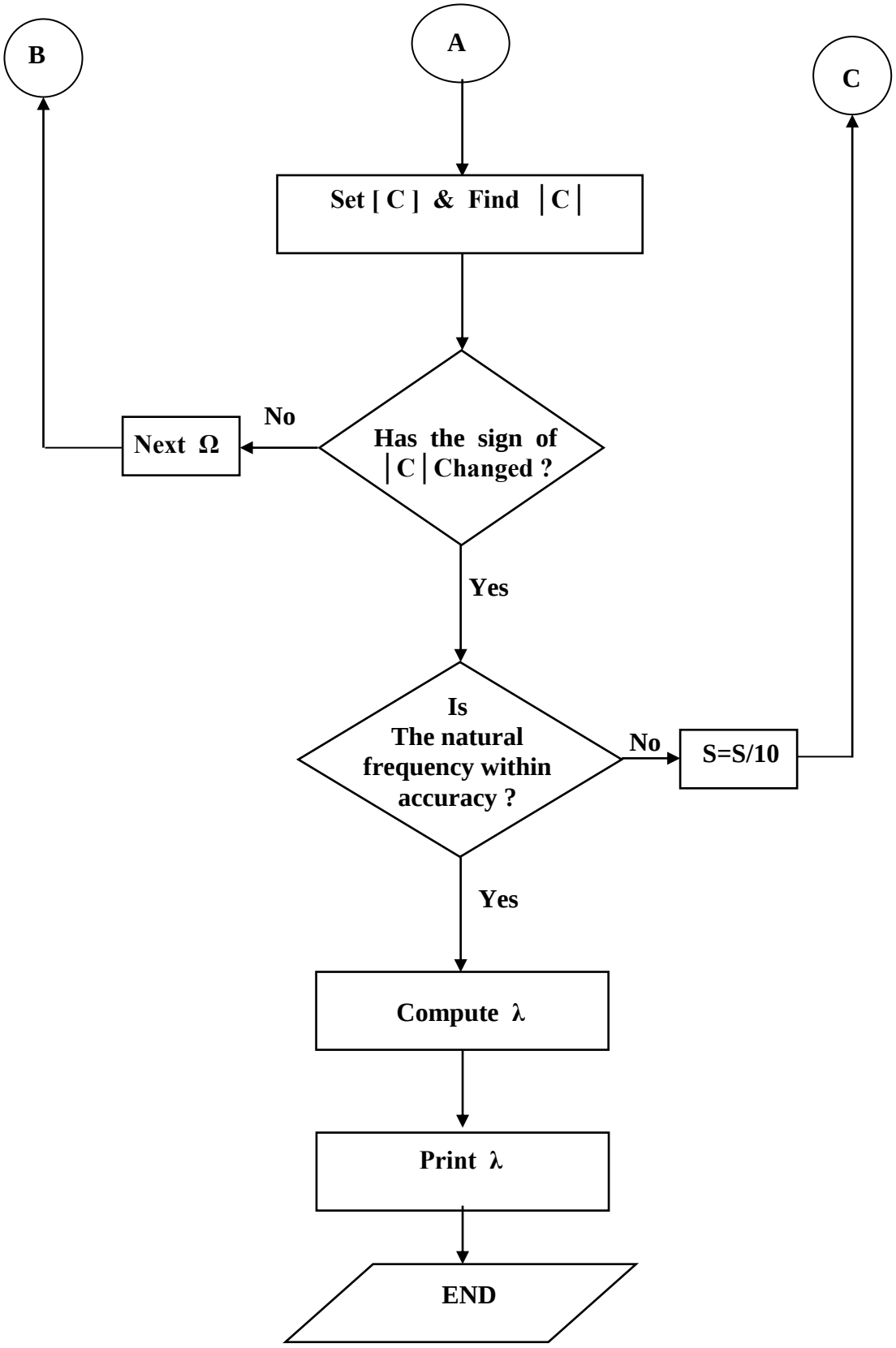
A
B
C
Set [C] & Find |C|
Has the sign of |C| Changed ?
No
Next Ω
Yes
Is The natural frequency within accuracy ?
No
S=S/10
Yes
Compute λ
Print λ
END

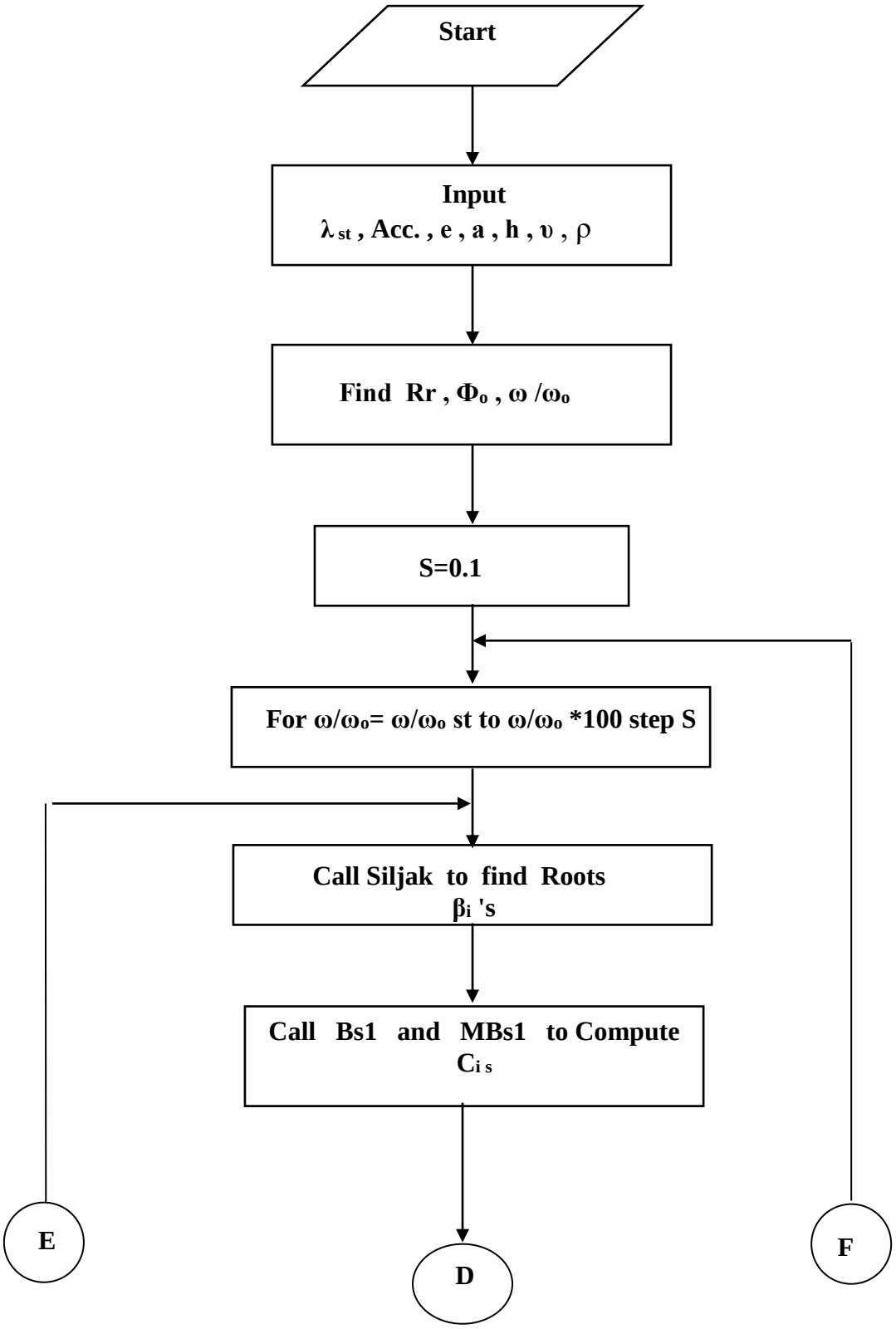

Fig. (3 – 9) Flow chart of shallow spheroidal shell. . . . Continue

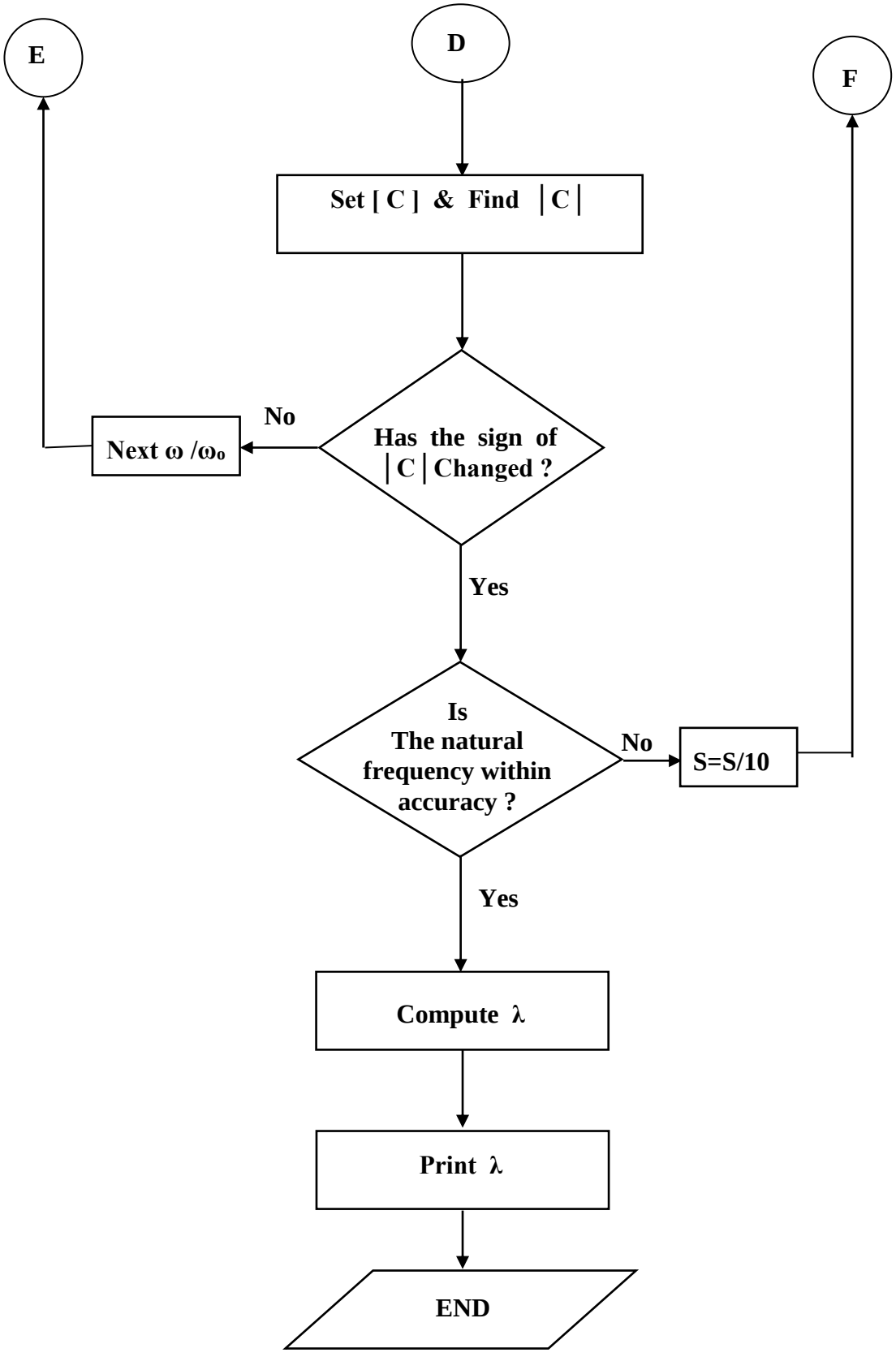
E
D
F
Set [C] & Find |C|
Has the sign of |C| Changed ?
No
Next ω /ωo
Yes
Is The natural frequency within accuracy ?
No
S=S/10
Yes
Compute λ
Print λ
END

CHAPTER Five

Conclusions and Recommendations

5 . 1 Conclusions

From the theoretical and experimental results presented in this work, the following conclusions may be drawn :

1. The Boundary Matching Method and Rayleigh – Ritz Method in this work predict fairly well the natural frequencies of an oblate spheroidal shell for all values of eccentricities while the Rayliegh Method (as pointed in the literature) was found to be limited to lower values of eccentricity (up to 0.6).
2. Natural frequencies are seen to have two types of behavior against increasing the shell thickness. One type, which is associated with the bending modes, tends to increase with the thickness, while the other type, which is associated with membrane modes remains unaffected by the thickness variation.
3. Bending modes natural frequencies tend to decrease with increasing eccentricity ratio.
4. Membrane modes natural frequencies tend to increase with increasing eccentricity ratio.

5 . 2 Recommendations for Future Work :

As a result of the work carried out here, further studies can be directed in this field. The following three points are recommended to be studied.

1. In the present work a Boundary Matching Method model of two spherical caps and Rayleigh – Ritz Method were used to predict the natural frequencies of oblate spheroidal shells, it would be interesting if the Boundary Matching Method is used for other structural model consisting of two spherical caps joined by a toroidal shell. Also it is interesting to use other method such as the Finite Element Method to the problem of this thesis.
2. It is felt that the method used in this work might be extended to include other types of practical boundary conditions such as an oblate spheroid with middle support.
3. Investigating experimentally several oblate spheroidal shells with various eccentricities , thickness ratios and boundary conditions.

REFERENCES

1 Sitzurgsber. Akard., "On the Small Free Vibration and Deformation of a Thin Elastic Shell", J. of App. Math., Vol., 146, PP. 505 – 514, 1937.

2 Reissner E., "Vibrations of shallow shell", J. of App. Math., Vol. 13, PP.169– 176, 1955.

3 Johnson M. W. and Reissner E., "On vibration of shallow spherical shell", J. App. Math., Vol. 15, PP. 367 – 380, 1958.

4 Kalnins A. and Naghdi P. M., "Axisymmetric vibration of shallow elastic spherical shells", J. Acoust. Soc. Amer., Vol. 32, PP. 342 – 347, 1960.

5 Dimaggio F. L. and Silibiger A., "Free extensional torsional vibrations of a prolate spheroidal shell", J. Acoust. Soc. Amer., Vol. 33, PP. 56 – 58, 1961.

6 Silibiger A. and. Dimaggio F. L., "Extensional axisymmetric second class vibration of a prolate spheroidal shell", Columbia University Technical Report No. 3, 1961.

7 Wilfred E. Baker " Axisymmetric modes of vibration of thin spherical shell", J. Acoust. Soc. Amer., Vol. 33, PP. 1749 – 1758, 1961.

8 Kalnins A. and Naghdi P. M., " On vibrations of elastic spherical shells", J. App. Mech., Vol. 29, PP. 65 – 72, 1962.

9 Shiraishi N. and Dimaggio F. L., "Perturbation solutions of a prolate spheroidal shells, " J. Acoust. Soc. Amer., Vol. 34, PP. 1725 – 1731, 1962.

10 Kalnins A. "Free Nonsymmetric Vibrations of Shallow Spherical Shells", J. of Appl. Mech., PP. 225 – 233, 1963.

11 Kalnins A., "Effect of bending on vibrations of spherical shells", J. Acoust. Soc. Amer., Vol. 36(1), PP. 74 – 81, 1964.

12 Kalinins A. "Free Vibration of Rotationally Symmetric Shells", J. Acoust. Soc. Amer., Vol. 36(7), PP. 1355 – 1365, 1964.

13 Numergut P. J. and Brand R. S., "Axisymmetric vibrations of a prolate spheroidal shell", J. Acoust. Soc. Amer., Vol. 38, PP. 262 – 265, 1965.

14 Penzes L. and Burgin G.," Free vibrations of thin isotropic oblate spheroidal shells", General Dynamic Report No. GD/C–BTD 65 – 113, 1965

15 Kalnins A. and Wilkinson F. P., "Natural frequencies of closed spherical shells", J. App. Mech. Vol. 9, PP. 65, 1965.

16 Dimaggio F. L. and Rand R., "Axisymmetric vibrations of prolate spheroidal shells", J. Acoust. Soc. Amer. Vol. 40, PP. 179 – 189, 1966.

17 Kraus H., "Thin elastic shells", John Wiley and Sons, New York 1967.

18 Yen T. and Dimaggio F. L., "Forced vibrations of submerged spheroidal shells", J. Acoust. Soc. Amer., Vol. 41, PP. 618 – 626, 1967.

19 Rand R. and Dimmagio F. L., "Vibrations of fluid – filled spherical and spheroidal shells", J. Acoust. Soc. Amer., Vol. 42, PP. 1278 – 1286, 1967.

20 Penzes L., " Free vibrations of thin orthotropic oblate spheroidal shells", J. Acoust. Soc. Amer., Vol. 45, pp. 500 – 505, 1969.

21 Huang H., "Transient Interaction of Plane Acoustic Waves with Spherical Elastic Shell", J. Acoust. Soc. Amer., Vol. 45(3), PP. 661 – 670, 1969.

22 Hayek S. and Dimaggio F. L., " Complex natural frequencies of vibration submerged spheroidal shells" J. of Solids and Structures Vol. 6, PP. 333 – 351, 1970.

23 Huang H. and Wang Y. F, "Transient Interaction of Spherical Acoustic Waves with Spherical Elastic Shell", J. of App. Mech., Vol. 38, PP. 71 – 74, 1971.

24 Bedrosian B. and Dimaggio F. L., "Transient response of submerged spheroidal shells", J. of Solids and Structures Vol. 8, PP. 111 – 129, 1972.

25 Baker E. H., Kovalevsky L. and Rish F. L., " Structural Analysis of Shells", Mc Graw – Hill, New York, 1972.

26 Berger B. S., "The dynamic response of a prolate spheroidal shell submerged in an acoustical medium", J. App. Mech., Vol. 41, PP. 925 – 929, 1974.

27 Warburton G. B. "The Dynamical Behavior of Shells", pergoman Press Ltd., England 1976.

28 Burroughs C. B. and Magrab E. B., "Natural frequencies of prolate spheroidal shells of constant thickness", J. of Sounds and Vibration, Vol. 57, PP. 571 – 581, 1978.

29 Gibson J. E., "Thin Shell", 1st. Ed., pergoman Press., New York, 1980.

30 Irie T., Yamada G. and Muramoto Y., " Free vibration of point – supported spherical shell", Transactions of ASME Vol. 52, PP. 890 – 896, 1985.

31 Tavakoli M. S. and Singh R., "Eigensolutions of joined / hermetic shell structures using the state space method", J. Sound and Vibration Vol. 100, PP. 97 – 123, 1989.

32 Hubert J. S. and Palencia E. S., "Vibration and Coupling of Continuous Systems", Asympotic Methods, Springer – Verlag, New York, 1989.

33 Fawaz Abbas Najim "An Investigation into the Free axisymmetric vibration characteristics of isotropic thin oblate spheroidal shells", M.Sc. thesis University of Baghdad, 1990.

34 Okazaki, A., Urata, Y. and Tatemichi, A., "Damping properties of three-layered shallow spherical shells with a constrained viscoelastic layers", JSME Intern. J., Series I., Vol. 33, PP. 145–151, 1990.

35 Zhang P. and Geer T. L., " Excitation of Fluid – Fluid, Submerged Spherical Shell by a Transient Acoustic Waves" J. Acoust. Soc. Amer. Vol. 93(2), PP. 696 – 705, 1993

36 Zhu. F., "Rayleigh – Ritz Method in Coupled Fluid – Structure Interacting Systems and Its Applications", J. Sound and Vibration Vol. 186(4), pp. 543 – 550, 1995.

37 Chang Y. C. and Demkowicz L., "A stability Analysis Vibrating Viscoelastic Spherical Shells", J. Appl. Math., Vol. 2(2), PP. 213 – 242, 1998.

38 Haym Benaroya, "Mechanical Vibration", Prentice – Hill, Inc., U.S.A., 1998.

39 Michael A. Spague and Thomas L. Geers, "Response of Empty and Fluid – Filled, Submerged Spherical Shells to plane and spherical, Step – Exponential Acoustic Waves" J. of Shock and Vibration, Vol. 6, PP. 147 – 157, 1999.

40 Aleksandr Korjanik, Rolands Rikards, Holmalte Bachand and Andris Chate, "Free Damped Vibrations of Sandwich Shells of Revolution", J.of Sandwich Structures and Materials, Vol.(3), PP. 171 – 196, 2001.

41 Antoine Chaigne, Mathieu Fontaine, Oliver Thomas, Michel Ferre, Cyril Tou., "Vibrations of Shallow Spherical Shells and Gongs", J. of Sound and Vibration, 2002.

APPENDIX

INTRODUCTION

Derivation of the differential equations of motion of an oblate spheroidal shell is conducted in terms of a curvilinear coordinate system based upon the radii , R_Φ , R_θ , which expresses the principal curvatures of the surface as function of the angle of inclination (Φ'). This appendix is provided for the purpose of deriving R_Φ and R_θ as function of (Φ') by transformation from the oblate spheroidal coordinate system, and , for deriving the actual differential equations of motion of an oblate spheroidal shell including the effect of bending resistance.

Finally all forces and moments are derived as functions of displacements.

APPENDIX A . 1

DERIVATION OF RADII OF CURVATURES

1 – OBLATE SPHEROIDAL COORDINATES

Consider the oblate spheroidal coordinate system

$x = p \cosh\alpha \cos\beta \cos\theta$ . . . (A . 1 . 1)

$y = p \cosh\alpha \cos\beta \sin\theta$ . . . (A . 1 . 2)

$z = p \sinh\alpha \sin\beta$ . . . (A . 1 . 3)

$p = a \cdot e$ . . . (A . 1 . 4)

For the equation of oblate spheroid, however, α must be constant, we can therefore write:

$\cosh\alpha = c$ . . . (A . 1 . 5)

$$e = \frac{1}{\cosh\alpha} = \frac{1}{c}$$ . . . (A . 1 . 6)

In view of these consideration, the equations of the oblate spheroidal shell can be written in the following form,

$x = p \cdot c \cdot \cos\beta \cdot \cos\theta = a \cdot \cos\beta \cdot \cos\theta$ . . . (A . 1 . 7)

$y = p \cdot c \cdot \cos\beta \cdot \sin\theta = a \cdot \cos\beta \cdot \sin\theta$ . . . (A . 1 . 8)

$z = p \cdot \sqrt{c^2 - 1} \cdot \sin\beta = a \cdot \sqrt{1 - e^2} \cdot \sin\beta$ . . . (A . 1 . 9)

2 – VECTORIAL REPRESENTATION OF THE SURFCE

Let the position vector of the ellipsoid be represented in the following form:

$r = x.i + y.j + z.k = a\cos\beta \cos\theta i + a\cos\beta \sin\theta j + a\sqrt{1 - e^2} \sin\beta k$

(A . 1 . 10)

now a rotational ellipsoid can be represented by the equation

$$\frac{\zeta^2}{a^2}+\frac{z^2}{a^2\tanh^2\alpha}=1 \qquad \ldots (A.1.11)$$

where $\zeta^2=x^2+y^2$

which represents an oblate spheroidal surface

3 – PROPERTIES OF THE SURFACE

The first fundamental form of an element of the arc of ellipsoid can be expressed as:

$$ds^2 = E \cdot d\beta^2 + 2F \cdot d\beta\, d\theta + G \cdot d\theta^2 \qquad \ldots (A.1.12)$$

where $r_\beta = \frac{\delta r}{\delta \beta}$

$$E = r_\beta \cdot r_\beta = a^2 (1 - e^2 \cos^2\beta) \qquad \ldots (A.1.13)$$

$$F = r_\beta\, r_\theta = 0 \qquad \ldots (A.1.14)$$

$$G = r_\theta\, r_\theta = a^2 \cos^2\beta \qquad \ldots (A.1.15)$$

The discriminate is

$$\sqrt{EG-F^2}=a^2\cos\beta\sqrt{1-e^2\cos^2\beta} \qquad \ldots (A.1.16)$$

The normal unit vector of the oblate spheroid is

$$N=\frac{(r_\theta * r_\beta)}{\sqrt{EG-F^2}} \qquad \ldots (A.1.17)$$

$$= \frac{1}{\sqrt{1-e^2\cos^2\beta}}(\sqrt{1-e^2}\cos\beta\cos\theta\, i+\sqrt{1-e^2}\cos\beta\cos\theta\, j+\sin\beta\, k \qquad \ldots (A.1.18)$$

or

$$N = N_1 \cdot i + N_2 \cdot j + N_3 \cdot k \qquad \ldots (A.1.19)$$

Where i, j, k are the unit vectors of the coordinate system. Now it can easily be calculate that.

$$\cos\Phi' = \frac{N_3}{|N|} = \frac{\sin\beta}{\sqrt{1-e^2\cos^2\beta}} \qquad \ldots (A.1.20)$$

where (Φ') is the angle in the space between the vertical axis and the normal vector.

The terms of the second fundamental form of the surface are:-

$$e^{\bullet} = \frac{r_{\beta\beta}.r_{\beta}.r_{\theta}}{\sqrt{EG-F^2}} = \sqrt{\frac{1-e^2}{1-e^2\cos^2\beta}} \qquad \ldots (A.1.21)$$

$$\left.\begin{aligned} .r_{\beta\beta} &= \frac{\delta^2 r}{\delta\beta^2} \\ r_{\theta\theta} &= \frac{\delta^2 r}{\delta\theta^2} \end{aligned}\right\} \qquad \ldots (A.1.22)$$

$$g = \frac{(r_{\theta\theta}\, r_{\beta}\, r_{\theta})}{\sqrt{EG-F^2}} = \frac{a\sqrt{1-e^2}.\cos^2\beta}{\sqrt{1-e^2\cos^2\beta}} \qquad \ldots (A.1.23)$$

The normal curvatures of the surface X1 and X2, in the two principle directions are

$$X1 = \frac{1}{R_{\Phi}} = \frac{e^{\bullet}}{E} = \frac{\sqrt{1-e^2}}{a(1-e^2.\cos^2\beta)^{3/2}} \qquad \ldots (A.1.24)$$

$$X2 = \frac{1}{R_{\theta}} = \frac{g}{G} = \frac{\sqrt{1-e^2}}{a(1-e^2.\cos^2\beta)} \qquad \ldots (A.1.25)$$

The two principal radii of the surface can be then written as

$$R_{\Phi} = \frac{a(1-e^2\cos^2\beta)^{3/2}}{\sqrt{1-e^2}} = \frac{(1-e^2).R_{\theta}^3}{a^2} \qquad \ldots (A.1.26)$$

$$R_{\theta} = \frac{a\sqrt{1-e^2\cos^2\beta}}{\sqrt{1-e^2}} \qquad \ldots (A.1.27)$$

Now the radii can be expressed as a function of the variable Φ' alone in the following form.

$$R_{\Phi} = \frac{a(1-e^2)}{(1-e^2\cos^2\Phi')^{3/2}} \quad \ldots (A.1.28)$$

$$R_{\theta} = \frac{a}{(1-e^2\cos^2\Phi')} \quad \ldots (A.1.29)$$

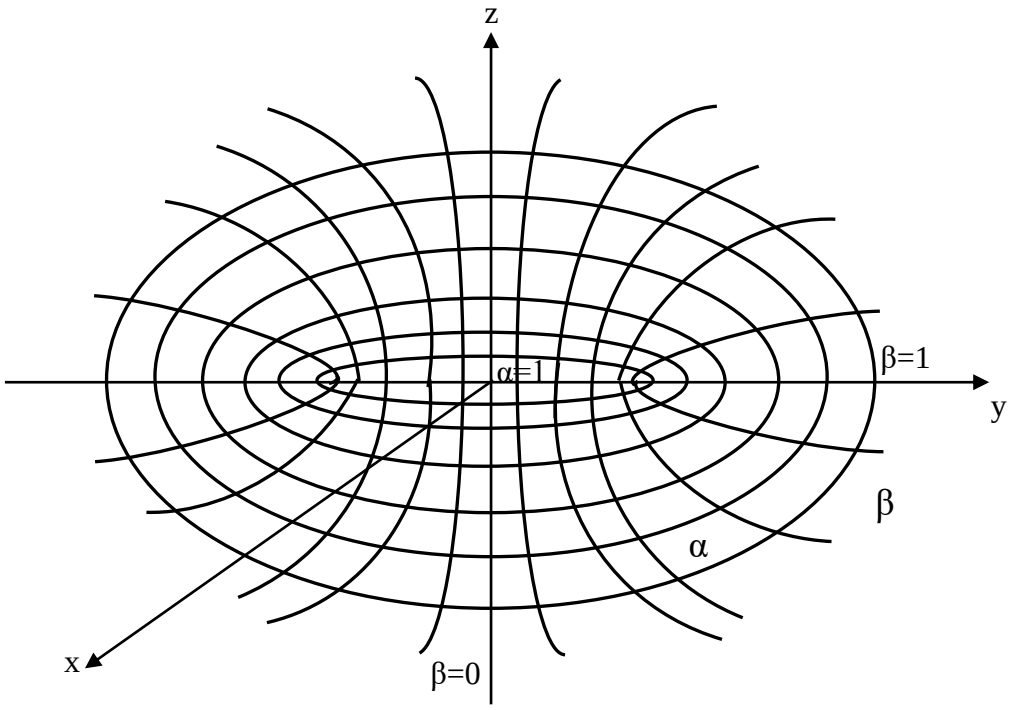

A1 Spheroidal Shell Coordinate System

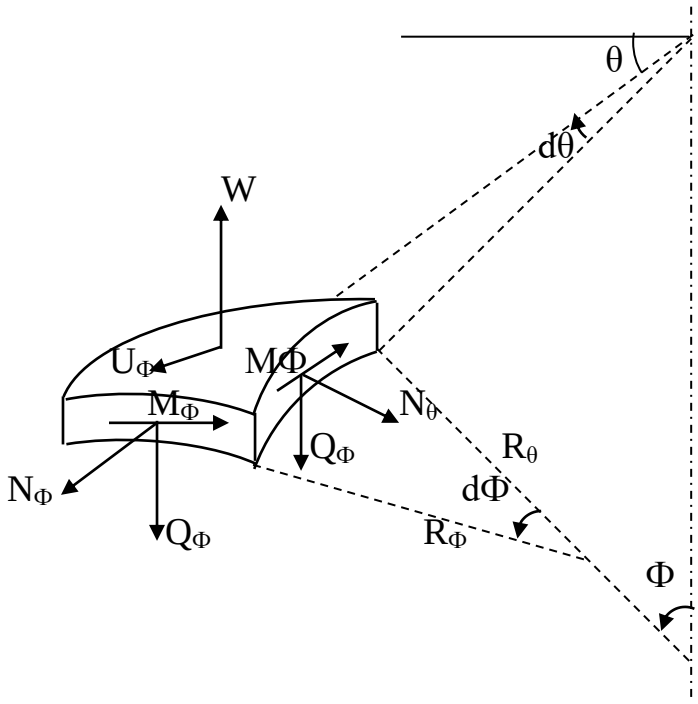

A2 Oblate Spheroidal Shell Element

APPENDIX A . 2

DERIVATION OF THE EQUATIONS OF MOTION

The vectors N_Φ and N_θ are the forces per unit length of the section corresponding to the stresses σ_Φ and σ_θ

The victors M_Φ and M_θ are the moment per unit length of the section corresponding to the stress couples. Finally the Q vector is the transverse shearing stress resultant, as represented in Fig. A2. The equations of motion may be derived by using Loves' assumptions :-

That if the shell is thin it may be assumed that the displacements in the θ and Φ direction vary linearly through the shell thickness while the displacements are independent of thickness. Moreover, if we assume that we may neglect shear deflections which implies that the normal shear strains are zero and neglecting the rotator inertia we get:-

$$\frac{\partial N_1 A_2}{\partial \alpha_1}+\frac{\partial N_{21} A_1}{\partial \alpha_2}+N_{12}\frac{\partial A_2}{\partial \alpha_2}-N_2\frac{\partial A_2}{\partial \alpha_1}+A_1 A_2\frac{Q_1}{R_1}=A_1 A_2 \rho\, h\frac{\partial^2 u_1}{\partial t} \qquad \ldots (A.2.1)$$

$$\frac{\partial N_{12} A_2}{\partial \alpha_1}+\frac{\partial N_2 A_1}{\partial \alpha_2}+N_{21}\frac{\partial A_2}{\partial \alpha_1}-N_1\frac{\partial A_1}{\partial \alpha_{21}}+A_1 A_2\frac{Q_2}{R_2}=A_1 A_2 \rho\, h\frac{\partial^2 u_2}{\partial t} \qquad \ldots (A.2.2)$$

$$\frac{\partial Q_1 A_2}{\partial \alpha_1}+\frac{\partial Q_2 A_1}{\partial \alpha_2}-\left(\frac{N_1}{R_1}+\frac{N_2}{R_2}\right)A_1 A_2 = A_1 A_2 \rho\frac{\partial^2 w}{\partial t} \qquad \ldots (A.2.3)$$

$$\frac{\partial M_1 A_2}{\partial \alpha_1}+\frac{\partial M_{21} A_1}{\partial \alpha_2}+M_{12}\frac{\partial A_1}{\partial \alpha_2}-M_2\frac{\partial A_2}{\partial \alpha_1}-Q_1 A_1 A_2=0 \qquad \ldots (A.2.4)$$

$$\frac{\partial M_{12} A_2}{\partial \alpha_1}+\frac{\partial M_2 A_1}{\partial \alpha_2}+M_{21}\frac{\partial A_2}{\partial \alpha_1}-M_1\frac{\partial A_1}{\partial \alpha_2}-Q_2 A_1 A_2=0 \qquad \ldots (A.2.5)$$

Now for our case applying the following terms,

$R_1 = R_\Phi$ . . . (A . 2 . 6)
$\alpha_1 = \Phi'$

$R_2 = R_\theta$ . . . (A . 2 . 7)
$\alpha_2 = \theta$

$A_1 = R_\Phi$ . . . (A . 2 . 8)

$A_2 = R_\theta \sin\Phi'$ . . . (A . 2 . 9)

$N_1 = N_\Phi,\ N_2 = N_\theta,\ M_1 = M_\Phi,\ M_2 = M_\theta,\ N_{12} = N_{\Phi\theta},\ M_{12} = M_{\Phi\theta}$
. . . (A . 2 . 10)

Moreover assuming axisymmetric motion where all derivatives with respect to θ are zero and

$N_{\Phi\theta} = M_{\Phi\theta} = Q_\theta = u_2 = 0$ . . . (A . 2 . 11)

we get the following equations

$$\frac{\partial}{\partial\Phi'}(N_\Phi R_\theta \sin\Phi') - N_\theta R_\Phi \cos\Phi' + Q_\Phi R_\theta \sin\Phi' = \rho\, h R_\Phi R_\theta \sin\Phi' \frac{\partial^2 u}{\partial t^2}$$
. . . (A . 2 . 12)

$$\frac{\partial}{\partial\Phi'}(Q R_\theta \sin\Phi') - \left(\frac{N_\Phi}{R_\Phi} + \frac{N_\theta}{R_\theta}\right) . R_\Phi R_\theta \sin\Phi' = \rho\, h R_\Phi R_\theta \sin\Phi' \frac{\partial^2 w}{\partial t^2}$$
. . . (A . 2 . 13)

$$\frac{\partial}{\partial\Phi'}(M_\Phi R_\theta \sin\Phi') - M_\theta R_\Phi \cos\Phi' - Q R_\Phi R_\theta \sin\Phi' = 0$$ . . . (A . 2 . 14)

The strains, expressed in terms of displacements, can be written as:

$$\varepsilon_\Phi^\circ = \frac{1}{R_\Phi}\left[\frac{\partial u_\Phi}{\partial\Phi'} + w\right]$$ . . . (A . 2 . 15)

$$\varepsilon_\theta^\circ = \frac{1}{R_\theta \sin\Phi'}\left[u_\Phi \cos\Phi' + w\sin\Phi'\right] = \frac{1}{R_\theta}\left[u_\Phi \cot\Phi' + w\right]$$ . . . (A . 2 . 16)

$$k_{\Phi} = \frac{1}{R_{\Phi}} \frac{\partial}{\partial \Phi'} \left[\frac{1}{R_{\Phi}} \left(u_{\Phi} - \frac{\partial w}{\partial \Phi'} \right) \right] \quad \ldots (A . 2 . 17)$$

$$k_{\theta} = \frac{1}{R_{\Phi} \sin \Phi'} \left[\frac{\cos \Phi'}{R_{\Phi}} \left(u_{\Phi} - \frac{\partial w}{\partial \Phi'} \right) \right] \quad \ldots (A . 2 . 18)$$

If E , υ are as in nomenclature then, the forces, moments and the shearing forces per unit length will be

$$N_{\Phi} = \frac{E\, h}{1-\upsilon^2} \left[\varepsilon_{\Phi}^{\circ} + \varepsilon_{\theta}^{\circ} \right] \quad \ldots (A . 2 . 19)$$

$$N_{\theta} = \frac{E\, h}{1-\upsilon^2} \left[\varepsilon_{\theta}^{\circ} + \upsilon\, \varepsilon_{\Phi}^{\circ} \right] \quad \ldots (A . 2 . 20)$$

$$M_{\Phi} = \frac{E\, h^3}{12(1-\upsilon^2)} \left[k_{\Phi} + \upsilon\, k_{\theta} \right] \quad \ldots (A . 2 . 21)$$

$$M_{\theta} = \frac{E\, h^3}{12(1-\upsilon^2)} \left[k_{\theta} + \upsilon\, k_{\Phi} \right] \quad \ldots (A . 2 . 22)$$

Substituting the relevant expressions we get :-

$$N_{\Phi} = \frac{E\, h}{1-\upsilon^2} \left[\frac{1}{R_{\Phi}} \left(\frac{\partial u_{\Phi}}{\partial \Phi'} + w \right) + \frac{\upsilon}{R_{\Phi}} \left(u_{\Phi} \cot \Phi' + w \right) \right] \quad \ldots (A . 2 . 23)$$

$$N_{\theta} = \frac{E\, h}{1-\upsilon^2} \left[\frac{1}{R_{\theta}} \left(u_{\Phi} \cot \Phi' + w \right) + \frac{\upsilon}{R_{\Phi}} \left(\frac{\partial u_{\Phi}}{\partial \Phi'} + w \right) \right] \quad \ldots (A . 2 . 24)$$

$$M_{\Phi} = \frac{E\, h^3}{12(1-\upsilon^2)} \left[\frac{1}{R_{\Phi}} \frac{\partial}{\partial \Phi'} \frac{1}{R_{\theta}} \left(u_{\Phi} - \frac{\partial w}{\partial \Phi'} \right) + \frac{\upsilon \cos \Phi'}{R_{\Phi} R_{\theta} \sin \Phi'} \left(u_{\Phi} - \frac{\partial w}{\partial \Phi'} \right) \right] \quad \ldots (A . 2 . 25)$$

$$M_{\theta} = \frac{E\, h^3}{12(1-\upsilon^2)} \left[\frac{\cos \Phi'}{R_{\Phi} R_{\theta} \sin \Phi'} \left(u_{\Phi} - \frac{\partial w}{\partial \Phi'} \right) + \frac{\upsilon}{R_{\Phi}} \frac{\partial}{\partial \Phi'} \left(\frac{1}{R_{\theta}} \left(u_{\Phi} - \frac{\partial w}{\partial \Phi'} \right) \right) \right]$$

APPENDIX

DERIVATION OF THE RAYLEIGH – RITZ'S ENERGY METHOD for NON – SHALLOW SPHEROIDAL SHELL:

From an expression for maximum potential energy [Umax]

$$
\begin{aligned}
U_{max} = \frac{E\,h}{2(1-\upsilon^2)} \int_0^{2\pi}\int_0^{2\pi} \frac{h^2}{12}\Bigg[\frac{1}{R_\Phi^2}\Bigg[\frac{\partial}{\partial\Phi'}\Bigg[\frac{U_\Phi}{R_\Phi} - \frac{\partial W}{R_\Phi\,\partial\Phi'}\Bigg]\Bigg]^2 \\
+ \frac{\cos^2\Phi'}{R_\Phi^2\,R_\theta^2\,\sin^2\Phi'}\Bigg[U_\Phi - \frac{\partial W}{\partial\Phi'}\Bigg]^2 + 2\,\upsilon\,\frac{\cos\Phi'}{R_\theta\,R_\Phi^2\,\sin\Phi'}\Bigg[U_\Phi - \frac{\partial W}{\partial\Phi'}\Bigg]. \\
\cdot\frac{\partial}{\partial\Phi'}\Bigg[\frac{U_\Phi}{R_\Phi} - \frac{\partial W}{R_\Phi\,\partial\Phi'}\Bigg]\Bigg] + \frac{1}{R_\Phi^2}\Bigg[\frac{\partial U_\Phi}{\partial\Phi'} + W\Bigg]^2 \\
+ \frac{1}{(R_\theta\,\sin\Phi')^2}(U_\Phi\cos\Phi' + W\sin\Phi')^2 \\
+ \frac{2\,\upsilon}{R_\theta\,R_\Phi\sin\Phi'}\Bigg[\frac{\partial U_\Phi}{\partial\Phi'} + W\Bigg].(U_\Phi\cos\Phi' + W\sin\Phi').\\
R_\Phi\,R_\theta\,\sin\Phi'\,d\Phi'\,d\theta
\end{aligned}
\qquad (B.1)
$$

but

$$
\left.
\begin{aligned}
W(\Phi') = \sum_{i=1}^{n} a_i\,.\,W_i(\Phi') \;,\; U_\Phi(\Phi') = \sum_{i=1}^{n} b_i\,.\,U_{\Phi i}(\Phi') \\
\frac{\partial W(\Phi')}{\partial\Phi} = \sum_{i=1}^{n} a_i\,.\,\frac{\partial W_i(\Phi')}{\partial\Phi} \;,\; \frac{\partial U_\Phi(\Phi')}{\partial\Phi} = \sum_{i=1}^{n} b_i\,.\,\frac{\partial U_{\Phi i}(\Phi')}{\partial\Phi}
\end{aligned}
\right\} \qquad (B.2)
$$

After substituting Eq.(B . 2) into Eq. (B . 1) yield the following expression:

$$U_{max} = \frac{E\,h}{2(1-\upsilon^2)} \int_0^{2\pi} \int_0^{2\pi} \frac{h^2}{12} \left[\frac{1}{R_\Phi^2} \left[\frac{\partial}{\partial \Phi'} \left[\frac{\sum_{i=1}^{n} b_i . U_{\Phi i}(\Phi')}{R_\Phi} - \sum_{i=1}^{n} a_i \frac{\partial W_i(\Phi')}{R_\Phi \, \partial \Phi'} \right] \right]^2 \right.$$

$$+ \frac{\cos^2 \Phi'}{R_\Phi^2 \; R_\theta^2 \; \sin^2 \Phi'} \left[\sum_{i=1}^{n} b_i . U_{\Phi i}(\Phi') - \sum_{i=1}^{n} a_i \frac{\partial W_i(\Phi')}{\partial \Phi'} \right]^2$$

$$+ \; 2\,\upsilon \frac{\cos \Phi'}{R_\theta \; R_\Phi^2 \; \sin \Phi'} \left[\sum_{i=1}^{n} b_i . U_{\Phi i}(\Phi') - \sum_{i=1}^{n} a_i \frac{\partial W_i(\Phi')}{\partial \Phi'} \right] .$$

$$\left. . \frac{\partial}{\partial \Phi'} \left[\frac{\sum_{i=1}^{n} b_i . U_{\Phi i}(\Phi')}{R_\Phi} - \sum_{i=1}^{n} a_i \frac{\partial W_i(\Phi')}{R_\Phi \, \partial \Phi'} \right] \right]$$

$$+ \frac{1}{R_\Phi^2} \left[\sum_{i=1}^{n} b_i . \frac{\partial U_{\Phi i}(\Phi')}{\partial \Phi} + \sum_{i=1}^{n} a_i . W_i(\Phi') \right]^2$$

$$+ \frac{1}{(R_\theta \; \sin \Phi')^2} \left(\sum_{i=1}^{n} b_i . U_{\Phi i}(\Phi') \cos \Phi' \; + \sum_{i=1}^{n} a_i . W_i(\Phi') \sin \Phi' \right)^2$$

$$+ \frac{2\,\upsilon}{R_\theta \; R_\Phi \sin \Phi'} \left[\sum_{i=1}^{n} b_i . \frac{\partial U_{\Phi i}(\Phi')}{\partial \Phi} + \sum_{i=1}^{n} a_i . W_i(\Phi') \right] .$$

$$. \left(\sum_{i=1}^{n} b_i . U_{\Phi i}(\Phi') \cos \Phi' + \sum_{i=1}^{n} a_i . W_i(\Phi') \sin \Phi' \right) .$$

$$R_\Phi \; R_\theta \; \sin \Phi' d\Phi' \, d\theta$$

(B . 3)

After algebraic simplification for Eq. (B . 3) yield the following expression :

$$U_{\max} = \frac{E\,h}{2(1-\upsilon^2)} \int_0^{2\pi} \int_0^{2\pi} \frac{h^2}{12} \left[\frac{1}{R_\Phi^2} \left[\left[\frac{1}{R_\Phi} \left(\sum_{i=1}^{n} b_i . \frac{\partial U_{\Phi i}(\Phi')}{\partial \Phi} - \sum_{i=1}^{n} a_i \frac{\partial^2 W_i(\Phi')}{R_\Phi \, \partial \Phi'^2} \right) \right] \right]^2 \right.$$

$$+ \frac{\cos^2 \Phi'}{R_\Phi^2 \; R_\theta^2 \; \sin^2 \Phi'} \left[\sum_{i=1}^{n} b_i . U_{\Phi i}(\Phi') - \sum_{i=1}^{n} a_i \frac{\partial W_i(\Phi')}{\partial \Phi'} \right]^2$$

$$+ \; 2\,\upsilon \frac{\cos\Phi'}{R_\theta \; R_\Phi^2 \; \sin\Phi'} \left[\sum_{i=1}^{n} b_i . U_{\Phi i}(\Phi') - \sum_{i=1}^{n} a_i \frac{\partial W_i(\Phi')}{\partial \Phi'} \right] .$$

$$\left. \cdot \left[\frac{1}{R_\Phi} \left(\sum_{i=1}^{n} b_i . \frac{\partial U_{\Phi i}(\Phi')}{\partial \Phi} - \sum_{i=1}^{n} a_i \frac{\partial^2 W_i(\Phi')}{R_\Phi \, \partial \Phi'^2} \right) \right] \right]$$

$$+ \frac{1}{R_\Phi^2} \left[\sum_{i=1}^{n} b_i . \frac{\partial U_{\Phi i}(\Phi')}{\partial \Phi} + \sum_{i=1}^{n} a_i . W_i(\Phi') \right]^2$$

$$+ \frac{1}{(R_\theta \sin\Phi')^2} \left(\sum_{i=1}^{n} b_i . U_{\Phi i}(\Phi') \cos\Phi' + \sum_{i=1}^{n} a_i . W_i(\Phi') \sin\Phi' \right)^2$$

$$+ \frac{2\,\upsilon}{R_\theta \; R_\Phi \sin\Phi'} \left[\sum_{i=1}^{n} b_i . \frac{\partial U_{\Phi i}(\Phi')}{\partial \Phi} + \sum_{i=1}^{n} a_i . W_i(\Phi') \right] .$$

$$\cdot \left(\sum_{i=1}^{n} b_i . U_{\Phi i}(\Phi') \cos\Phi' + \sum_{i=1}^{n} a_i . W_i(\Phi') \sin\Phi' \right) .$$

$$R_\Phi \; R_\theta \; \sin\Phi' d\Phi' \, d\theta$$

$$U_{max} = \frac{E\,h}{2(1-\upsilon^2)} \int_0^{2\pi} \int_0^{2\pi} \frac{h^2}{12} \left[\frac{1}{R_\Phi^2} \left[\frac{1}{R_\Phi{}^2} \left\{ \left(\sum_{i=1}^{n} b_i . \frac{\partial U_{\Phi i}(\Phi')}{\partial \Phi} \right)^2 - 2 \sum_{i=1}^{n} b_i . \frac{\partial U_{\Phi i}(\Phi')}{\partial \Phi} . \right. \right. \right.$$

$$\left. \left. \left. . \sum_{i=1}^{n} a_i \frac{\partial^2 W_i(\Phi')}{R_\Phi \, \partial \Phi'^2} + \left(\sum_{i=1}^{n} a_i \frac{\partial^2 W_i(\Phi')}{R_\Phi \, \partial \Phi'^2} \right)^2 \right\} \right]$$

$$+ \frac{\cos^2 \Phi'}{R_\Phi^2 \; R_\theta^2 \; \sin^2 \Phi'} \left[\left(\sum_{i=1}^{n} b_i . U_{\Phi i}(\Phi') \right)^2 - 2 \sum_{i=1}^{n} b_i . U_{\Phi i}(\Phi') . \sum_{i=1}^{n} a_i \frac{\partial W_i(\Phi')}{\partial \Phi'} \right.$$

$$\left. + \left(\sum_{i=1}^{n} a_i \frac{\partial W_i(\Phi')}{\partial \Phi'} \right)^2 \right]$$

$$+ 2\,\upsilon \frac{\cos\Phi'}{R_\theta \; R_\Phi^3 \; \sin\Phi'} \left[\sum_{i=1}^{n} b_i . U_{\Phi i}(\Phi') . \sum_{i=1}^{n} b_i \frac{\partial U_{\Phi i}(\Phi')}{\partial \Phi} - \sum_{i=1}^{n} b_i . U_{\Phi i}(\Phi') . \right.$$

$$. \sum_{i=1}^{n} a_i \frac{\partial W_i{}^2(\Phi')}{\partial \Phi'^2} - \sum_{i=1}^{n} a_i \frac{\partial W_i(\Phi')}{\partial \Phi'} . \sum_{i=1}^{n} b_i \frac{\partial U_{\Phi i}(\Phi')}{\partial \Phi}$$

$$\left. + \sum_{i=1}^{n} a_i \frac{\partial W_i(\Phi')}{\partial \Phi'} . \sum_{i=1}^{n} a_i \frac{\partial W_i{}^2(\Phi')}{\partial \Phi'^2} \right]$$

$$+ \frac{1}{R_\Phi^2} \left[\left(\sum_{i=1}^{n} b_i . \frac{\partial U_{\Phi i}(\Phi')}{\partial \Phi} \right)^2 + 2 \sum_{i=1}^{n} b_i . \frac{\partial U_{\Phi i}(\Phi')}{\partial \Phi} . \sum_{i=1}^{n} a_i . W_i(\Phi') \right.$$

$$\left. + \left(\sum_{i=1}^{n} a_i . W_i(\Phi') \right)^2 \right]$$

$$+ \frac{1}{(R_\theta \; \sin\Phi')^2} \left[\left(\sum_{i=1}^{n} b_i . U_{\Phi i}(\Phi') \cos\Phi' \right)^2 + 2 \sum_{i=1}^{n} b_i . U_{\Phi i}(\Phi') \cos\Phi' . \right.$$

$$\left. . \sum_{i=1}^{n} a_i . W_i(\Phi') \sin\Phi' + \left(\sum_{i=1}^{n} a_i . W_i(\Phi') \sin\Phi' \right)^2 \right]$$

$$+ \frac{2\,\upsilon}{R_\theta \; R_\Phi \sin\Phi'} \left[\left(\sum_{i=1}^{n} b_i . \frac{\partial U_{\Phi i}(\Phi')}{\partial \Phi} . \sum_{i=1}^{n} b_i . U_{\Phi i}(\Phi') \cos\Phi' \right) \right.$$

$$+ \left(\sum_{i=1}^{n} b_i . \frac{\partial U_{\Phi i}(\Phi')}{\partial \Phi} . \sum_{i=1}^{n} a_i . W_i(\Phi') \sin\Phi' \right)$$

$$+ \left(\sum_{i=1}^{n} a_i . W_i(\Phi') . \sum_{i=1}^{n} b_i . U_{\Phi i}(\Phi') \cos\Phi' \right)$$

$$\left. + \left(\sum_{i=1}^{n} a_i . W_i(\Phi') . \sum_{i=1}^{n} a_i . W_i(\Phi') \sin\Phi' \right) \right] \; R_\Phi \; R_\theta \; \sin\Phi' d\Phi' \, d\theta \qquad (B.4)$$

but

$$\left.\begin{aligned}\left(\sum_{i=1}^{n} a_i . W_i(\Phi')\right)^2 &= \sum_{i=1}^{n}\sum_{j=1}^{n} a_i\, a_j\, W_i(\Phi').W_j(\Phi') \\ \left(\sum_{i=1}^{n} b_i . U_{\Phi i}(\Phi')\right)^2 &= \sum_{i=1}^{n}\sum_{j=1}^{n} b_i\, b_j\, U_{\Phi\ i}(\Phi').U_{\Phi\, j}(\Phi')\end{aligned}\right\} \qquad (B.5)$$

hence

$$\begin{aligned}U_{\max} = \frac{E\,h}{2(1-\upsilon^2)}\Bigg[\frac{h^2}{12}\Bigg\{\frac{1}{R_\Phi{}^4}\Bigg[&\sum_{i=1}^{n}\sum_{j=i}^{n} b_i b_j . \int_0^{2\pi}\int_0^{2\pi} \frac{\partial U_{\Phi i}}{\partial\Phi}\cdot\frac{\partial U_{\Phi j}}{\partial\Phi} \\ &- 2\sum_{i=1}^{n} b_i \sum_{j=i}^{n} a_i \int_0^{2\pi}\int_0^{2\pi} \frac{\partial U_{\Phi i}}{\partial\Phi}\cdot\frac{\partial^2 W_i}{\partial\Phi^2} \\ &+ \sum_{i=1}^{n}\sum_{j=1}^{n} a_i a_j \int_0^{2\pi}\int_0^{2\pi} \frac{\partial^2 W_i}{\partial\Phi'^2}\cdot\frac{\partial^2 W_j}{\partial\Phi'^2}\Bigg] \\ &+ \frac{\cos^2\Phi'}{R_\Phi^2\, R_\theta^2\, \sin^2\Phi'}\Bigg[\sum_{i=1}^{n}\sum_{j=1}^{n} b_i b_j \int_0^{2\pi}\int_0^{2\pi} U_{\Phi i}.U_{\Phi j} - 2\sum_{i=1}^{n} b_i \sum_{i=1}^{n} a_i \int_0^{2\pi}\int_0^{2\pi} U_{\Phi i}\cdot\frac{\partial W_i}{\partial\Phi'} \\ &+ \sum_{i=1}^{n}\sum_{j=1}^{n} a_i a_j \int_0^{2\pi}\int_0^{2\pi} \frac{\partial W_i}{\partial\Phi'}\cdot\frac{\partial W_j}{\partial\Phi'}\Bigg] \\ &+ 2\upsilon\,\frac{\cos\Phi'}{R_\theta\, R_\Phi^3\, \sin\Phi'}\Bigg[\sum_{i=1}^{n} b_i \sum_{i=1}^{n} b_i \int_0^{2\pi}\int_0^{2\pi} U_{\Phi i}\cdot\frac{\partial U_{\Phi i}}{\partial\Phi} - \sum_{i=1}^{n} b_i \sum_{i=1}^{n} a_i \int_0^{2\pi}\int_0^{2\pi} U_{\Phi i}\cdot\frac{\partial W_i^{\,2}}{\partial\Phi'^2} \\ &- \sum_{i=1}^{n} a_i \sum_{i=1}^{n} b_i \int_0^{2\pi}\int_0^{2\pi} \frac{\partial W_i}{\partial\Phi'}\cdot\frac{\partial U_{\Phi i}}{\partial\Phi} + \sum_{i=1}^{n} a_i \sum_{i=1}^{n} a_i \int_0^{2\pi}\int_0^{2\pi} \frac{\partial W_i}{\partial\Phi'}\cdot\frac{\partial W_i^{\,2}}{\partial\Phi^2} \\ &+ \sum_{i=1}^{n} a_i \sum_{i=1}^{n} a_i \int_0^{2\pi}\int_0^{2\pi} \frac{\partial W_i(\Phi')}{\partial\Phi'}\cdot\frac{\partial W_i^{\,2}(\Phi')}{\partial\Phi'^2}\Bigg]\Bigg\} \\ &+ \frac{1}{R_\Phi^2}\Bigg[\sum_{i=1}^{n}\sum_{i=1}^{n} b\, b_j \int_0^{2\pi}\int_0^{2\pi} \frac{\partial U_{\Phi i}}{\partial\Phi}\cdot\frac{\partial U_{\Phi j}}{\partial\Phi} + 2\sum_{i=1}^{n} b_i \sum_{i=1}^{n} a_i \int_0^{2\pi}\int_0^{2\pi} \frac{\partial U_{\Phi i}}{\partial\Phi}.W_i \\ &+ \sum_{i=1}^{n}\sum_{ji=1}^{n} a_i . a_j \int_0^{2\pi}\int_0^{2\pi} W_i . W_j\Bigg] \\ &+ \frac{1}{(R_\theta\,\sin\Phi')^2}\Bigg[\sum_{i=1}^{n}\sum_{j=1}^{n} b_i b_j \int_0^{2\pi}\int_0^{2\pi} U_{\Phi i}\cos\Phi . U_{\Phi j}\cos\Phi' \\ &+ 2\sum_{i=1}^{n} b_i \sum_{i=1}^{n} a_i \int_0^{2\pi}\int_0^{2\pi} U_{\Phi i}\cos\Phi' .\, W_i \sin\Phi' \\ &+ \sum_{i=1}^{n}\sum_{j=1}^{n} a_i\, a_j \int_0^{2\pi}\int_0^{2\pi} W_i \sin\Phi' . W_j \sin\Phi\Bigg]\end{aligned}$$

$$+\frac{2\upsilon}{R_\theta\ R_\Phi \sin\Phi'}\left[\sum_{i=1}^{n} b_i \sum_{i=1}^{n} b_i \int_0^{2\pi}\int_0^{2\pi} \frac{\partial U_{\Phi i}}{\partial \Phi}\ .U_{\Phi i}\cos\Phi'\right.$$

$$+\sum_{i=1}^{n} b_i \sum_{i=1}^{n} a_i \int_0^{2\pi}\int_0^{2\pi} \frac{\partial U_{\Phi i}}{\partial \Phi}\ .W_i \sin\Phi'$$

$$+\sum_{i=1}^{n} a_i \sum_{i=1}^{n} b_i \int_0^{2\pi}\int_0^{2\pi} W_i\ .U_{\Phi i}\cos\Phi'$$

$$\left.+\sum_{i=1}^{n} a_i \sum_{i=1}^{n} a_i \int_0^{2\pi}\int_0^{2\pi} W_i\ .W_i(\Phi')\sin\Phi'\right)\ R_\Phi\ R_\theta \sin\Phi' d\Phi'\ d\theta$$

. . . (B . 6)

After simplified Eq. (B . 6) and some arrangements yield the following expression :-

$$U_{\max} = \sum_{i=1}^{n}\sum_{j=1}^{n} c_i c_j \frac{E h \pi}{(1-\upsilon^2)} \int_0^{2\pi} \frac{h^2}{12 R_\Phi^4}\left[U'_{\Phi i} U_{\Phi j}' - 2U_{\Phi i}' W_i'' + W_i'' W_j''\right]\sin\Phi'$$

$$+\frac{\upsilon\, h^2}{6 R_\theta\ R_\Phi^3}\left[U_{\Phi i} U_{\Phi i}' - U_{\Phi i} W_i'' - U_{\Phi i}' W_i' + W_i' W_i''\right]\cos\Phi'$$

$$+\frac{h^2}{12 R_\Phi^2\ R_\theta^2}\left[U_{\Phi i} U_{\Phi j} - 2U_{\Phi i} W_i' + W_i' W_j'\right]\frac{\cos^2\Phi'}{\sin\Phi'}$$

$$+\frac{1}{R_\Phi^2}\left[U_{\Phi i}' U_{\Phi j}' + 2U_{\Phi i}' W_i + W_i W_j\right]\sin\Phi'$$

$$+\frac{1}{R_\theta^2}\left[U_{\Phi i} U_{\Phi j}\frac{\cos^2\Phi'}{\sin\Phi'} + 2U_{\Phi i}\ W_i \cos\Phi' + W_i W_j \sin\Phi'\right]$$

$$+\frac{2\upsilon}{R_\Phi\ R_\theta}\left[U_{\Phi i} U_{\Phi i}'\ \cos\Phi' + U_{\Phi i}' W_i \sin\Phi' + U_{\Phi i} W_i \cos\Phi' + W_i W_i \sin\Phi'\right].$$

$$. R_\Phi\ R_\theta\ d\Phi'$$

. . . (B . 7)

where

$$U_{\max} = \sum_{i=1}^{n}\sum_{j=1}^{n} c_i c_j \frac{E h \pi}{(1-\upsilon^2)} \int_0^{2\pi} k_{i\,j} \qquad \ldots (B . 8)$$

Hence

$$K_{ij} = \frac{E h \pi}{(1-\upsilon^2)} \int_0^{2\pi} \frac{h^2}{12 R_\Phi^4} \left[U'_{\Phi i} U_{\Phi j}' - 2 U_{\Phi i}' W_i'' + W_i'' W_j'' \right] \sin\Phi'$$

$$+ \frac{\upsilon\, h^2}{6 R_\theta R_\Phi^3} \left[U_{\Phi i} U_{\Phi i}' - U_{\Phi i} W_i'' - U_{\Phi i}' W_i' + W_i' W_i'' \right] \cos\Phi'$$

$$+ \frac{h^2}{12 R_\Phi^2 R_\theta^2} \left[U_{\Phi i} U_{\Phi j} - 2 U_{\Phi i} W_i' + W_i' W_j' \right] \frac{\cos^2\Phi'}{\sin\Phi'}$$

$$+ \frac{1}{R_\Phi^2} \left[U_{\Phi i}' U_{\Phi j}' + 2 U_{\Phi i}' W_i + W_i W_j \right] \sin\Phi'$$

$$+ \frac{1}{R_\theta^2} \left[U_{\Phi i} U_{\Phi j} \frac{\cos^2\Phi'}{\sin\Phi'} + 2 U_{\Phi i} W_i \cos\Phi' + W_i W_j \sin\Phi' \right]$$

$$+ \frac{2\upsilon}{R_\Phi R_\theta} \left[U_{\Phi i} U_{\Phi i}' \cos\Phi' + U_{\Phi i}' W_i \sin\Phi' + U_{\Phi i} W_i \cos\Phi' + W_i W_i \sin\Phi' \right].$$

$$. R_\Phi R_\theta \, d\Phi' \qquad \ldots (B . 9)$$

where

k_{ij} is the tow dimensional of stiffness matrix of spheroidal shell.

In order to find the mass matrix of spheroidal shell can be begin from the maximum kinetic energy as in the following expression :-

$$K_{max} = \frac{\omega^2 \rho h}{2} \int_0^{2\pi} \int_0^{2\pi} (U_\Phi^2 + W^2) R_\Phi R_\theta \sin\Phi' \, d\Phi' \, d\theta \qquad \ldots (B . 10)$$

The same procedure in the maximum potential energy, after simplified and some arranged for Eq. (B . 10) yield :-

$$K_{max} = \sum_{i=1}^{n} \sum_{j=1}^{n} c_i c_j \int_0^{2\pi} \rho\, h \pi \left[U_i U_j + W_i W_j \right] R_\Phi R_\theta \sin\Phi' \, d\Phi' \qquad \ldots (B . 11)$$

where

$$K_{max} = \sum_{i=1}^{n} \sum_{j=1}^{n} c_i c_j \int_0^{2\pi} m_{ij} \qquad \ldots (B . 12)$$

hence

$$m_{ij} = \int_0^{2\pi} \rho\, h \pi \left[U_i U_j + W_i W_j \right] R_\Phi R_\theta \sin\Phi' \, d\Phi' \qquad \ldots (B . 13)$$

where, m_{ij} is the tow dimensional of mass matrix of spheroidal shell.

ACKNOWLEDGMENTS

(In The Name of Allah, The Gracious, The Merciful)

*Praise be to " **ALLAH** " and pride to his Prophet " **Mohammed** "*

*I would like to express my deep thanks and gratitude to my supervisors, **Dr. Ahmed A. Al – Rajihy** and **Dr. Ala M.H. Al – Jesany** for their support, guidance, advice and assistance throughout the various stages of the present work.*

I record my sincere gratitude to my family and my friends for their encouragement and moral support during the period of preparing this work.

I am also grateful to all those who have helped me in one way or another in carrying out this research.

Nawal Hussein Abdul – Ameer
July 2005

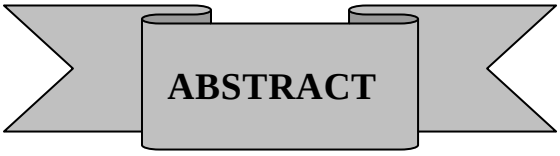

This thesis presents a theoretical investigation of the axisymmetric free vibration of an isotropic thin oblate spheroid shells. The analysis depends on two approaches which are the Rayliegh–Ritz's Method and the Boundary Matching Method. Both of the shallow shells and non – shallow shells theories are used for the analysis.

Rayliegh–Ritz's Method as well as an approximate modeling technique are adopted to estimate the natural frequencies for the shells. This technique is based on considering the oblate spheroid as a continuous system constructed from two spherical shell elements matched at the continuous boundaries.

Some experiments, which were taken from the literature, are used to improve the theoretical work. The experimental model satisfies the same requirements and conditions of this thesis.

Throughout the results, it is shown that when the eccentricity ratio reaches zero, an exact thin sphere solution emerges and when the eccentricity ratio approaches one an exact thin circular plate solution emerges. Therefore, the eccentricity ratio of an oblate shell at medium value lies between these two values.

The Rayleigh Method is found to be suitable for eccentricities less than 0.6, while for the Rayleigh–Ritz's Method and Boundary Matching Method are suitable for all eccentricities.

The effect of different boundary conditions (such as: clamped – clamped, clamped – free and pined – pined) of the oblate spheroid shells on the free vibration characteristics is investigated.

LIST OF CONTENTS

NOMENCLATURE

Symbol	Description	Units
A_i , B_i	Arbitrary constants.	
a , b	Major and minor semi – axis of an oblate spheroid shell respectively.	m
$C_{i,j}$	Element of the boundary conditions matrix.	
D_b	Plate or shell rigidity ($E.h^3 / 12 (1 - \upsilon^2)$.	N/m
d	Shallow spherical shells' base radius (Fig. 3–7).	m
E	Young's modulus of elasticity.	N/m^2
e	Eccentricity ratio ($\sqrt{1-b^2/a^2}$).	N.D.
H	Shallow spherical shells' height (Fig.3–7).	m
h	Shell thickness.	=
$J_o(x$	Bessel function of the first kind of order zero.	
$J_1(x)$	Bessel function of the first kind of order one.	
k_ϕ, k_θ, k_r	Changes of curvature in the ϕ, θ, r directions respectively.	
M_Φ , M_θ , M_r	Moments per unit length.	N.m/m
N_Φ , N_θ , N_r	Membrane forces per unit length.	N/m
$P_n(x)$	Legendre function of the first kind.	
$P'_n(x)$	First derivative of the Legendre function of the first kind.	
$P''_n(x)$	Second derivative of the Legendre function of the first kind.	
Q_Φ , Q_r	Transverse shearing force per unit length.	N/m
$Q_n(x)$	Legendre function of the second kind.	
$Q'_n(x)$	Derivative of the Legendre function of the second kind	
R_r	Effective radius.	m

R_Φ , R_θ	Principal radii of curvatures of an oblate spheroid surface.	m
U	Strain energy.	
U_r	The displacement of a shallow spherical shell parallel to horizontal axis	m
U_Φ	Tangential displacement mode.	=
u_Φ	Tangential displacement of points on shell middle surface.	=
W_r	The displacement of a shallow spherical shell parallel to vertical axis.	=
W	Transverse or radial displacement mode.	=
w	Transverse displacement of points on shell middle surface.	=
$Y_o(x)$	Bessel function of the second kind of order zero.	
$Y_1(x)$	Bessel function of the second kind of order one.	
z	Distance from the middle surface in the Z – direction	m

Greek Symbols

β_i	Roots of the non – shallow shell cubic equation.	
$\varepsilon_{\phi'}', \varepsilon_\theta', \varepsilon_r'$	Direct strains in the ϕ, θ, r directions respectively at a distance z from the middle surface.	
$\varepsilon_\phi^\circ, \varepsilon_\theta^\circ, \varepsilon_r^\circ$	Strains in the ϕ, θ, r directions respectively for the middle surface.	
Φ'	Inclination angle of an oblate spheroid.	degree
Φ	Inclination angle of a spherical shell model.	=
Φ_o	Opening angle of the approximate spherical shell..	=
λ	Non – dimensional frequency parameter $\sqrt{\rho/E}\,\omega.a$ (used for oblate spheroid shells).	
μ_i	Roots of the shallow shell equation.	
θ	Angle of rotation in the meridian direction.	degree
ρ	Mass density.	kg/m^3
Ω	Non – dimensional frequency parameter $\sqrt{\rho/E}\,\omega.R$ (used for spherical shells).	

ω	Circular frequency	rad/sec
ω_o	Natural frequency parameter define $h/d\sqrt{E/\rho}$	=
υ	Poisson ratio.	N.D.
$б_{\Phi'}$, $б_{\theta}$	Stress resultants.	N/m^2

Note : Other symbols are given in their corresponding chapters.